D688986

185

D 68899/86

KALUSOWILA. P. W.

185

CITY OF LONDON POLY.

DIFFUSION PROBLEMS IN LEAD-TIN OVERLAY BEARINGS

Thesis submitted in partial fulfilment of the
requirements of the degree of

DOCTOR OF PHILOSOPHY

to the

COUNCIL FOR NATIONAL ACADEMIC AWARDS

by

PREMATILAKE WIMALADARMA KALUBOWILA

-

Sponsoring
Establishment

Department of Metallurgy and
Materials Engineering
City of London Polytechnic
Central House
Whitechapel High Street
London E1 7PF.

Collaborating
Establishment

Shell Research Limited
Thornton Research Centre
PO Box 1
Chester CH1 3SH.

DIFFUSION PROBLEMS IN LEAD-TIN OVERLAY BEARINGS

Thesis submitted in partial fulfilment of the
requirements of the degree of

DOCTOR OF PHILOSOPHY

to the

COUNCIL FOR NATIONAL ACADEMIC AWARDS

by
PREMATILAKE WIMALADARMA KALUBOWILA

-

Sponsoring
Establishment

Department of Metallurgy and
Materials Engineering
City of London Polytechnic
Central House
Whitechapel High Street
London E1 7PF.

Collaborating
Establishment

Shell Research Limited
Thornton Research Centre
PO Box 1
Chester CH1 3SH.

CONTENTS

Page No.

Page No.

ACKNOWLEDGEMENTS

I would like to express my gratitude to my supervisors: Dr S P Wach for advising me throughout the project and Dr M B Levens for the advice and arrangement of financial support.

My thanks are also due to Dr C J L Booker, Dr M Clarke, Mr E J Easterbrook, Dr R P H Fleming and Mr M Perry for useful discussions at various stages; Mr P Cook, Mr A Mandal and all the other technicians in the Department of Metallurgy and Materials Engineering at the City of London Polytechnic; Mr P Marks and Mr D Singleton at the Thornton Research Centre for helping in the experiments.

I also acknowledge the help given by Dr D Cook in preparing a computer program, and Mr K Z Czoch for arranging a visit to Glacier Metals Company.

Finally, my sincere thanks are due to Ms I Mansouri-Azar for spending long hours in helping in various ways at all stages from the beginning of the project to the final binding of the thesis.

ABSTRACT

The corrosion of lead-tin overlay bearings in hot lubricating oils, through the depletion of tin in the overlay, has been recognised as a problem of some severity in the automotive bearing industry. The inter-diffusion of tin in the overlay and the copper in the underlying substrate results in the formation of copper-tin intermetallic compounds, consequently depleting tin in the overlay. This renders the bearing subject to corrosion in degraded oil. Attempts have been made to slow down this diffusion process by placing electrodeposited barriers between the bonding material and the overlay. The most common barrier is a thin electrodeposit of nickel. Claims have been made that this nickel barrier retards the growth of intermetallic compounds. However, no evidence to this effect has been found in the present work. The nickel barrier, as well as other barriers, forms intermetallic compounds with tin at almost the same rate as when a barrier is not present.

This work was carried out to investigate the problem of diffusion in detail and to search for possible solutions. The kinetics of the diffusion processes involved was studied. After experimenting on a number of barriers, two successful barriers were discovered. These are electrodeposited alloys of Cu-P and Cu-B. A mechanism of prevention of intermetallic compound growth and tin depletion by the two barriers is discussed.

Another important outcome of the investigation is that it has been established that the diffusion of copper and nickel are the rate controlling elements in the process of formation of the respective intermetallic compounds with tin. This disproves the frequently held view that the diffusion of tin, commonly associated with its low melting point, is the rate controlling step.

1. GENERAL INTRODUCTION

A bearing is a means of positioning one part of a machine with respect to another part in such a way that a relative motion is possible. Plain bearings of slider type were used first, dating back thousands of years. These include all types of bearings in which the primary motion is a sliding of one surface over another. Journal or sleeve bearings which are used to position a shaft, or a moving part in a radial direction, and thrust bearings used in general to prevent movement of shaft in an axial direction and as guides for linear motion, fall into the category of plain bearings. Overlay plated bearing is one particular type of plain bearings developed in the 1940's. A great many types of journal bearings have been developed over the years. Some surround the shaft completely in one form or another and others may encompass the shaft partially. In many cases a lubricant is used to facilitate motion and reduce friction between the bearing surface and the shaft. Liquid lubricants such as oil, water and grease as well as solid lubricants such as graphite and molybdenum disulphide are in common use.

In selecting a type of bearing for a particular application, factors such as mechanical requirements, environmental requirements and the economics of production are considered [1] . In automotive engines, both the crank shaft bearings and connecting rod bearings are subject to very high cyclic loading, demanding a high fatigue strength. At first glance rolling element bearings might be considered the first

choice for this type of service. However, for a number of reasons all motor engine manufacturers use journal bearings for the crank shaft big-end and main bearings. Low cost of production and the successful functioning by careful attention to the lubricant of the journal bearings have been the major reasons for its choice in the above application [1]. Larger radial spaces for housing a rolling type bearing and the damping capacity of the oil film in the slide bearing where large and rapid variations in load occur, have also been taken into account.

Requirements that a plain bearing must satisfy, in addition to its economical production are [3, 4]:

(i) fatigue strength and compressive strength;

(ii) embeddability;

(iii) compatibility;

(iv) corrosion resistance.

The materials generally used as the bearing material in the plain bearings fall into three main categories:

(i) White metals

These are the well-known 'babbits' which are either tin-base or lead-base alloys. The alloys have low melting points and have an outstanding embeddability and are compatible with virtually any type of mating surface. The corrosion resistance of tin-base alloys is high, but the lead-base alloys are susceptible to corrosion by the acidic products of the partial oxidation of oil. They are also economical

to produce. However, their fatigue strength at the service temperatures of the present day engine is low, hence these alloys are not used any more in modern automotive engines.

(ii) Copper alloys

This category consists of a wide range of copper-base alloys with lead, zinc, aluminium, phosphorus, nickel and other alloying elements [2,3,4]. The load carrying component in these alloys is the copper matrix and other elements are used to improve properties such as fatigue strength. Copper-lead alloys are in wide use; the lead being insoluble in copper is dispersed in the copper matrix as separate 'islands'. One shortcoming of the lead phase not being in solution is that it is susceptible to corrosion by acidic oil oxidation products [2,7]. Copper-tin-lead alloys are also in common use. Here, the tin and copper form a bronze matrix in which free lead is distributed. Phosphorus is sometimes added to tin-bronzes for improving the fatigue strength and compressive strength, although it lowers the embeddability and compatibility.

(iii) Aluminium-base alloys

There are two main classifications. In the first category, high melting point constituents such as chromium, nickel, manganese, iron and silicon are added to aluminium for improved fatigue strength. The alloys can be used as 'solid' half bearings, whereas the alloys with low melting point constituents, which form the other class have to be steel backed for their fatigue strength in most cases. Aluminium alloys of tin or cadmium fall into this class. The embeddability

and compatibility of the aluminium are generally lower than those of copper base alloys. These are also in wide use in automotive engines. A recently developed aluminium alloy containing 20 ^{w}/o tin, or more, of tin and steel backed, is claimed [3] to have a greatly improved embeddability and comformability.

It is not possible to find all the desired bearing properties in one bearing material, hence the normal practice is to meet a compromise depending on the application. The harder materials, although good in their fatigue strength and compressive strength, have poor embeddability and conformability. To overcome this problem overlays have been developed (Table 1).

An overlay is an electrodeposit of about 15 - 25 μm thickness deposited on the bearing surface. Copper-base alloys are in many cases coated with an overlay of a lead-tin alloy or a lead-indium alloy. Typical nominal overlay compositions are [3] :

(i) Pb 90 ^{w}/o - Sn 10 ^{w}/o

(ii) Pb 88 ^{w}/o - Sn 10 ^{w}/o - Cu 2 ^{w}/o

(iii) Pb 95 ^{w}/o - In 5 ^{w}/o

The thickness of the overlay varies with the size of the bearing. The thinner the overlay, the greater is its fatigue strength (Figure 1). Crank shaft journal bearings of heavy truck engines are usually provided with 15 μm thick overlay and those of light motor car engines with a thicker (25 μm) overlay.

TABLE 1. Fatigue ratings of engine bearing alloys as obtained on a hydraulically loaded bearing test rig (After Pratt Ref 2)

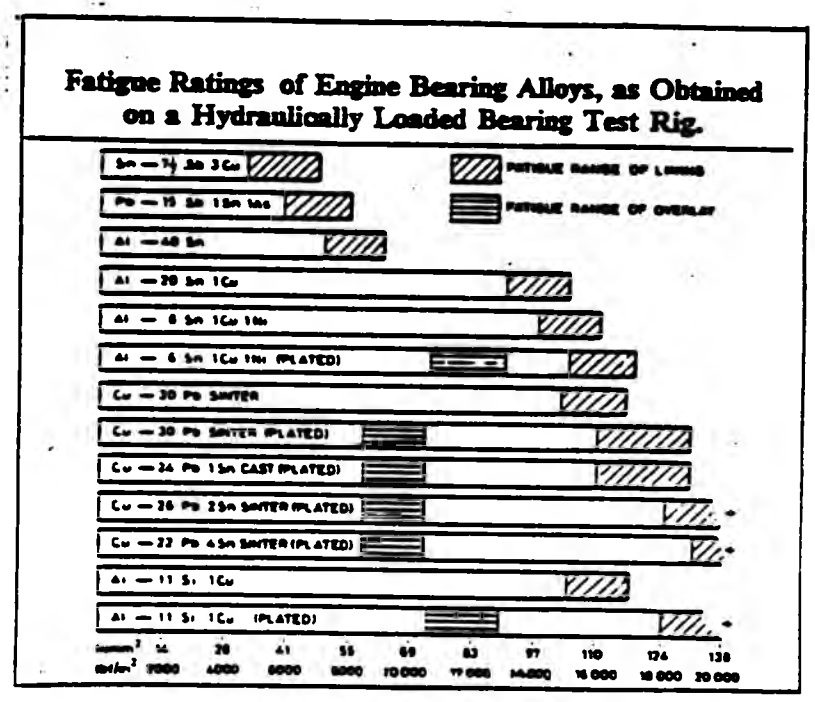

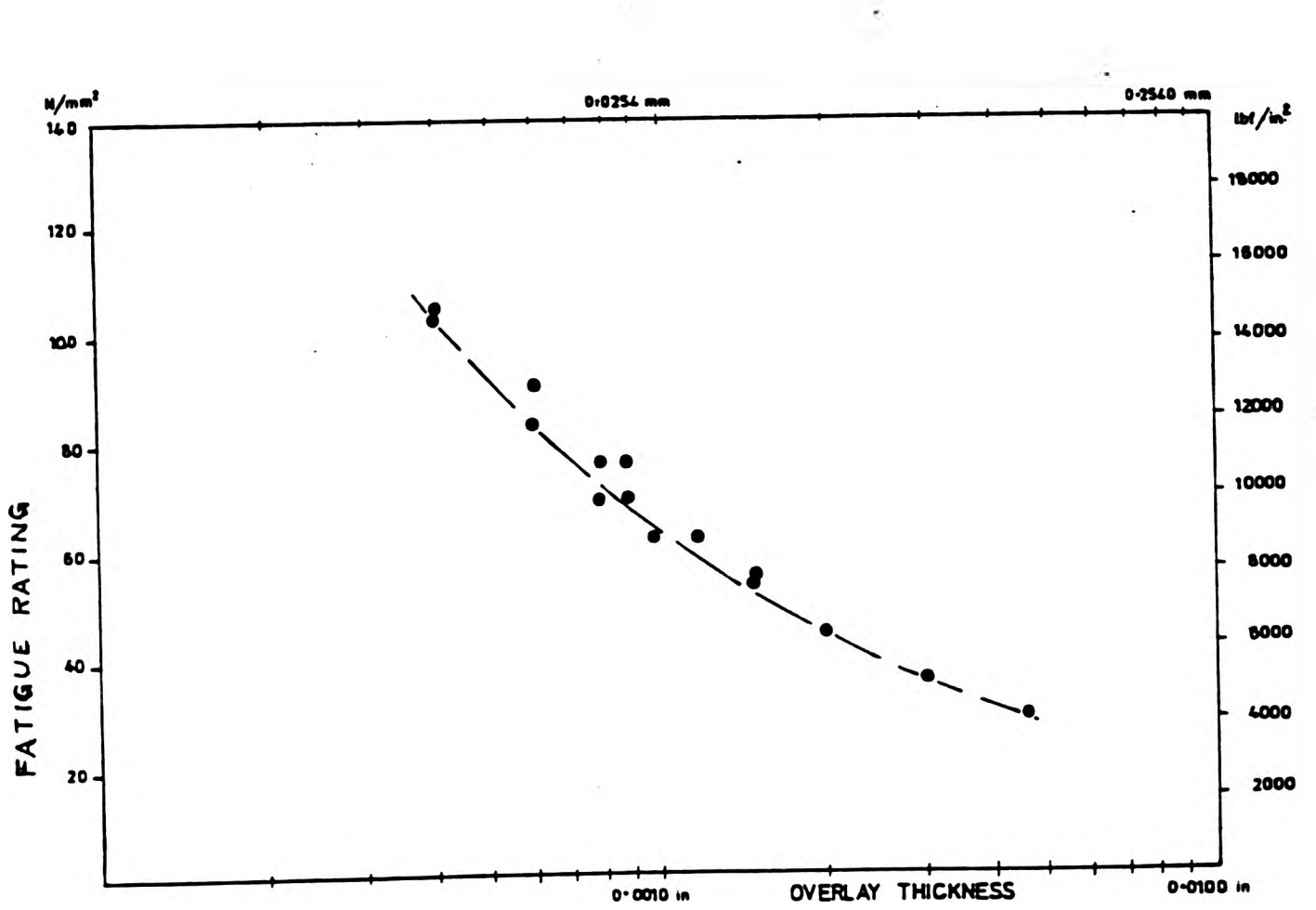

Figure 1. The Fatigue Strength/Thickness Relationship for Lead-Tin overlays. (After Pratt. Ref 2)

The provision of an overlay has the following benefits to the bearing:

(i) Improved ability to tolerate and embed entrapped matter within the limits imposed by the thickness of the overlay and dirt particle size.

(ii) Greater corrosion resistance than that of the underlying material. In the case of copper-lead bearings, the lead phase is attacked by acidic oil oxidation products, if not coated with an overlay.

(iii) Improved load distribution because the soft overlay is able to conform with minor irregularities in the mating surface, so distributing the imposed loading over a greater effective area.

(iv) Improved compatibility. The lead alloy overlays have a greater compatibility with mating surfaces.

The corrosion resistance of the overlay is due to the presence of tin in it. The minimum level of tin required for corrosion protection is thought[7] to be about 2 $^{w}/_{o}$. Under service conditions the tin in the overlay reacts with the copper substrate forming intermetallic compounds (Cu_6Sn_5 and Cu_3Sn), consequently depleting the overlay of tin beyond this minimum level. The rate of depletion of tin from the overlay, hence the susceptibility to corrosion, increases with the operating temperature. In modern high performance engines with high compression ratios, the normal running temperatures are high and 140^{o}C is not uncommon. At this

temperature the diffusion rates are quite high and premature failure in bearings due to corrosion is not uncommon. The efficiencies of the engines are being constantly improved by the manufacturers and the compression ratios increased, with the result of higher operating temperatures. It is known that engines are being developed from ceramic materials to run at much higher temperatures than those of the conventional engines, and bearing problems in such situations could be anticipated.

This work was carried out to investigate into the diffusion of tin in the lead-tin overlays and to alleviate the problem.

2. LITERATURE SURVEY

2.1 INTRODUCTION

Corrosion of lead-tin overlays in automotive bearings has been recognised as due to the depletion of tin from the overlay, below minimum limits. Under operating conditions, interdiffusion of tin and copper forms Cu_6Sn_5 and Cu_3Sn intermetallic compounds in between the overlay and the copper substrate. In cases where barriers such as nickel, cobalt and iron are placed, intermetallic compounds of tin with those metals are formed. Thus, such barriers do not seem to perform successfully as diffusion barriers. A mechanism of corrosion of lead-tin and lead-indium has been proposed by Wilson and Shone [7].

Generally accepted methods of measuring diffusion coefficients are presented together with recently published methods. The effect of temperature on diffusion kinetics is given by the generally accepted Arrhenius equation, although in some cases this equation does not fully agree with the experimental results. Alternative expressions for temperature dependence of diffusion have been reviewed.

Factors affecting intermetallic compound formation and some controlling attempts have been discussed. Recent work on diffusion barrier layers and their effectiveness has been studied. Electroplating techniques of some barrier layers and lead-tin alloys relevant to the plain overlay bearings have been presented.

2.2 CORROSION OF OVERLAY BEARINGS

Bearing corrosion became an important problem to the petroleum and automotive industry during the period 1934-1935, at which time the use of Cu-Pb, Cd-Ag and Cd-Ni bearings became fairly wide spread [9], instead of the previously used babbit bearings. Since then, there have been developments in the engine design, bearing materials and the lubricants. With the development of high performance up-rated engines, bearing materials to satisfy their more stringent performance requirements were also developed. The cyclic loading of the modern engine is very high compared to the earlier ones. To withstand the fatigue conditions, new bearing materials based on copper and aluminium were developed. Copper may serve as a good bearing material, specially when steel-backed, and shows an improved performance when incorporated with softer lead to obtain good embeddability and conformability. Lead is virtually insoluble in copper, hence Cu-Pb is not a true alloy, but consists of lead distributed as 'islands' in a dendritic copper matrix. Cu-Pb bearings are readily corroded by oil oxidation products, which preferentially attack the lead, leaving a porous structure.

The overlay plating of Cu-Pb and Pb-bronze bearings, with a Pb-Sn or Sn-based electrodeposited overlay was introduced in the late 1930's, primarily with the object of enabling the harder and stronger Pb-bronzes to be used as engine bearing linings. This also reduced the seizure problem posed by the rather incompatible Pb-bronze alloys [2]. The overlay also served to protect the lead

phase in copper from corrosion. Lead overlays could be made corrosion-resistant by the addition of a few percent of tin or indium. Indium was used in the USA and tin was widely used in the UK and in Europe. Alloying is an effective and a common method of improving corrosion resistance of metallic materials. An Fe - 8 ^{w}/o Al alloy is reported to have the same oxidation resistance as an 80Ni - 20Cr alloy [11].

Chromium or aluminium in iron improves the oxidation resistance[12]. Copper, phosphorus, nickel and chromium alloyed in such concentrations with iron to sustain the presence of a protective oxide, improves its corrosion resistance [12]. Alloys of gold with copper or silver retain the corrosion resistance of gold, above a critical alloy concentration, called by Tammann,[13] the reaction limit. Below the critical limit the alloy corrodes in certain environments, eg. strong acids. This behaviour of noble metal alloys is known as parting and the mechanism is probably related to dezincification of brasses. The tin content of the Pb-Sn overlay [2,7], when new, is about 8 - 12 ^{w}/o and this content of tin is in far excess of the amount required to prevent corrosion of lead in hot oils. However under service conditions, where the temperatures can rise up to about 150^{o}C, tin depletion takes place due to the formation of diffusion compounds with the substrate. An overlay bearing depleted of tin becomes susceptible to corrosion. Lead-indium alloys also suffer from the same problem.

Wilson and Shone [7] attribute the prevention of corrosion of lead-tin and lead-indium overlays, to the presence of a continuous protective

surface layer of tin oxide or indium oxide. When the tin content of the overlay is less than 3 ^{w}/o and indium 5 ^{w}/o, the oxide layer is not continuous; some lead oxide is formed in the discontinuous areas of the tin or indium oxide as shown schematically in Figure 2. As a result of this pitting is initiated at the lead oxide covered areas, in lead-tin alloys. In the case of lead-indium alloys (< 5 ^{w}/o In), indium oxide is formed in the grain boundaries and consequently intergranular corrosion occurs. Corrosion resistance of an electrodeposited Pb - 6 ^{w}/o Sn alloy has been attributed by Du-Rose [121] to tin being in solid solution in the alloy. Narcus [122] and Voyda [123] found that an electrodeposited alloy containing up to 8 ^{w}/o of tin was a solid solution, although a lower solid solubility is indicated at room temperature in the equilibrium diagram (Figure 22g).

2.3 DIFFUSION

Diffusion is a process whereby the distribution of each component in a phase tends to uniformity [20-30]. One simple, but important, concept in diffusion is that it is the result of the tendency to random motion of the individual atoms. Because of thermal energy, the atoms in a metal crystal are in constant motion around their equilibrium positions. Occasionally, as a result of this random motion, an atom will jump into a neighbouring vacant site. At room temperature, the frequency of jumps is relatively small. However, as the temperature rises, the jump frequencies increase, and the net rate of atomic migration eventually becoms large enough to provide readily observable effects,

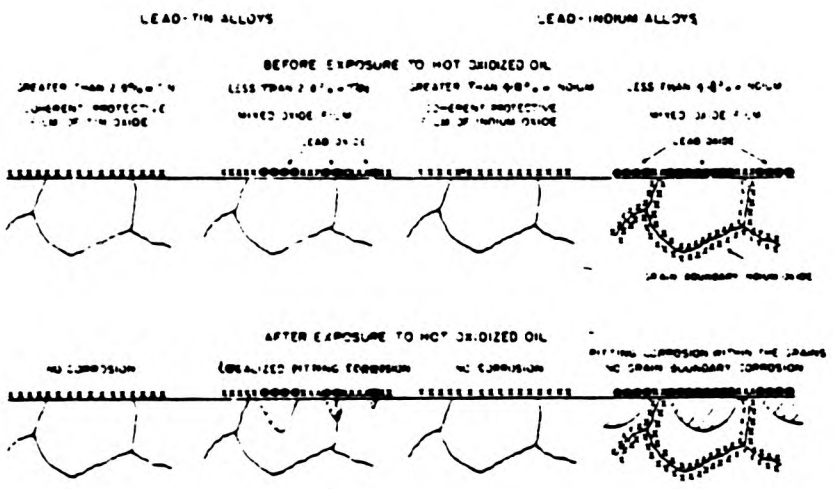

Figure 2. Schematic Representation of the Mechanism by which Lead-Tin and Lead-Indium Alloys corrode in Medicinal White Oil at 140°C. (After Wilson & Shone, Ref 7).

including transport of atoms over considerable distances. Changes in chemical composition, phase transformations and compound formation can also be brought about as a result of atomic migration when atom of a species migrate to different positions in a matrix of the same species, the process is known as self diffusion. Interdiffusion or chemical diffusion are the terms used to denote the atomic migration of one species in another matrix.

2.3.1 Diffusion Mechanisms

There are four generally recognised mechanisms of diffusion:

(i) Vacancy mechanism

This is a very common type of mechanism in metals and alloys. A certain number of vacancies can be expected to be present in a crystal in thermodynamic equilibrium. Any atom in the neighbourhood of the vacant site can diffuse by jumping into the vacancy.

(ii) Interstitial mechanism.

Interstitial atoms move from one interstitial site to another, without causing net motion of any other atoms.

(iii) Interstitialcy mechanism

Interstitial atom moves to a normal lattice site pressing the atom in the normal site to an interstitial position.

(iv) Exchange mechanism

This occurs very frequently in practice, and involves simultaneous motion of two lattice atoms.

Diffusion in crystals is generally agreed to take place by a series of jumps of individual atoms. Vacancy mechanism is the dominant mechanism in most pure metals and substitutional solid solutions [44-48]. Interstitial mechanism is assumed to play a major role in diffusion of the noble metals in lead, tin, indium and thallium [32]. For the exchange mechanism to take place in a dilute binary alloy, the diffusion coefficients of the two elements must be equal [31]. The diffusion coefficients in a homogeneous phase are usually different for the different components and this effect was first demonstrated by Smigelskas and Kirkendall [33]. Several experimental techniques provide information on the nature of point defects present in thermal equilibrium [31]. In such experiments, vacancies have been found to be the dominant defect in all metals investigated: (Aluminium [34,35], Copper [36], Silver [37], Gold [38], Lead [39], Sodium [40], Lithium [41], Cadmium [42], Magnesium [43]). Interstitial diffusion is rarely possible when two metals inter-diffuse, for their atomic radii are usually of the same order. Electrodeposited base metal composites are substitutional systems [20], and diffusion in them occur predominantly by vacancy mechanisms [21,25-27]. All diffusion processes are thermally activated; a thermal fluctuation must occur to supply the energy to surmount the energy barrier, in their transition, between lattice positions.

2.3.2 Rates of Mass Transport by Diffusion

In diffusion studies it is assumed that atomic migration occurs as a result of gradient in concentration. Strictly speaking, this is not

correct. First of all, it is the gradient in activity, not concentration, which is the true driving force for atomic migration. Secondly, self diffusion and diffusion of trace quantities occur without a concentration or an activity gradient. A gradient of concentration is required only for chemical diffusion or interdiffusion.

The analysis of diffusion data is based on Fick's first or second law. Fick's first law relates the flux (J) to the concentration gradient of solute i, $\frac{dc_i}{dx}$.

Mathematically it is written as:

$$J_i = - D_i \frac{dc_i}{dx} \qquad (2.1)$$

In the above equation the proportionality constant D_i is referred to as the diffusivity or the diffusion coefficient. This relationship assumes steady state and a constant D over the entire range of composition at a fixed temperature.

Fick's second law is mathematically expressed as:

$$\frac{\partial c}{\partial t} = \frac{\partial}{\partial x}\left(\tilde{D} \frac{\partial c}{\partial x}\right) \qquad (2.2)$$

where $\tilde{D}$ is the chemical or interdiffusion coefficient. For

conditions of constant $\tilde{D}$ equation (2.2) can be written as:

$$\frac{\partial c}{\partial t} = \tilde{D} \frac{\partial^2 c}{\partial x^2} \tag{2.3}$$

The interdiffusion coefficient $\tilde{D}$ for substitutional alloys depend on the actual coefficients for the individual components A and B. The relationship of the interdiffusion coefficients to the individual coefficients D_A and D_B are given by Darken's[49] equation:

$$\tilde{D} = N_A D_A + N_B D_B \tag{2.4}$$

where, D_A and D_B are the intrinsic diffusivities and N_A and N_B are the mole fractions of the components A and B in a binary system.

2.3.3 Methods of Determination of Interdiffusion Coefficient

The expression for Fick's second law is the general equation employed in the studies of isothermal diffusion, where D may not remain constant. Equation (2.3) can be solved for particular boundary conditions by two methods. First method, called Grube's method, is based on the assumption that the diffusivity, D, is not a function of concentration. The second approach, by Boltzmann and Matano[50,51], utilizes graphical integration to determine a concentration dependent diffusion coefficient.

(i) Grube's method

Generally the diffusion coefficient increases with the increase in concentration, but an approximate solution can be obtained by taking an average value, and this gives the simple solution:[44]

$$c = c_s - \tfrac{1}{2}(c_s - c_o)\ \mathrm{erf}\ \frac{x}{2\sqrt{Dt}} \qquad (2.5)$$

where, c = concentration at a distance x

c_s = original concentration from x = o to - ∞

c_o = original concentration from x = o to + ∞

The Grube's method is quite straightforward and easy to perform. The most difficult task is obtaining an accurate concentration-penetration profile. The limitations of the method must, however, be borne in mind or else this simplified solution might be applied to a system in which the diffusivities are strongly dependent upon composition. In reality, all chemical diffusion coefficients are concentration dependent and this method should only be applied to those whose dependence is small.

(ii) The Boltzmann-Matano method

In this method, a concentration penetration profile is plotted as the first step. Next the Matano interface is determined graphically

as shown in Figure 3a. It divides the two areas N and M equally. Boltzmann's solution to Fick's second law is given as:

$$\tilde{D}\,(N_A) = -\frac{1}{2t}\left(\frac{\partial x}{\partial N_A}\right)_{N_A} \int_{x_{A_2}}^{x_A} x \; dN_A \qquad (2.6)$$

Using the above equation, the interdiffusion coefficient at mole concentration N_A, $\tilde{D}\,(N_A)$, is determined. As shown in Figure 3b, $\left(\frac{\partial x}{\partial N_A}\right)_A$ is the reciprocal of the gradient at N_A of the concentration profile and N_{A_2} is the concentration as $x \to \infty$. The integral is the area between the Matano interface and the curve between the values $N = N_{A_2}$ and $N = N_A$.

Several computer programs have been devised to eliminate the time consuming exercise of graphical analysis. Hartley [52], has devised a program using the Boltzmann-Matano analysis. Heizwegan and Visser [53] have developed a more accurate program which does not assume a constant partial molar volume as in Boltzmann-Matano method.

(iii) Einstein-Smoluchowski method

An approximate value for the interdiffusion coefficient, can also be obtained using the Einstein-Smoluchowski equation:

$$x^2 = 2\tilde{D}t \qquad (2.7)$$

where, x = distance of penetration; m

$\tilde{D}$ = interdiffusion coefficient; $m^2 s^{-1}$

t = time; s

Plotting x^2 versus time, the interdiffusion coefficient can be obtained from the gradient.

(iv) Other methods

Another method of determining self-diffusion coefficients using tracer concentration profiles has been described by Mrowec [142]. This method can also be used to determine the diffusivity of any other diffusant provided that the diffusant has not reached the opposite side of the solvent. Figure 4 shows a typical distribution curve under such circumstances. From the point of view of the theory of diffusion it is a semi-infinite system, and in this case the solution of Fick's second law gives the equation:

$$c = \frac{c_o}{2\sqrt{\pi Dt}} \exp\left(-\frac{x^2}{4Dt}\right) \qquad (2.8)$$

where, c is the concentration of the diffusant at a distance x from the interface, c_o is the original concentration of the diffusant before diffusion has taken place and t is the time of annealing.

Equation (2.8) can be written in the form:

$$\ln \frac{c}{c_o} = -\ln (4\pi Dt)^{\frac{1}{2}} - \frac{x^2}{4Dt} \qquad (2.9)$$

Thus the slope of the plot of $\ln c/c_o$ versus x^2 gives the value $-1/4Dt$. Hence, it can be seen that it is not necessary to determine the absolute concentration of the diffusant to obtain the diffusion coefficient. The ratio of c/c_o can be obtained from a radiation

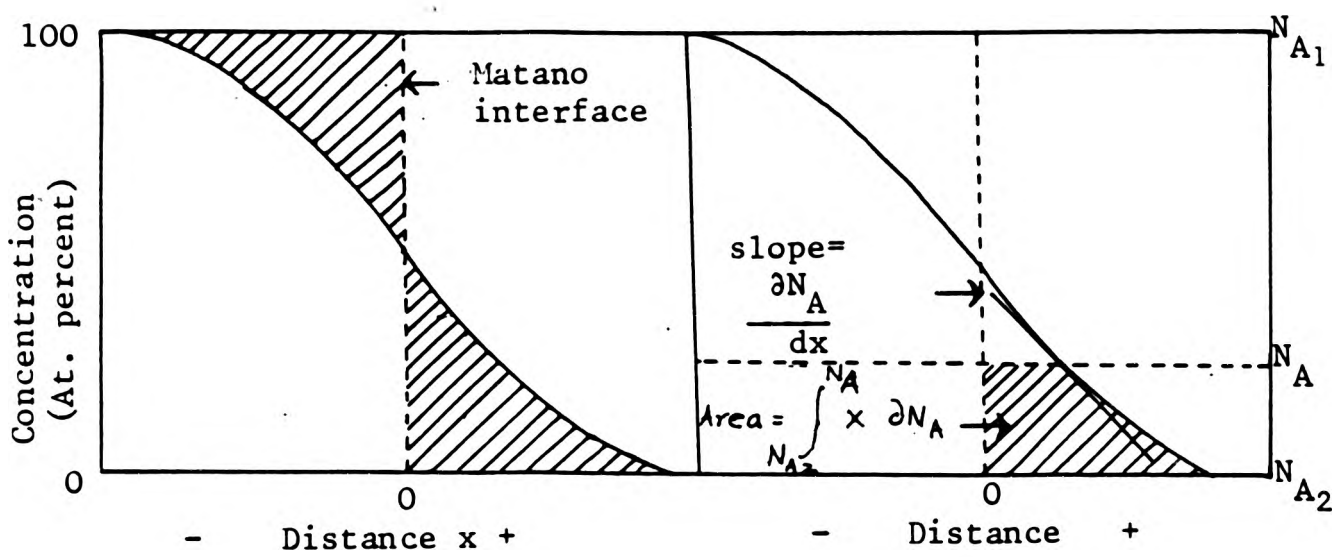

Figure 3a

Figure 3b

Concentration-penetration profiles illustrating the application of the Boltzmann-Matano solutions for D (After Owen Ref 40).

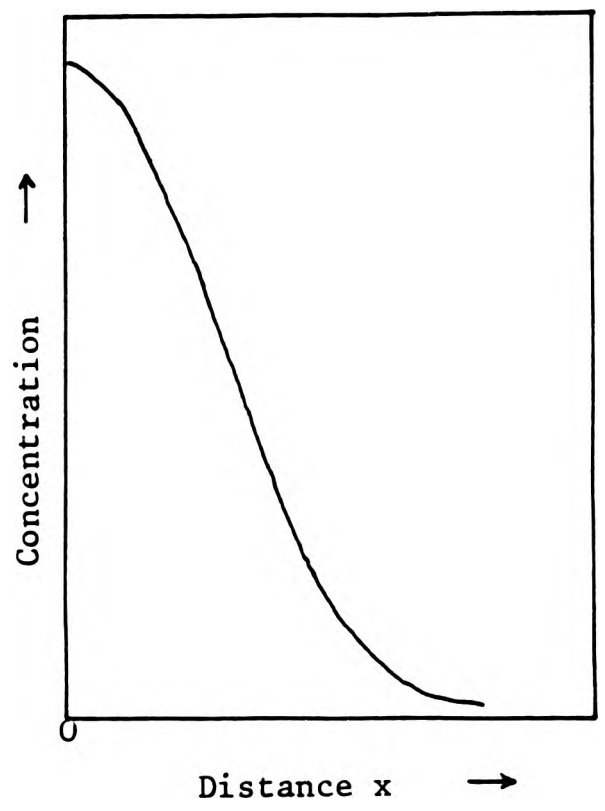

Figure 4. Schematic tracer concentration profile.

technique such as electron probe microanalysis, where the intensity of radiation is proportional to the concentration. Equation (2.9) can be written in terms of intensity of radiation, in the form:

$$\frac{\partial \ln \dfrac{I - I_b}{I_o - I_b}}{\partial x^2} = -\frac{1}{4Dt} \qquad (2.10)$$

where, I_o is the intensity at the interface before diffusion, I_b is the intensity of background signal and I is the intensity at any other point at a distance x from the interface.

Using Fick's first law, Wach [103,137] has deduced equations showing the relationship of rational rate coefficient of Wagner [104], Pilling and Bedworth [105] parabolic rate coefficient and Tammann [106] rate coefficient to the chemical diffusion coefficient. At steady state, when the concentration does not vary with time, the Fick's first law can be applied to a binary system. When the concentration gradient is constant and the concentration varies from c_i at $x = x_1$, to zero at $x = x_2$ the following relationship has been obtained:

$$k_r = D_i c_i = D_i \rho w_i \qquad (2.11)$$

where ρ = density of the medium; kg m^{-3} or mol m^{-3}

w_i = mass fraction of diffusant in the compound formed;

D_i = chemical diffusion coefficient; m^2 s^{-1}

c_i = concentration of the diffusant; kg m^{-3} or mol m^{-3}

k_r = rational rate coefficient (Wagner); kg m^{-1} s^{-1} or mol m^{-1} s^{-1}

Similarly, it has been shown that the Pilling and Bedworth [105] rate coefficient k_p is related to the chemical diffusion coefficient as in the equation:

$$k_p = 2 D_i c_i^2 = 2 D_i \rho^2 w_i^2 \qquad (2.12)$$

The Tammann rate coefficient [106] has been shown [103,137] to be equivalent to the diffusion coefficient, and comes from differentiated Einstein-Smoluchowski equation:

$$\frac{dx}{dt} = \frac{D}{x} = \frac{k_T}{x} \qquad (2.13)$$

The above equations can be used to evaluate the chemical diffusion coefficients in binary systems at steady state where the concentration varies from a particular value to zero as in the case of permeation of hydrogen, or in the formation of near-stoichiometric compounds.

Using Fick's second law, Bockris et al [132] have derived equations similar to Wach's for the diffusion of hydrogen from a uniformly precharged specimen, which involves the boundary conditions:

$$\frac{\partial c}{\partial x} = 0 \quad , \quad x = 0 \quad , \quad t \geq 0$$

$$c = 0 \quad , \quad x = L \quad , \quad t > 0$$

$$c = c_o \quad , \quad 0<x<L \quad , \quad t \leq 0$$

For the above boundary conditions Bockris et al have derived

the equation:

$$\frac{J_t}{zF} = \left(\frac{D}{\pi t}\right)^{\frac{1}{2}} c_o \qquad (2.14)$$

For conditions where the initial concentration profile is not uniform and the initial boundary conditions are:

$$c = 0 \quad , \quad x = 0 \quad , \quad t > 0$$

$$c = 0 \quad , \quad 0<x<L \quad , \quad t \leq 0$$

the authors have derived the following equation:

$$\frac{J_t}{zF} = \left(\frac{D}{\pi}\right)^{\frac{1}{2}} c_o\left[t^{-\frac{1}{2}} - (t + t_o)^{-\frac{1}{2}} \right] \qquad (2.15)$$

where t_o is the time interval.

From equations (2.14) and (2.15), the quantity $D^{\frac{1}{2}}c$ can be obtained. Knowing the diffusion coefficient, the original c_o can be obtained.

Wach [103,137] also emphasises the importance of the quantity given by the product of concentration and the square root of the diffusion coefficient ($D^{\frac{1}{2}}$ c), and shows that it gives a measure of the activity, or the propensity for change, of the species diffusing at the particular time.

2.3.4 Temperature Dependence of Diffusion

In general, all diffusion coefficients follow an Arrhenius type behaviour. This is generally expressed as:

$$D = D_o \exp\left(-\frac{Q_D}{RT}\right) \qquad (2.16)$$

where D = Diffusion coefficient; $m^2 s^{-1}$

D_o = Pre-exponential factor or frequency factor; $m^2 s^{-1}$

Q_D = Activation energy; $J\ mol^{-1}$

R = Gas constant = 8.314 $J\ K^{-1}\ mol^{-1}$

T = Temperature; K

The quantities D_o and Q_D are assumed to be constant over the limited temperature range. D can be the interdiffusion coefficient, self-diffusion coefficient or intrinsic diffusion coefficient.

The above equation can be written in the following forms:

$$\ln D = \ln D_o - \frac{Q_D}{RT} \qquad (2.17)$$

$$\text{and} \quad \log D = \log D_o - \frac{Q_D}{2.303\ R} \cdot \frac{1}{T} \qquad (2.18)$$

Plotting log D versus T^{-1} yields a straight line from which D_o and Q_D may be evaluated.

Until recently, equation (2.16) was an adequate representation of self-diffusion measurements in most solids. The well-known exceptions were the 'anomalous' body-centred cubic metals γ-U, β-Ti, β-Zr and

Vanadium [54] . However, recent developments have shown that small deviations from the Arrhenius equation are common for self-diffusion in pure metals. Two possible causes for small deviations from the Arrhenius equation are:

(1) temperature dependence of the activation energy for diffusion;
(2) two or more mechanisms contribute to lattice diffusion.

Curvature of the Arrhenius plot due to either of these causes will partially invalidate the defect quantity deduced from force fitting of the data to the Arrhenius equation. Seeger and Mehrer [55] have presented an interpolation of self-diffusion data that takes into account the temperature dependence of activation energy and two mechanisms of diffusion; single vacancies and divacancies. The equation derived by the above authors for the tracer self-diffusion coefficient, D^T , is as follows:

$$\ln D^T = \ln D_{10} - \frac{Q_1}{kT} + 2\,\alpha \ln\left(\frac{T}{T_o}\right) - 2\,\alpha\,\frac{T-T_o}{T} + \ln\left[1 + D_{21}\exp\left(-\frac{Q_{21}}{kT}\right)\right] \quad (2.19)$$

where, the following notations and abbreviations have been used:

$$Q_1 \equiv H^F_{1V} + H^M_{1V}$$

$$D_{10} \equiv a^2 \nu_{1V}\, f_{1V} \exp\,(S^M_{1V}/k) \exp\,(S^F_{1V}/k)$$

$$Q_{21} \equiv Q_2 - Q_1 = H^F_{1V} - H^M_{1V} + H^M_{2V} - H^B_{2V}$$

$$D_{21} \equiv D_{20}/D_{10} = 4\frac{f_{2V}}{f_{1V}} \exp\frac{S^F_{1V} + \Delta S_{2V}}{k} \quad \frac{\nu^o_{2V} \exp\,(S^M_{2V}/k)}{\nu^o_{1V} \exp\,(S^H_{1V}/k)}$$

$H^F_{2V} \equiv H^F_{1V} - H^B_{2V}$ = divacancy formation enthalpy,

$S^F_{2V} = 2S^F_{1V} + \Delta S^F_{2V}$ = divacancy formation entropy,

H^B_{2V} = divacancy binding enthalpy,

ΔS_{2V} = divacancy association entropy,

H^M_{2V} = divacancy migration enthalpy,

$\nu^o_{2V} \exp (S^M_{2V}/k)$ = frequency factor for divacancy migration

$2\alpha = \alpha^F + \alpha^M$

α^F = coefficient associated with monovacancy formation ≃ 0.1

α^M = coefficient associated with monovacancy migration (somewhat larger than α^F)

a = edge length of the elementary cubic lattice

ν_{1V} = jump frequency of an atom adjacent to the vacancy

H^M_{1V} = activation enthalpy associated with jumps

$\nu^o_{1V} \exp (S^M_{1V}/k)$ = pre-exponential factor associated with jumps

A much simpler equation to the one above (2.19) has been derived by Wach [56] as a modified version of the generally accepted Arrhenius equation (2.16). The pre-exponential factor D_o in equation (2.16) is given by the Wert-Zener-Le Claire equation:

$$D_o = \gamma\, a^2\, f\, \nu \exp (\beta\, Q_D / R\, T_M) \qquad (2.20)$$

where γ, a, β and T_M are constants associated with the matrix lattice. By plotting log D_o versus Q_D for hydrogen and other species in metals and other matrices, Wach [56] obtained a linear

relationship (compensation effect). This linear relationship is not expected from equation (2.20). Hence the author modified equation (2.16) by introducing two constants D_θ and θ, characteristic of the diffusing element and independent of the lattice. At the hypothetical temperature $T = \infty$, the equation is:

$$D_o = D_\theta \exp \frac{Q_D}{R\theta} \qquad (2.21)$$

$$\text{or} \quad \ln D_o = \ln D_\theta + \frac{Q_D}{R\theta} \qquad (2.22)$$

where, D_o = pre-exponential factor of the Arrhenius equation; $m^2\ s^{-1}$

$D_\theta = \frac{h}{4\pi m}$; $m^2\ s^{-1}$ (comes from the minimum value of the uncertainty principle)

h = Plank constant = 6.625×10^{-34} Js

m = atomic mass; kg

$\theta = \frac{h\nu}{k}$; K ν = frequency factor; Hz

R = Gas constant = 8.314 J K^{-1} mol^{-1}

At any temperature T, the diffusion coefficient is given by:

$$D = D_\theta \exp\left(\frac{Q_D}{R\theta} - \frac{Q_D}{RT}\right) \qquad (2.23)$$

values of D_θ and θ for some metals [57] are given in Table 2. Equation (2.23) is very useful for interdiffusion calculations, and activation energy Q_D can be determined from a single value of D determined at a temperature T.

TABLE 2. The constants θ, $\nu = k\theta/h$ and $D_\theta = h/4\pi m$ for some elements. (After Wach Ref 57,140)

Element	θ/K	ν/Hz	D_θ/m^2s^{-1}	Element	θ/K	ν/Hz	D_θ/m^2s^{-1}
H	1150	2.4	3.15×10^{-8}	Fe	2570	5.3	5.69×10^{-10}
He	16660	34.7	7.93×10^{-9}	Ni	2740	5.6	5.41×10^{-10}
B	1950	4.1	2.94×10^{-9}	Cu	1890	4.0	5.00×10^{-10}
C	4098	8.5	2.65×10^{-9}	Zn	1600	3.5	4.84×10^{-10}
O	2050	4.3	1.99×10^{-9}	Nb	3410	7.1	3.42×10^{-10}
Na	1590	3.3	1.38×10^{-9}	Mo	3960	8.2	3.31×10^{-10}
Mg	1370	2.9	1.31×10^{-9}	Ag	1750	3.6	2.94×10^{-10}
P	1150	2.4	1.025×10^{-9}	Cd	1150	2.4	2.83×10^{-10}
Ar	1230	2.6	7.95×10^{-10}	Sn	870	1.8	2.68×10^{-10}
V	2590	5.4	6.23×10^{-10}	Xe	2840	5.9	2.42×10^{-10}
Cr	3950	8.2	6.11×10^{-10}	Pb	965	2.0	1.53×10^{-10}

Arrhenius type equations for the temperature dependence of diffusion have been derived by other authors. Frenkel [133], derived a formula for the diffusion coefficient:

$$D = \frac{\delta^2}{6\tau} \exp\left(-\frac{Q}{RT}\right) \qquad (2.24)$$

where, δ = mean distance of jump ≃ distance between neighbouring atoms,

τ = mean duration of oscillation of an atom,

Q = activation energy of transition from one equilibrium position to another,

T = absolute temperature.

Polanyi and Wigner [134] suggested a somewhat different formula for the temperature dependence of the diffusion coefficient in crystalline solids. The characteristic feature of their formula is that the pre-exponential factor D_o depends on the temperature and also the activation energy. The formula of Polanyi and Wigner is:

$$D = \frac{2\delta^2 \nu Q}{RT} \exp\left(-\frac{Q}{RT}\right) \qquad (2.25)$$

where, δ = distance between neighbouring atoms,

ν = maximum frequency of oscillation of atoms.

At low temperatures the above formula approximates to:

$$D = \frac{2Q\delta^2}{N_A h} \exp\left(-\frac{Q}{RT}\right) \qquad (2.26)$$

where, N_A = Avogadro constant

h = Planck constant

By analysing the experimental data on lead, gold and copper, Bugakov [102], has shown a relationship between the diffusion coefficient, temperature, the self-diffusion coefficient at the melting point and the melting point. Bugakov's formula is somewhat similar to Wach's equation (2.23), and is given as:

$$D = D_s \exp\left(-\frac{Q}{R}\left(\frac{1}{T} - \frac{1}{T_s}\right)\right) \qquad (2.27)$$

where, D_s = self diffusion coefficient at the melting point,

T_s = melting point,

Q = activation energy,

R = gas constant,

T = absolute temperature.

In the above formula, Bugakov assumes the self-diffusion coefficient at the melting point is a constant.

2.3.5 Driving force for diffusion:

In the original formulation of Fick's laws it is assumed that diffusion takes place down a concentration gradient. This is certainly true in cases where the equilibrium state is a single phase, as in most cases in practice. The diffusion of atoms takes place in order to lower the free energy of the system. The true driving force for diffusion is the chemical potential of the diffusing species. At equilibrium the chemical potential of the particular species is the same throughout the system, or in other words, the change in chemical potential at equilibrium is zero. Thus it is more logical to write diffusion equations in terms of chemical potentials rather than compositions, based on the assumption that diffusion occurs down the chemical potential gradient.

Darken [49] developed a phenomenological theory of diffusion based on the above assumption. A more general phenomenological theory has been given by Bardeen and Herring [144,145] and this has the advantage of being readily applied to an assembly of a multiple of components. Their theories have been developed as given below. The diffusion current of a species is directly proportional to the number of atoms per unit volume and also to the chemical potential gradient. Thus it can be mathematically stated as:

$$T_i = - c_i M_i \frac{\partial \mu_i}{\partial x} \qquad (2.28)$$

where, T_i = diffusion current,

c_i = number of i atoms per unit volume,

μ_i = chemical potential of the ith component per atom,

M_i = proportionality constant termed the mobility of the component i .

This equation gives the diffusion current in terms of a diffusion "force" $\frac{\partial \mu_i}{\partial x}$ on the atom.

However, the flux of i atoms, although mainly dependent on the chemical potential μ_i of the i component, may also be influenced by the gradients of the chemical potentials of other components and of the vacancies if present. A more general expression has also been derived by the authors [144,145] taking into consideration the influence of the chemical potentials of the other components and vacancies.

For a binary alloy of A and B the above authors have derived an equation for the diffusion coefficients of A and B. For A, the diffusion coefficient D_A is given as:

$$D_A = \frac{\partial \mu_A}{\partial \ln c_A} \cdot M_A \qquad (2.29)$$

and for B,

$$D_B = \frac{\partial \mu_B}{\partial \ln c_B} \cdot M_B \qquad (2.30)$$

In the above equations, M_A and M_B are the mobility of A and B

in the alloy respectively. It can be seen from the above two equations that D_A and D_B differ only due to the mobility terms, since the other atoms are equal according to the Gibbs-Duhem equations:

$$\frac{\partial \mu_A}{\partial \ln c_A} = \frac{\partial \mu_B}{\partial \ln c_B} \qquad (2.31)$$

2.4 THERMODYNAMICS OF SOLUTIONS

In a binary solution of A and B , if the forces of attraction between like atoms and unlike atoms are the same, the solution will then behave ideally and obey Raoult's law. In such cases the heat of mixing ΔH_m is zero. In reality most of solid solutions do not behave according to Raoult's law and have either a positive or a negative deviation from it. When the force of attraction between A-A or B-B atoms is greater than that of A-B atoms, there will be a positive deviation and a positive heat of mixing(endothermic reaction). If the force of attraction between A-B atoms is greater than A-A or B-B, a negative deviation from Raoults law and a negative heat of mixing will occur. When there is a negative heat of mixing, generally intermediate compounds are formed.

The chemical potential of an ideal solution can be written as:

$$\mu_A - \mu_A^{\ominus} = RT \ln N_A \qquad (2.32)$$

and

$$\mu_B - \mu_B^{\ominus} = RT \ln N_B \qquad (2.33)$$

Guggenheim [146], Wach [137] and other workers use a function called the absolute activity λ, which is related to the chemical potential by the equation:

$$\mu_A = RT \ln \lambda_A \qquad (2.34)$$

In terms of these absolute activities, equations(2.32) and (2.33) become:

$$\lambda_A / \lambda_A^{\theta} = N_A \qquad (2.35)$$

and

$$\lambda_B / \lambda_B^{\theta} = N_B \qquad (2.36)$$

Wach [56,137] gives an expression for the absolute chemical potential of a solution as:

$$\mu = R\theta \ln(D_c^{\frac{1}{2}} / D_\theta^{\frac{1}{2}} C_\theta) \qquad (2.37)$$

For a non-ideal solution, equation (2.35) and (2.36) can be written[147] as:

$$\lambda_A / \lambda_A^{\theta} = \gamma_A N_A \qquad (2.38)$$

and

$$\lambda_B / \lambda_B^{\theta} = \gamma_B N_B \qquad (2.39)$$

where, γ_A and γ_B are activity coefficients of A and B respectively.

An alternative way of measuring the deviations from "ideal" behaviour is in terms of the "excess" thermodynamic functions. The excess free enthalpy, excess heat of mixing and the excess entropy are related by the equation:

$$\Delta G_{xs} = \Delta H_{xs} - T \Delta S_{xs} \qquad (2.40)$$

For very dilute solutions the excess heat of mixing (heat of mixing in an ideal solution is zero) and excess entropy of mixing can be obtained from solubility data using the equation [146] (2.41):

$$\ln N = \frac{\Delta S_{xs}}{R} - \frac{\Delta H_{xs}}{RT} \qquad (2.41)$$

From a plot of ln N, the mole fraction of the solute, versus 1/T, the excess heat and entropy of mixing can be obtained from the slope and the intercept with the ln N axis respectively. Thus from the plot some knowledge of the interaction forces of the A-A or B-B and A-B atoms can be obtained.

2.5 INTERMEDIATE PHASES IN METALLIC SYSTEMS

Interdiffusion of two metals may result in the formation of intermediate phases in the diffusion zone. Often the configuration which has the minimum free enthalpy after mixing does not have the same crystal structure as either of the pure components. In such cases intermediate phases are formed. These are usually stoichiometric compounds. The volume per atom in some intermediate phases is less

than that in pure metals. Hence the intermediate phases formed as a result of interdiffusion are under tensile stress, eg. Copper-Zinc [58] and Iron-Aluminium[59]. The tensile stress may lead to the formation of cracks finally resulting in failure of components.

In the lead-tin or tin plated copper system, (as in some bearing materials), intermediate phases formed have been identified as Cu_6Sn_5 and Cu_3Sn by Creydt [60], and by others [61]. The tin rich, light coloured sompound Cu_6Sn_5, is formed first at the interface, and with time transforms into the copper rich darker compound Cu_3Sn. Tin reacts with other metals such as silver, nickel, cobalt and iron to form intermetallic compounds. With silver, tin forms Ag_3Sn as a single layer [60]. Iron, cobalt and nickel have been used in the bearing industry as diffusion barriers placed between the overlay and the underlying copper based material. Cobalt forms $CoSn_2$ at 170^oC [64]. Nickel reacts with tin at temperatures of 100^oC, or even below, to form a predominantly plate-like phase of composition 86 $^w/o$ Sn - 14 $^w/o$ Ni corresponding to a compound $NiSn_3$, which transforms into a columnar form identified [63,64] as Ni_3Sn_4. Iron forms $FeSn_2$ with tin at temperatures above 170^oC [63].

The incidence of metastable structures which decompose on heating, in diffusion compounds is quite common. For example, the Fe-Sn couple has been reported [66] to form an intermetallic compound Fe_3Sn_2 at 300^oC which is thermodynamically not stable below 630^oC.

In the Pt-Mo couple a new η phase has been reported [67] containing about 35 ^{w}/o Pt. The compound NiSn formed on the Ni-Sn interface, decomposes on heat-treatment [68,69]. Another case is the formation of a solid solution of Mo and Ni on heat-treatment of the Ni_4Mo compound [70].

2.5.1 Nucleation

Nucleation of phases in metals and alloys is predominantly heterogeneous. Suitable nucleation sites are non-equilibrium defects such as excess vacancies, dislocations, grain boundaries, stacking faults, inclusions, and free surfaces, all of which increase the free enthalpy and hence the local activity of the material. If the creation of a nucleus results in the destruction of a defect some free enthalpy (ΔG_d) will be released, thus assisting the moving atoms to surmount the activation energy barrier. The free enthalpy change associated with the heterogeneous nucleation ΔG_{het} is given as:

$$\Delta G_{het} = - V(\Delta G_V - \Delta G_S) + A\gamma - \Delta G_d \qquad (2.42)$$

where, V = volume of the new phase at the nucleation site initially,

ΔG_V = volume free enthalpy associated with one unit of volume,

ΔG_S = change in strain energy associated with the change in volume,

A = interfacial area between the parent material and the new phase,

γ = free enthalpy per unit area of the interface.

Excess vacancies can assist nucleation by increasing diffusion rates or by relieving misfit strain energies, ie. reduction of ΔG_S. The vacancies may influence the nucleation individually or collectively by grouping into clusters.

If the concentrations of heterogeneous nucleation sites per unit volume is c_1, then the heterogeneous nucleation rate N_{het} will be given [45] by the following equation:

$$N_{het} = w\, c_1 \exp\left(-\frac{\Delta G_m}{kT}\right) \cdot \exp\left(-\frac{\Delta G^*}{kT}\right) \qquad (2.43)$$

where, N_{het} = heterogeneous nucleation rate; nuclei m^{-3} s^{-1}

w = a factor incorporating the vibrational frequency of the atoms, and the surface area of the critical nucleus,

ΔG_m = activation energy for atomic migration per atom,

k = Boltzmann's constant,

T = temperature; K

ΔG^* = activation energy for nucleation.

Although the growth of alloy layers has been studied quite extensively, relatively few have paid attention to the nucleation stage.

Barry and Phillips [81] have studied the nucleation stage of $FeSn_2$ in tin plated steel, and observed that initial nucleation of $FeSn_2$ takes place during the electroplating process itself even in acid electroplates. Castell-Evans [82] has investigated the nucleation of $FeSn_2$ alloy layer in tin plate, and attempted to modify the structure of the alloy layer to produce a compact and continuous structure for better corrosion resistance. Continuity of the alloy layer is a major factor in determining the corrosion behaviour [83,84], and the pattern of discontinuity has been reported [85,86] by isolating the alloy layers and examining them in the transmission electron microscope. The nucleation of the alloy layer in hot-dipped tin coatings is thought to take place in the zinc chloride flux layer by a reaction of the type [87]:

$$ZnCl_2 + Sn = Zn + SnCl_2 \qquad (2.44)$$

$$Fe + SnCl_2 = FeCl_2 + Sn \qquad (2.45)$$

$$2Sn + Fe = FeSn_2 \qquad (2.46)$$

2.5.2 Growth

The great majority of phase transformations in metals and alloys occurs by nucleation followed by growth of the new phase. An interface is created during the nucleation stage and then advances into the surrounding parent phase during the growth stage. The nucleation stage is very important and determines many features in the transformation. However, the bulk of the transformation product is formed in the growth stage by the transfer of atoms across the moving parent/product interface. There are two types of interface: glissile

and non-glissile. Glissile interfaces migrate by dislocation glide resulting in shearing of the parent lattice into the product. Non-glissile interfaces migrate by the more-or-less random jumps of individual atoms. The extra energy needed for the jumps is supplied by thermal activation. Hence, the migration of non-glissile interfaces is extremely sensitive to temperature. Most of the interfaces are non-glissile. Transformations produced by the migration of glissile interfaces are referred to as military transformations as opposed to civilian transformations produced by the migration of non-glissile interefaces. During a military transformation the nearest neighbours of any atom are essentially unchanged and as a result the parent and product must have the same composition, and no diffusion is involved in the transformation. During civilian transformations, the parent and product may or may not have the same composition. If there is no change in composition, the new phase will be able to grow as fast as the atoms cross the interface. Therefore, such transformations are interface controlled. When the parent and product have different composition the growth of the new phase will require long-range diffusion. If the interfacial reaction is faster, the rate at which the new phase can grow is governed by the rate at which lattice diffusion can remove the excess ahead of the interface. Hence, this type of transformation is diffusion controlled. However, if the interface reaction is slower the transformation will be interface-controlled. It is also possible that the rates of the interface reaction and the diffusion process are equal, in which case the

transformation will be under mixed-control.

The laws governing the mass transport by diffusion can not be directly applied in the case of reactive diffusion. But sometimes under certain conditions this law holds. Solution of Fick's law gives a parabolic growth relationship.

$$x^2 = kDt \qquad (2.47)$$

where, x = diffusion path (thickness of the compound being formed),

D = interdiffusion coefficient,

t = time,

k = proportionality constant.

The parabolic law is the most important rate law for high temperature heterogeneous reactions in which a reaction product separates the reactants, and where mass transport takes place by diffusion through the product. The growth reactions are stated in terms of rate coefficients. The term "rate coefficient" is preferred to "rate constant" since the quantity for a given reaction is seldom constant[103]. Lustman & Mehl [88] and Van Horn [89] have suggested that the parabolic behaviour may best be established by plotting log x against log t so that the slope gives the power index of ½ as in equation (2.48).

$$\log x = \log kD + \frac{1}{n} \log t \qquad (2.48)$$

Van Horn [89] has examined the significance of small deviations from n = 2 in equation (2.48) and attributed them to structural factors

such as grain size. The above author recognises the variation of the power index as n = 1.7 for lattice diffusion, n = 2 for grain boundary and lattice diffusion in combination, and n>2 for grain boundary diffusion. There is also an implication of n < 1.7 when diffusion is only partially rate controlling. Van Horn concludes that a power law could be a general type of solution and a parabolic law (ie. n = 2) is merely a special case. The departure from n = 2 appears to take place when several diffusion mechanisms occur simultaneously, or where large volume changes influence transformation.

In single phase growth studies, the Grube solution (section 2.2.3(i)), has frequently been used. In the Fe-Cr system, the parabolic law has been well established [90]. A parabolic law has been found in the Al-Zn system, when intermetallic compounds form to a limited extent [91]. In the Fe-Zn system also a similar relationship has been observed [92,102]. Bugakov [102] has observed parabolic growth in the Cu-Zn system. Peterson and Ogilvie [92] have established a parabolic law in the U-Nb system.

Gabe attributes the deviations from the parabolic behaviour to:

(i) formation of intermetallic compounds in diffusion layer;

(ii) formation of compounds between the coating metal and substrate impurities;

(iii) the presence of a second phase in the substrate which may affect the diffusion interface structure;

(iv) exhaustion of one of the diffusion couple metals.

Some deviation from the parabolic growth law has been observed in many systems which form intermediate intermetallic compounds; eg. Al-Nb [94], Al-Zn [95], Fe-Zn [96,97].

For the case of multiphase systems Kirkaldy [98,99] and Rodigin [100] have both used the Grube solution. By relating each layer as a part of two binary diffusion couples, the authors have independently deduced the overall diffusion laws for the whole system. In radioactive tracer techniques, Pawel and Lundy [101] have used an extension of the Grube's solution. For a thin coating of thickness h the solution is given by:

$$a_{x,t} = \frac{a_o}{2}\left(\text{erf} \frac{h-x}{2\sqrt{Dt}} + \text{erf} \frac{h+x}{2\sqrt{Dt}} \right) \qquad (2.49)$$

where, $a_{x,t}$ = the activity at x at time t;

a_o = the activity at x at t = 0

The rate of formation of a compound by diffusion, called rational rate coefficient by Wagner [104], has been shown to be equal to the product of concentration and the diffusivity of the diffusant by Wach [103]. Wach has used Fick's first law under the boundary conditions, the concentration gradient is constant and the concentration varies from c = 0 at $x = x_1$, to $c = c_1$ at $x = x_2$ to obtain the relationship (2.11) as stated in section (2.2.3)

$$k_r = D_i c_i = D_i \rho w_i \qquad (2.11)$$

For the same boundary conditions, the above author has also shown that Pilling and Bedworth [105] parabolic rate coefficient k_p, is related to the diffusivity and the concentration as in equation (2.12) (section 2.2.3).

2.5.2.1 Growth kinetics of intermetallic phases of Cu-Sn and Ni-Sn

Tu and Thompson [80] have found in experiments with thin films of Cu and Sn at temperatures ranging from 115°C to 150°C, that the growth of Cu_6Sn_5 showed a linear rate, and the rate of consumption of the Cu_6Sn_5 due to the formation of Cu_3Sn showed a parabolic rate with an activation energy of 96.5 kJ mol^{-1}. They have also observed that Cu atoms were the dominant diffusing species in the growth of Cu_6Sn_5 between Cu and Sn films at room temperature, and have estimated that the minimum interdiffusion coefficient to be $1.5 \times 10^{-20} m^2 s^{-1}$.

Kang and Ramachandran [150] have studied the growth kinetics of intermetallic phases at the liquid Sn and solid Ni interface, and conclude that the rate determining step in the diffusion process is the diffusion of Ni in the liquid Sn. The authors also confirm a parabolic growth rate for the initial and final stages and a very slow intermediate stage for the Ni-Sn interdiffusion in a temperature range of 300-520°C. They found Q_D = 15 kJ mol^{-1}.

Kay and Mackay [63] have measured the rate of growth of the total compound (Cu_6Sn_5 + Cu_3Sn) at room temperature and found that the growth was parabolic. Kay and Mackay [64] have also examined the effect of the substrate on the rate of growth of intermetallic compounds. The authors state that at any temperature, coatings of the same composition on the various substrates, the growth rate of

the total compound layer will be highest in silver, followed by copper and then brass. The authors also state that at room temperature, except for 10 ^{w}/o Pb-Sn coating, the hard copper basis metal always gives a faster growth rate than does the soft copper basis metal. However, at 170^{o}C the two materials give very similar values. The authors also claim that the effect of different coating compositions also depends upon temperature. However, from their Arrhenius plots [63] for total intermetallic and Cu_3Sn grown from coatings of different compositions of Sn and Pb, it is seen that the composition of Sn in the overlay hardly affects the growth rate of the Cu-Sn compounds. The experiments have been carried out with lead-tin coatings of compositions 40, 60, 90 and 100 ^{w}/o of Sn. The condition of the electroplated coating also has an effect on the growth rate.

The activation energies calculated by the above authors [63,64] for the copper-tin system are around 39 kJ mol^{-1}, and for the nickel-tin system 37 kJ mol^{-1}. The values of activation energies for the formation of Cu_6Sn_5 and Cu_3Sn evaluated from the inter-diffusion values given by Smithells [139] are 127 and 130 kJ mol^{-1} respectively.

2.5.3 Factors affecting the formation of intermetallic compounds

Daniels [108] suggests a criterion of band formation between coating and the substrate and considers that if a liquid coating metal wets the substrate, a solid solution alloy or intermetallic compound must form and the coating becomes satisfactorily bonded to the substrate. In cases where a liquid metal does not wet the substrate

(eg. lead on steel), the presence of small amounts of a third metal may enable an intermediate, coherent compound, to form. The behaviour of Ni, Sn or Zn in molten Pb can serve as appropriate examples. A fluxing process, prior to hot dipping and soldering, may have two functions in promoting bonding. The flux may remove oxides, greases, etc., from the surface by chemical reaction or surface tension effects, or it may initiate nucleation by forming an intermediate compound prior to the actual coating process.

The formation of solid solution alloys between a coating and a substrate is thought to have a dependence on the relative atomic sizes of the two metal atoms. Gorbunov [109] considers the size difference of 15-16% may not be exceeded if a solid solution is formed. Data presented by Drewitt[110] for metal coatings on iron supports this view.

The bond between an electrodeposited coating and a substrate may be attributed to electrostatic cohesion forces between atoms. Some evidence has been reported for the existence of an intermediate layer or phase shortly after electrodeposition of tin on iron [107,111].

Three aspects of intermetallic compound formation can be recognised:

(i) nucleation of the compound;

(ii) topography of growth;

(iii) thermodynamics of formation.

For an intermetallic compound to nucleate in the parent phase, the atoms which predominate the intermetallic compound must be transferred to the site by a diffusion process. In a hot dipping process the nucleation must occur on the solid substrate surface and there is evidence that the diffusion of the coating metal through the alloy layer is the rate-controlling process [112,113]. In Cu-Sn system the diffusion of Cu through the alloy layer appears to be rate-controlling [80]. However, the steel substrate in the Al-Fe and Fe-Sn systems can provide nuclei for the solid state process. Cold work, which should increase the density of the surface defects may promote alloy formation.

The topography of the surface of the substrate can influence the alloy growth [82]. There is also evidence that surface pretreatments can alter the form of individual alloy crystallites [83]. Buck and Leidheiser [114] have shown that $FeSn_2$ can be nucleated during plating Sn from alkaline electrolytes. Barry and Phillips [81] observed that nucleation of $FeSn_2$ occurred during plating of Sn or steel from acid electrolytes.

The free enthalpies and the heats of formation at the temperature concerned are the thermodynamic factors relevant in the formation of intermetallic compounds. From the principles of the equilibrium diagrams it is understood that the free enthalpies of the compounds must be favourable. If more than one compound can form, the one with the highest heat of formation can form in preference to the others [87]. If all the compounds have similar heats of formation,

then the thermodynamic factor may be unimportant.

2.5.4 Control of the thickness of the diffusion layer

Formation of diffusion compounds in diffusion coatings in some industrial applications is not desired but unavoidable. In certain cases however, compound formation to a certain limit is preferred [135], as in soldered copper joints, from the point of view of stronger adhesion of the coating to the substrate. In Pb-Sn overlay bearings, the compound formation can cause premature failure, especially when the service temperatures are high (above 100°C) and the lubricants are contaminated with weak organic acids resulting from the break-down of the lubricant itself and the fuel [7]. In printed circuit boards, formation of the intermetallic compounds with tin and copper, makes the tin (or lead-tin) surface less solderable [8].

Three basic mechanisms can be recognised in the control of alloy growth. Controlling the nucleation stage has received little attention. The energy for nucleation may be either described in thermodynamic terms (see section 2.5.1) or in terms of the enthalpy of intermetallic compound formation, which corresponds to the chemical reaction involved [71]. If several compounds form, those having the highest negative heat of formation may be expected to form preferentially. Thirdly, the factor becoming increasingly important is the topography and the orientation of growth, while nucleation will affect the number of growth sites, the relative rate of growth of each nucleus will depend upon crystallographic and orientation factors as they affect diffusion.

For example, in the Al-Fe system, where Fe_2Al_5 is the predominant intermetallic phase, very rapid growth at the Fe/Fe_2Al_5 interface with preferred orientation in the intermetallic layer (epitaxy with c axis normal to the interface plane) has been observed [72]. This effect is primarily due to the defective structure, and is also found in $MoBe_{22}$ which is thought to be cubic [71]. In the Ni-Al system, aluminium atoms have a higher diffusivity, probably due to deficit of Al in δ-Ni_2Al_3. Likewise, nickel atoms have a higher diffusivity in β-NiAl. This results in the initial predominance of Ni_2Al_3 phase which is later transformed to NiAl [71].

In practice, two categories of controlling attempts of alloy growth can be distinguished:

(i) solid solution alloying within the diffusion alloy layer, with the new element inhibiting atomic diffusion processes;

(ii) imposing barrier layers at the interface of the main diffusion couple.

As an example of the first method, it is a well known practice to add up to 0.25 ^{w}/o Al to zinc galvanising baths [72,73], and up to 8 ^{w}/o Si to hot-dip aluminising baths [74,75]. Aluminium appears to promote formation of a ternary Al-Fe-Zn compound which restrains attack on the iron substrate, while silicon is thought to occupy the vacant lattice sites in Fe_2Al_5 thereby minimising the ability of aluminium to diffuse and to promote the growth of $FeAl_2$ and $FeAl_3$ preferentially in the intermediate layers [71].

In cases where preferential diffusion takes place along grain boundaries, as has been reported in systems Nb-Ta [76] and Cr-Al [77], poisoning the diffusion paths by the use of precipitates suggests itself as an answer. Equally well, alloying elements may promote the diffusion process. An example is the case of using increased silicon contents in mild steel for hot-dip zinc galvanising, which probably stabilises the columnar non-coherent δ-phase [87].

The most common example of a diffusion barrier is an electrodeposit of nickel [7] between the copper and the lead-tin (or lead-indium) overlay. However, the formation of diffusion layers have not been completely arrested by these barriers [7,64]. It has been observed that the barrier layers react with tin in the overlay to form intermetallic compounds [64]. Nickel forms Ni_3Sn_4 and $NiSn_3$. A number of electrodeposited metals and alloys have been experimented as barriers in the copper-tin system [64], and none of them have proved successful in preventing the formation of intermetallic compound. However, Kay and Mackay [64], claim that the rate of growth of the iron-tin compound $FeSn_2$, with an interposed iron barrier between a copper-tin couple, was extremely slow at 170°C. Even at the end of the annealing period of 400 days the 5 μm thick barrier layer was not wholly consumed. Other barrier layers which these authors have studied were: tin-nickel alloy, speculum (Cu_6Sn_5), lead, silver, cobalt and iron-nickel alloy.

2.6 ELECTROPLATING PROCESSES IN THE PLAIN BEARING INDUSTRY.

Electroplates in the plain bearing industry are to be found in three main applications [78] :

(i) overlay plates;

(ii) as bonding layers and barrier layers, eg. copper and nickel plates on steel;

(iii) as protective and decorative plates as in tin plating of steel backed bearings.

The main electrodeposited overlays, as mentioned earlier, are lead-tin, lead-indium and lead-tin-copper alloys. Certain customary preferences have an effect on usage. For example, lead-tin-copper overlays are widely used in the USA. Lead-tin overlays are more popular among the engine builders in the UK, and are normally produced by co-deposition from fluoborate solution. The composition of a typical bath for plating overlays to contain 10 $^{w}/_{o}$ tin is given in Table 3.

TABLE 3. Composition of a fluoborate bath for Pb-10 $^{w}/_{o}$ Sn Plating[115]

Substance	Concentration/g dm^{-3}
Pb^{2+}(as basic lead carbonate)	200
Sn^{2+}(as $SnCl_2$)	20
free fluoboric acid (HBF_4)	50
boric acid (H_3BO_4)	25
gelatine	0.5

The deposition is usually performed at room temperature. As mentioned earlier (see section 2.2), the tin content of the as-plated lead-tin overlay is expected to be around 10 $^{w}/_{o}$. The Sn content in the alloy can be increased by increasing the relative tin content of the bath, by increasing the amount of the addition agent (gelatine or bone glue), or by increasing the current density [79] . The usual current density employed is in the range 1 - 10 A dm^{-2} .

2.6.1 Electrodeposition of alloys

Electrodeposition of alloy layers as barriers against diffusion has received little attention. Speculum (Cu_6Sn_5) and Ni-Fe alloys have been tested as barriers by Kay and Mackay [64] . Although the two alloys mentioned by the authors had shown good results as barriers, it is the author's experience that some of the alloys mentioned later are more efficient barriers than pure metals. Therefore, it is thought important to discuss some of the general principles and recent work published on alloy electrodeposition.

Brenner [115] describes five types of alloy plating:

(i) regular codeposition;

(ii) irregular codeposition;

(iii) equilibrium codeposition;

(iv) anomalous codeposition;

(v) induced codeposition.

(i) Regular Codeposition

This is a diffusion controlled mechanism and the effects of the plating variables on the composition of the deposited alloy are determined by the changes in concentrations of metal ions in the cathode diffusion layer. Thus the percentage of the more noble metal in the deposit is increased by processes which increase the metal ion concentration of the more noble metal in the cathode diffusion layer. Hence, increase in total metal content of the bath, decrease of current density, elevation of bath temperature and increased agitation of the bath, can increase the percentage of the more noble metal in the deposit. It is most likely to occur in baths in which the equilibrium potentials are far apart and with metals that do not form solid solutions.

(ii) Irregular Codeposition

In irregular codeposition as opposed to regular codeposition, the process does not depend totally on diffusion phenomena. The effects of plating variables on the composition of the deposit are much smaller than with regular alloy plating systems. This is most likely to occur in systems where the equilibrium potentials are closer to each other, and also with metals which form solid solutions.

(iii) Equilibrium Codeposition

Equilibrium codeposition occurs in solutions which are in chemical equilibrium with both of the parent metals. The ratio of the metals deposited is same as that of the metal ions in the plating solution, at low current densities. Copper-bismuth and lead-tin alloys deposited from acid baths are examples of this category.

(iv) Anomalous Codeposition

In anomalous codeposition, the less noble metal is deposited in preference to the more noble one. In a given plating bath, this type of codeposition occurs only under certain conditions of concentration and operating variables. This is a rare type of codeposition, but occurs frequently in association with the three metals in the iron group.

(v) Induced Codeposition

This type occurs in the deposition of metals such as molybdenum, tungsten and germanium, which cannot be deposited alone, without an inducing metal such as iron, nickel and cobalt. The effects of the plating variables on the composition of the deposit are not predictable and do not obey an established rule.

2.6.1.1 Electrodeposition of Lead-Tin Alloys

Lead-tin alloys are among the small number of electrodeposited alloys of commercial interest. They are used as corrosion resistant, protective coatings on steel, as a surface layer on bearings, solderable coatings on copper in printed circuits in electronic equipment. Electrodeposition of lead-tin is also made use of in the reclamation of the alloy from scrap metals in the form of solder.

The alloy is commercially electrodeposited in a fluoborate bath containing the two metal ions in the ratio of the metals in the desired composition. The common plating systems used in industry belong to the regular type with tin as the less noble metal.

Concentrated solutions of lead and tin fluoborates are available commercially. The compositions of baths for depositing the different types of alloys are listed in Table 4. The data were obtained from Brenner [115], based on data from Carlson and Kane [116].

About 25 g dm^{-3} of boric acid is necessary in the bath to prevent hydrolysis of fluoborate. If the fluoborate hydrolyses, hydrofluoric acid or fluorides are formed and lead fluoride precipitates. Free fluoboric acid improves the stability of the bath by preventing hydrolysis, particularly of stannous fluoborate. Addition agents such as glue are made to the bath, since without them smooth, adherent deposits are not obtained. The addition agents also influence the tin content of the deposit (Figure 5b), and improve the throwing power of the bath. Glue is the most common addition agent in the industry. A number of others have been suggested: resorcinol [117], nicotine and beta-napthol [118], derivatives of monohydroxy biphenyls [119] and dihydroxy phenylmethane [120]. Glue is gradually used up during operation of the bath, through inclusion in the deposit, precipitation or decomposition. Usually, glue is added daily to the operating bath in small quantities to compensate for the loss. Du Rose and Hutchinson [79] noted that a bath containing glue or resorcinal deteriorated on standing. International Tin Research Institute [136] recommends a current density of 3A dm^{-2} for still vat plating, and for barrel plating with rotating anodes or solution movement a higher current density of 6A dm^{-2}. The anodes used are usually a lead-tin alloy of the same composition as the deposited alloy. The temperature of the bath is maintained between 25 - 30°C.

TABLE 4. Composition of Fluoborate Baths for Electroplating Lead-Tin alloys of various compositions. (After Brenner Ref 115).

Tin content of deposit	Composition of bath							
	Tin content			Lead content		Total metal	Sn	Glue
%	Total g/liter	Stannous g/liter	*M*/liter	g/liter	*M*/liter	*M*/liter	Sn + Pb Wt-%	g/liter
5	5	4	0.034	90	0.435	0.469	4.3	0.5
7	7	6	0.051	90	0.435	0.486	6.3	0.5
10	10	9	0.076	90	0.435	0.511	9.1	0.5
15	15	13	0.110	80	0.385	0.495	16	1.0
25	25	22	0.185	65	0.314	0.500	25	1.5
40	40	35	0.295	44	0.212	0.507	44	3.0
50	50	45	0.380	35	0.170	0.550	56	4.0
60	60	55	0.465	25	0.120	0.585	69	5.0

TABLE 5. Typical Baths for Electrodeposited Phosphorus Alloys containing Nickel or Cobalt. (After Brenner Ref 115)

Bath no.	Bath type	$NiSO_4 \cdot 6H_2O$		$NiCl_2 \cdot 6H_2O$		Metal added as phosphate[b] or phosphite[b]	H_3PO_4	
		M/liter	g/liter	*M*/liter	g/liter	*M*/liter	*M*/liter	g/liter
1	Ni	0.67	175	0.21	50	0.12	0.5	50
2	Ni	0.57	150	0.19	45	0.24	0.5	50
2A	Ni	0.57	150	0.21	50	—	—	200 ml
3	Ni	—	—	—	—	1.0	—	—
				$CoCl_2 \cdot 6H_2O$	$CoCl_2 \cdot 6H_2O$			
4	Co	—	—	0.88	210	0.12	0.5	50
5	Co	—	—	0.76	180	0.24	0.5	50
6	Co	—	—	—	—	1.0	—	—
7	Co	—	—	1.0	240	—	1 *M* HCOOH	45 g/liter

Bath no.	Bath type	H_3PO_2		Current density amp/dm^2	pH	Temp. °C	Cathode efficiency 75°C %	P in deposit %	Type of deposit
		M/liter	g/liter						
1	Ni	0.015	1.3	5-40	0.5-1	75-95	65	2-3	Dull, mat, strong
2	Ni	0.5[d]	40	5-40	0.5-1	75-95	50	12-15	Bright, strong, brittle
2A	Ni	0.5	40	30	—	90	12	12	Bright
3	Ni	2.0	160	5-40	0.5-1	75-95	—	—	Bright, strong, brittle
4	Co	0.02	2.0	5-40	0.5-1	75-95	90	1-2	Dull, mat, strong
5	Co	0.5	40	5-40	0.5-1	75-95	55	9-11	Bright, strong, brittle
6	Co	2.0	160	5-40	0.5-1	75-95	45	11-12	Bright, strong, brittle
7	Co	0.02	2.0	5-30	1.5-2	75-95	95	0.8-1.2	Dull, mat, strong, some ductility

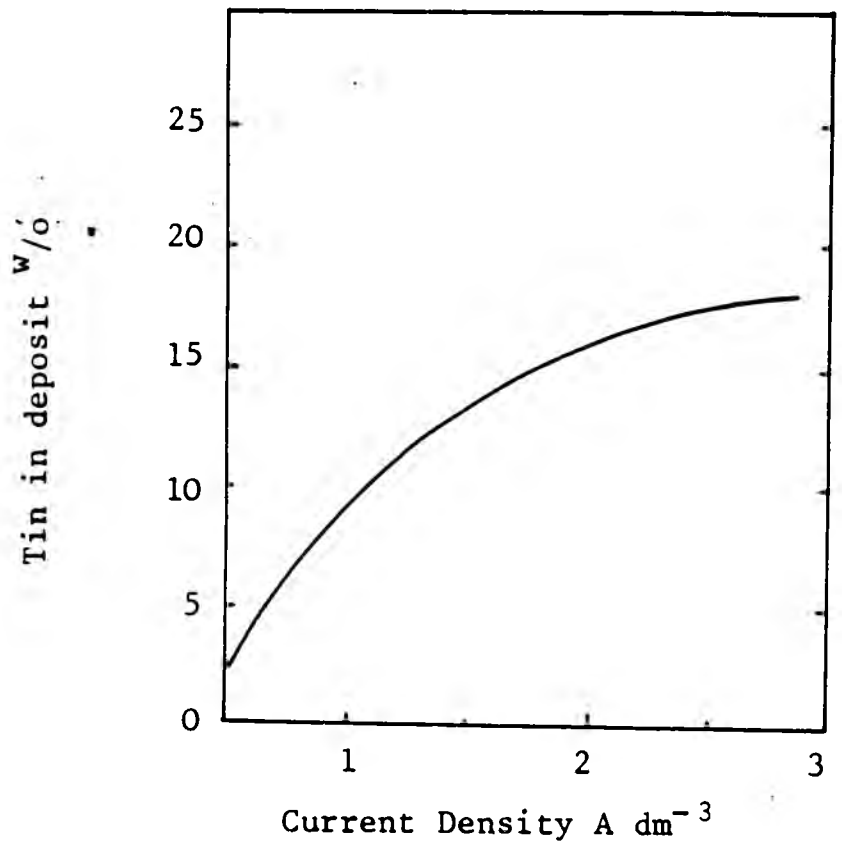

Figure 5a. Effect of current density on composition of electrodeposited Pb-Sn from fluoborate bath; metal content of bath 13 w/o Sn. (After Brenner Ref 115).

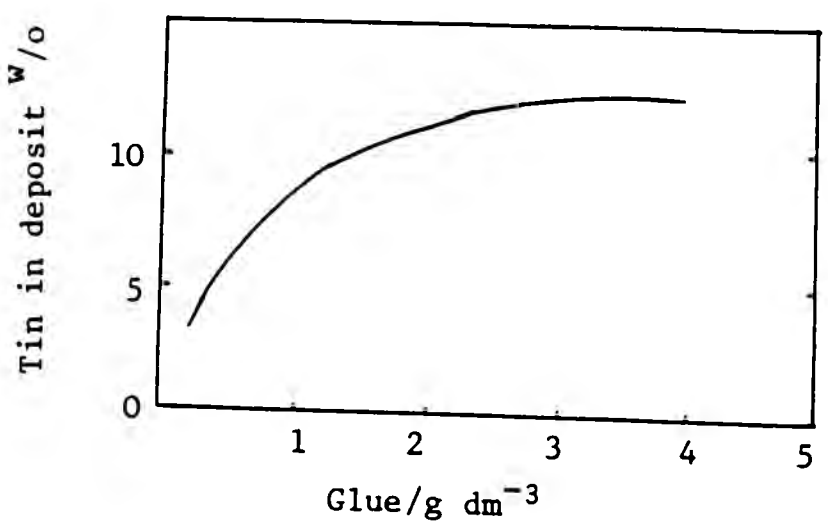

Figure 5b. Variation of tin content of electrodeposited lead-tin alloys with the content of glue in a fluoborate plating bath 10 w/o Sn, 175 g dm^{-3} total metal content, 2.5 A dm^{-2}. (After Brenner Ref 115).

As mentioned earlier, the composition of the deposit depends on the plating variables. Figure 5a, 5b, 5c and 5d show the effect of current density, glue content, tin content in the bath, and the total metal content in the bath, on the tin content of the deposit [115]. From the above plots, it is seen that the increase in current density, glue content and the tin content of the bath result in an increase in the tin content of the deposit.

2.6.1.2 Electrodeposition of Alloys Containing Phosphorus

Literature on the electrodeposition of alloys containing phosphorus is very scarce. Nickel and cobalt alloys containing phosphorus were first deposited by the electroless plating process developed by Brenner and Riddell [124]. An electrolytic process for the deposition of nickel and cobalt alloys containing phosphorus has also been developed by Brenner and co-workers [125]. The above workers obtained alloys containing as much as 15% of phosphorus from acid solutions containing phosphites. In addition to nickel and cobalt alloys with phosphorus, Brenner et al [125] have examined the influence of the presence of phosphites and hypophosphites in other electroplating baths. However, no interesting results have been obtained in these experiments. An alloy containing iron and a few percent of phosphorus has been obtained from a hot ferrous chloride solution containing phosphorous acid [115]. Brenner [115] states that the presence of phosphites in acid copper, acid zinc, cyanide silver, cyanide zinc, alkaline tin and ammoniacal cobalt-tungsten plating baths, did not have any effect on the appearance of deposits. In some instances it caused roughening of the deposits.

As mentioned earlier, the composition of the deposit depends on the plating variables. Figure 5a, 5b, 5c and 5d show the effect of current density, glue content, tin content in the bath, and the total metal content in the bath, on the tin content of the deposit [115]. From the above plots, it is seen that the increase in current density, glue content and the tin content of the bath result in an increase in the tin content of the deposit.

2.6.1.2 Electrodeposition of Alloys Containing Phosphorus

Literature on the electrodeposition of alloys containing phosphorus is very scarce. Nickel and cobalt alloys containing phosphorus were first deposited by the electroless plating process developed by Brenner and Riddell [124]. An electrolytic process for the deposition of nickel and cobalt alloys containing phosphorus has also been developed by Brenner and co-workers [125]. The above workers obtained alloys containing as much as 15% of phosphorus from acid solutions containing phosphites. In addition to nickel and cobalt alloys with phosphorus, Brenner et al [125] have examined the influence of the presence of phosphites and hypophosphites in other electroplating baths. However, no interesting results have been obtained in these experiments. An alloy containing iron and a few percent of phosphorus has been obtained from a hot ferrous chloride solution containing phosphorous acid [115]. Brenner [115] states that the presence of phosphites in acid copper, acid zinc, cyanide silver, cyanide zinc, alkaline tin and ammoniacal cobalt-tungsten plating baths, did not have any effect on the appearance of deposits. In some instances it caused roughening of the deposits.

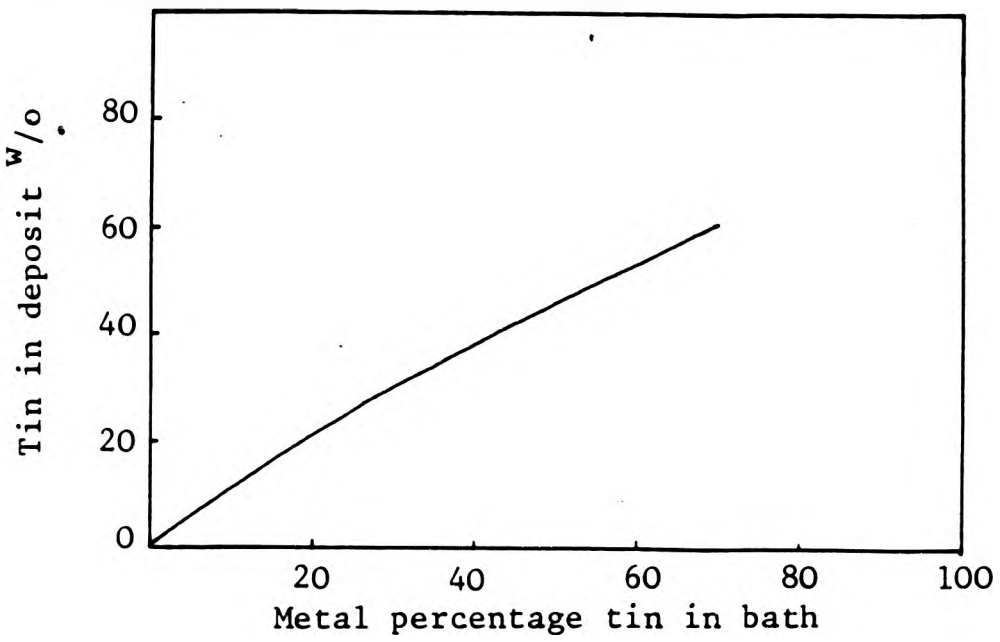

Figure 5c. Variation of tin content of electrodeposited lead-tin alloys with the tin percentage in the bath; fluoborate bath with total metal content 80-90 g dm^{-3} free fluoboric acid 40 g dm^{-3}, free boric acid 25 g dm^{-3}, glue 0.5 - 5 g dm^{-3}, current density 3.2 A dm^{-2}.
(After Brenner Ref 115)

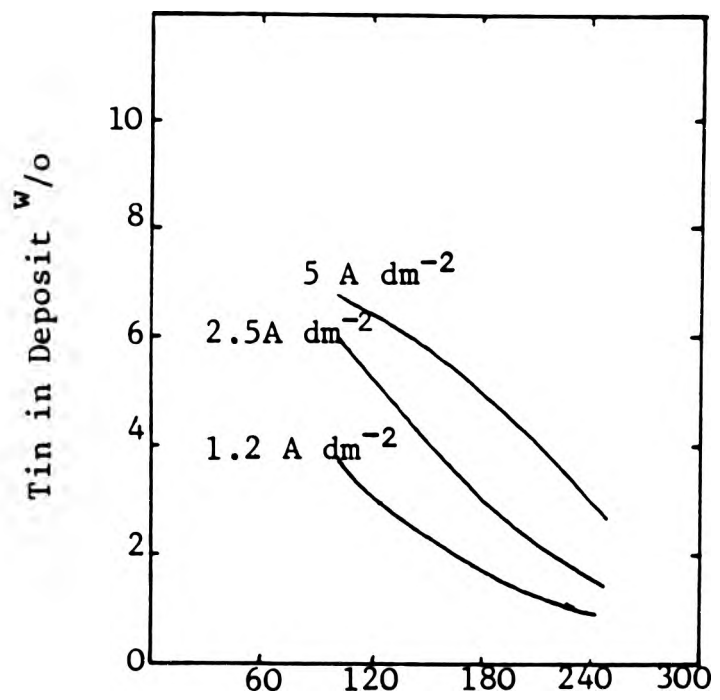

Figure 5d. Relation between tin content of the electrodeposited lead-tin alloys and total metal content in a fluoborate bath; deposition done at three current densities $60^{w}/o$ Sn in solution; 0.4 g dm^{-3} glue.
(After Brenner Ref 115)

Baths developed by Brenner et al [125] for depositing nickel and cobalt with phosphorus were ordinary nickel or cobalt acid sulphate and chloride baths to which phosphoric acid was added. Phosphorus acid, which is more expensive, has offered no advantage over phosphoric acid. Table 5 gives compositions and conditions for plating of different baths for depositing nickel and cobalt with phosphorus.

The inclusions of phosphorus in electrolytic copper deposits, obtained from pyrophosphate baths, has been reported by Sorkin et al [126] and Owen et al [127]. The mechanism of inclusion of phosphorus in copper deposits has not been studied. Furlani et al [128] refer to formation of phosphites at the cathode during electrodeposition. Sorkin et al [126] conclude that the main factors influencing the inclusion of phosphorus in the deposit are the electrodeposition potential and the pH of the electrolyte. The maximum phosphorus content is obtained at potentials between - 0.25 V and - 0.75 V and at pH values around 6. Brenner [115] has studied the effect of phosphorous acid and phosphoric acid content in the bath, and the current density of deposition, on the phosphorus content of the deposit of Ni-P and Co-P alloys. Figures 6a, 6b and 6c show that increasing the current density or the phosphoric acid concentration result in a decrease in phosphorus content in the deposit, and an increase in phosphorous acid content results in an increase in the phosphorus content in the deposit. The baths recommended by Brenner (Table 5) have pH values around 1.

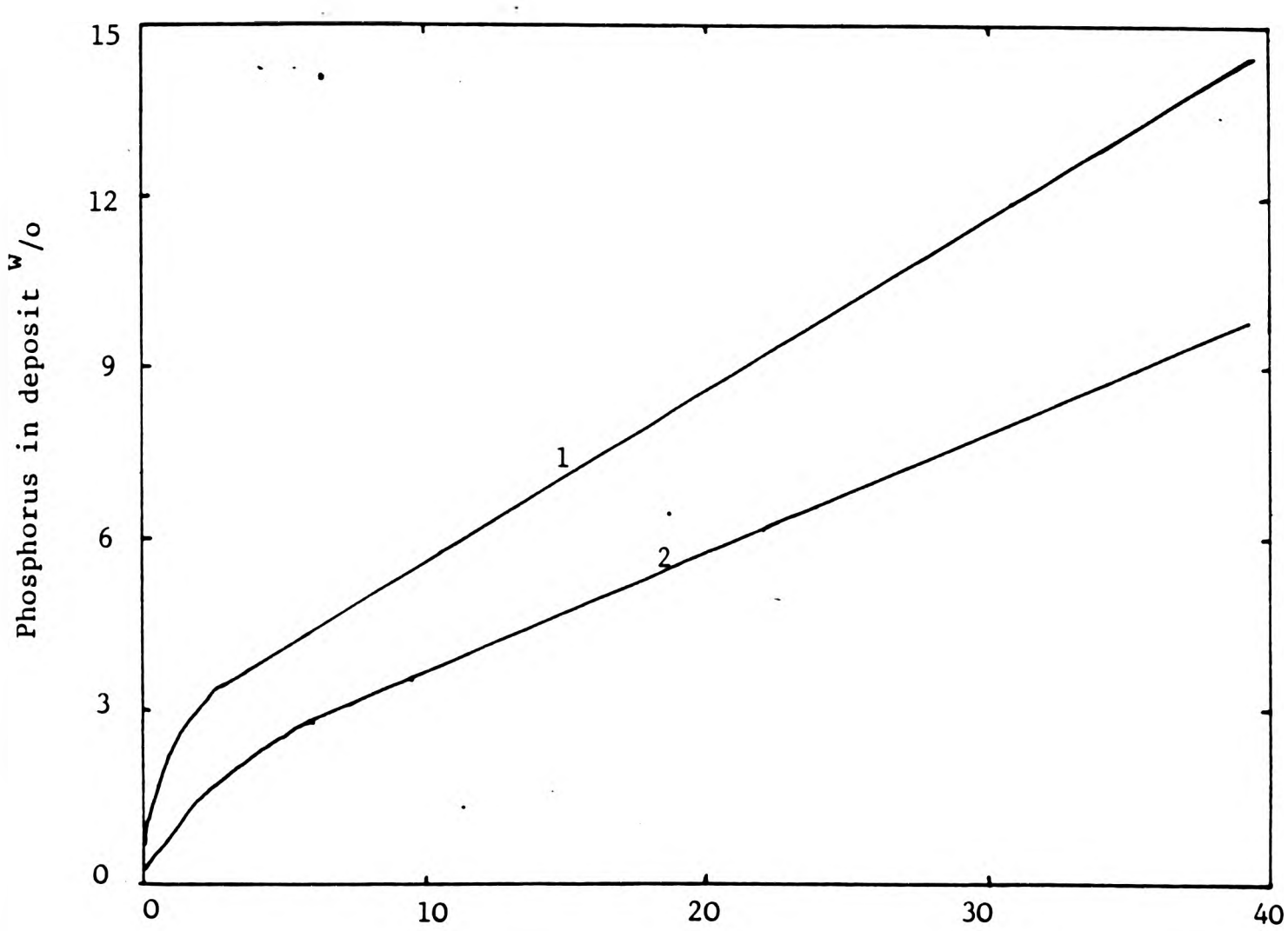

Figure 6a. Variation of the phosphorous content of electrodeposited nickel- and cobalt-phosphorus alloys with the phosphorus acid content of the bath.

Curve 1. Nickel-phosphorus alloys.
Curve 2. Cobalt-phosphorus alloys.

(After Brenner, Ref 115)

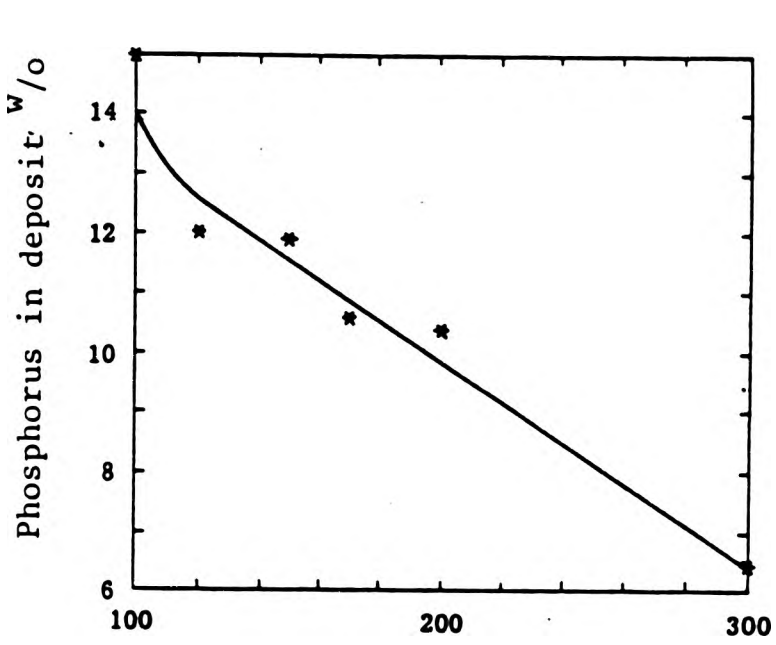

Concentration of Phosphoric acid in bath, ml dm^{-3}

Figure 6b. Variation of the phosphorus content of electrodeposited nickel-phosphorus alloys with the phosphoric acid content in the bath; current density 40 A dm^{-2}; temperature 90°C.
(After Brenner Ref 115)

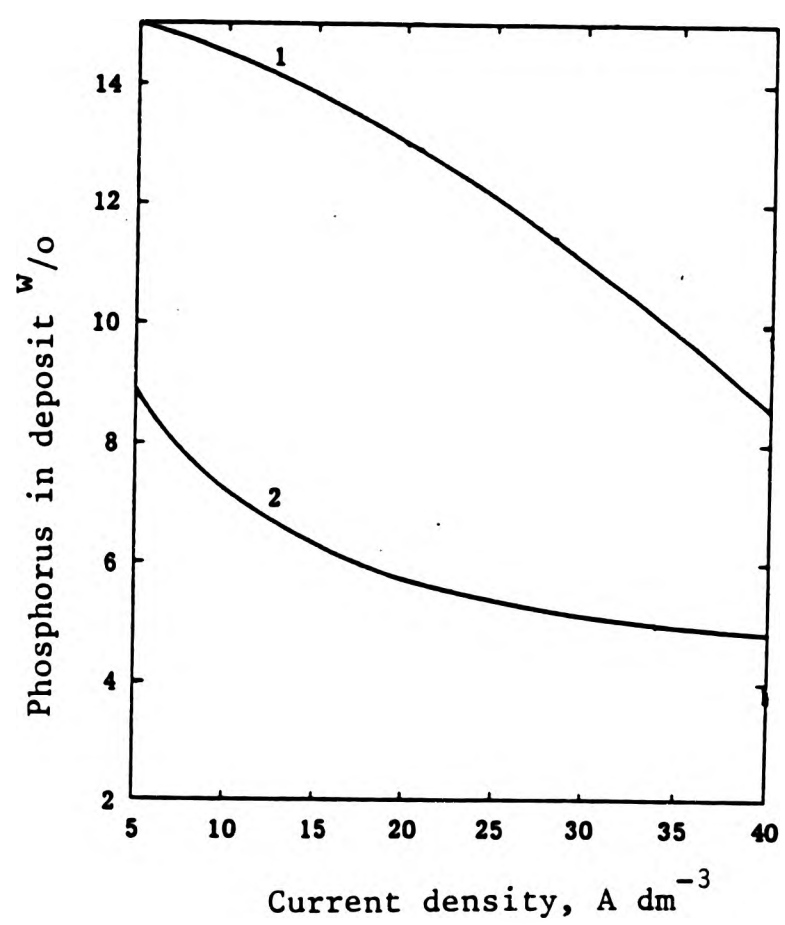

Figure 6c. Variation of the phosphorus content of electrodeposited nickel- and cobalt-phosphorus alloys with current density.

Curve 1. Ni-P alloy.
Curve 2. Co-P alloy.

(After Brenner Ref 115)

The influence of bath temperature on the deposits has also been studied by Brenner et al [125], who observed that higher operating temperatures gave better deposits.

3. LABORATORY EQUIPMENT AND EXPERIMENTAL PROCEDURE

3.1 INTRODUCTION

The different layers of a bearing material other than the overlay, which is generally electrodeposited, are usually cast one onto the other. In a patent granted to Glacier Metal Co [129], a method of casting continuous composite strips of bearing material is given. Molten metal is allowed to fall onto two rolling drums, which are cooled, in an inert gas atmosphere. The molten metal containers are arranged in such a way that three layers are cast on one another (Figure 7). The Pb-Sn overlay may also be cast, but the usual practice is electrodeposition.

Initially, three systems of samples of bearing material supplied by Shell Research Limited (Thornton Research Centre) were investigated. Their behaviour was studied during heat treatment in non-oxidising oils in the temperature range 100 - 160°C, over a period of time ranging from 20 to 220 days. It was observed that most of the diffusion processes had taken place during the initial 20 days. For that reason subsequent heat treatment experiments were of shorter duration, lasting from one to 20 days. The heat treated samples were mounted in a cold mounting resin, polished and examined metallographically. The thickness of the layers of compounds formed were measured under the optical microscope. These results were then used to evaluate the kinetics parameters of the diffusion processes involved in the compounds formation. Microprobe analyses were carried out on cross-sections to obtain depths of diffusion and concentration profiles of the different elements involved. X-ray

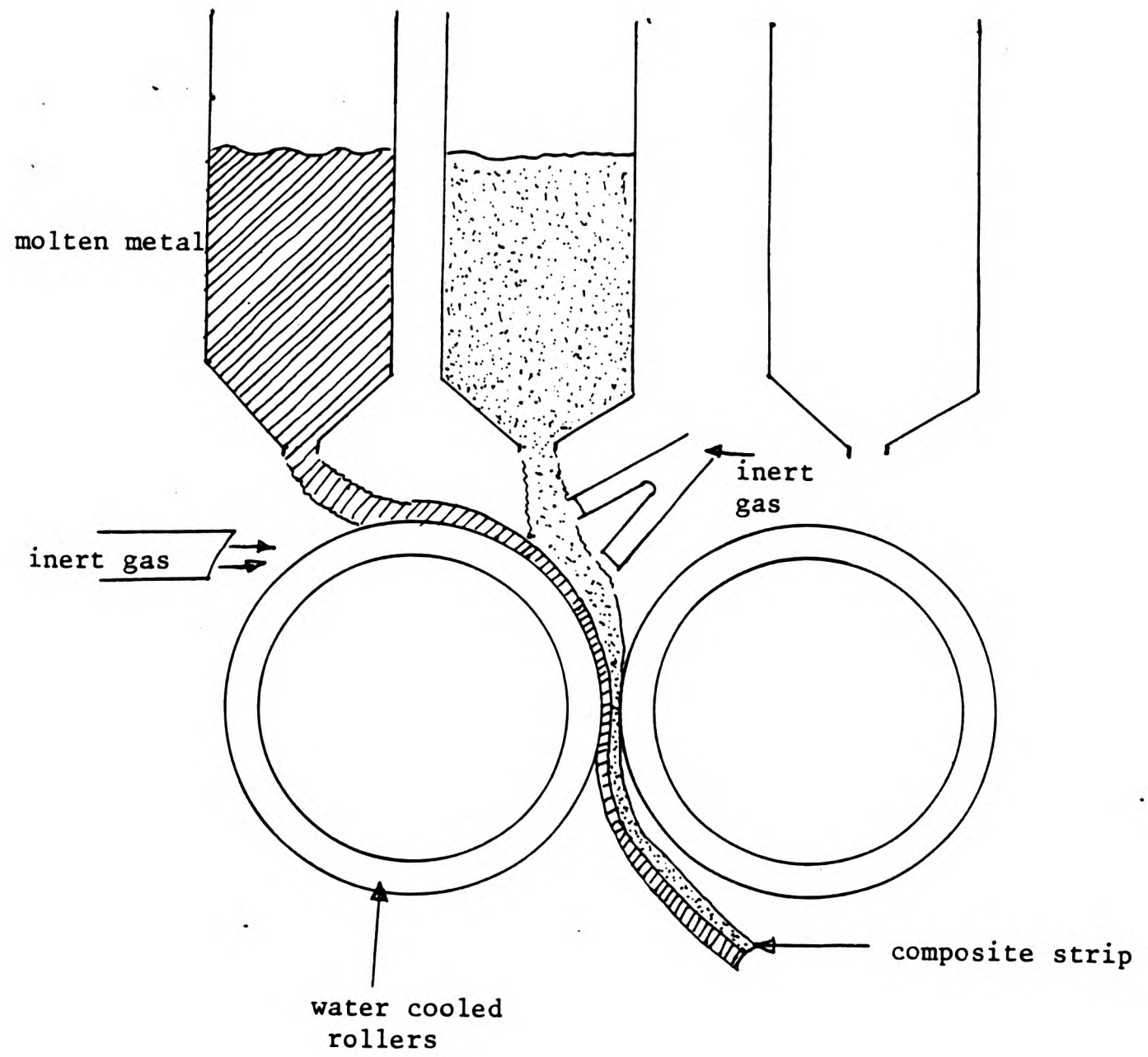

Figure 7. Arrangement for making a composite strip for bearing material. British Patent 1335961, 17.11.1970 Glacier Metal Co.[129] (a bimetal strip is shown)

diffraction methods were used to identify some of the compounds formed in the heat treatment operations.

Different barrier layers were plated on fresh samples and their behaviour, on heat treatment, was studied using optical methods and probe analysis.

One of the barriers tested was an electrodeposited alloy of copper and phosphorus which proved very successful as a barrier to diffusion and compound formation. A wet chemical analysis was carried out to estimate the content of phosphorus in the above barrier. Copper-boron was another diffusion barrier proved to be successful and attempts to estimate its boron content were not fruitful. Some conductivity measurements were taken on Cu-P and Cu-B plating solutions, in order to establish a mechanism of inclusion of phosphorus in the copper deposit.

Copper-phosphorus and copper-boron barriers were further tested at higher temperatures and longer exposure times. The techniques of depositing Cu-P and Cu-B barrier layers have now been patented. A mechanism of phosphorus and boron preventing formation of intermetallic compounds of Cu and Sn is discussed.

3.2 METALLOGRAPHIC TECHNIQUE

Three systems of bearing material, all provided with a Pb-Sn electrodeposited overlay, were investigated originally. The three systems are:

(i) Pb-Sn on Copper

(ii) Pb-Sn on Copper-Lead-Tin

(iii) Pb-Sn on Nickel on Copper

The samples were provided by the Thornton Research Centre, and had been supplied by a bearing manufacturer. Samples from the above three systems were cut into small parts of approximately 3 cm x 5 cm and heat treated in non-oxidising silicone oil in order to prevent corrosion of the Pb-Sn overlay during the heat treatment. The temperatures selected for heat treatment were 100, 115, 125, 135, 145, 160^{o}C over periods of 1, 2.5, 5, 10, 20, 60 and 90 days.

The oil baths used for heat treatment consisted of a large oil tank, the walls of which were made of insulating material, and 500 cm^3 glass beakers containing the silicone oil were dipped to about $\frac{3}{4}$ of their depth. The main tank was heated by a heating element on the side of its walls. Motor driven propellers in each beaker were used to keep the temperature fluctuation of the oil in the beakers to a minimum. By careful adjustment it was possible to reduce the fluctuation of the temperature to a $\pm 1^{o}$C. An independent propeller kept the oil in the tank circulating to have an even temperature at all depths. The set up is shown in Figure 8a.

The cut samples were arranged vertically along the side of the beakers with their overlay plated side facing the centre of the beakers. A separate beaker was chosen for each system of samples.

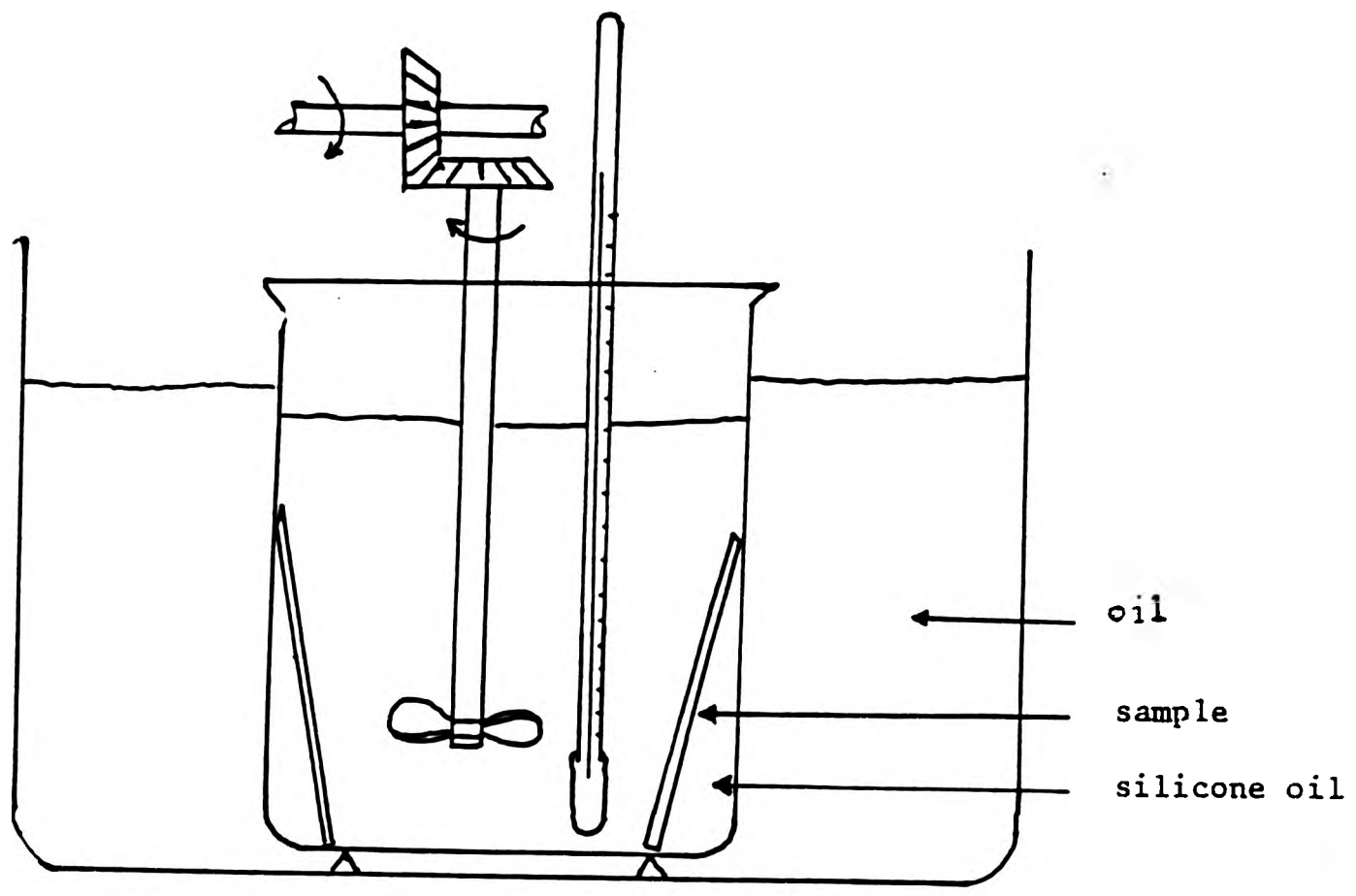

Figure 8a. Arrangement for annealing the specimens.

It was possible to take out samples from the oil filled beakers after the specific time, without disturbing the rest of the samples.

The heat treated samples were cut into mountable sizes and mounted in a clear cold mounting resin. The samples were mounted at an angle so that the measurement of the widths of diffusion layers was made easier. The actual widths measured ranged from 0.5 to about 1.0 μm; by mounting the samples obliquely it was possible to enlarge these widths about threefold.

A great deal of care had to be taken in polishing the samples. The soft overlay tended to wear out preferentially, particularly when associated with a hard nickel barrier. An attempt to polish a number of samples at a time on an automatic polishing device was not successful. It was experienced that polishing should be performed for a minimum length of time in order to prevent bevelling of the section. Hence, a few scratch marks still remaining on harder material was inevitable. However, the widths of the intermetallic layers were quite conspicuous after etching particularly, and could be measured with resonable accuracy using a graticule in the optical microscope at a magnification of 1000 times. Alternate etching and polishing was found effective in obtaining a good result with little bevelling effect. The final polish was done on 1 μm diamond polishing wheel.

In order to get reproducible results, it was necessary to take the average of 20 thickness measurements on each sample. While in some samples the intermetallic layers were fairly uniform throughout

the entire length, in some it was very uneven, particularly in samples with Pb in the substrate. Various combinations of etching solutions were tried, and it was finally decided to use a NH_4OH solution with 10 ^{v}/o of 20 vol H_2O_2 for copper based systems, and a solution of potassium dichromate with few drops of concentrated HCl for Ni based systems, with 5 seconds immersion time in each case. The real thicknesses were obtained by multiplying the measured thickness (oblique thickness)by a factor obtained by comparing the measured thickness of the as-mounted sample with the actual thickness of the sample. This factor is the cosine of the angle between the vertical and the mounted sample.

3.3 ELECTROPLATING PROCESSES OF THE DIFFUSION BARRIERS

Interpositioning of barriers could be divided into two categories: (i) electroplating processes and (ii) electroless processes. Iron and four other alloys were electroplated as barriers between the lead-tin overlay and the copper substrate. Electroless plating of nickel, chromating and phosphating as barriers are in the electroless category. Copper strips, 0.8 mm in thickness, commercially pure and known as "high conductivity copper" (cold rolled, 99.9 ^{w}/o Cu, 0.03 ^{w}/o Oxygen; BS2870 C101) were used as the substrate in all experiments on barrier plating. Laboratory pre-treatments to electroplating included cleaning the surface mechanically, vapour degreasing and cathodic cleaning followed by washing with distilled water and acetone and then blow-drying.

3.3.1 Iron Plating

The iron barrier was plated with a $FeSO_4$ bath, the composition of which is given in Table 6.

The plating was done at room temperature at a cathode current density of 2.0 A dm^{-2} on pretreated copper strips, in a 250 cm^3 bath. The time of deposition was 5 minutes and a thickness of about 5 μm was obtained. The deposit was smooth and adherent. The voltage of the D C source used was 6 V. Cast iron anode was used with approximately the same area as the cathode. Deposition was obtained only on the side facing the anode, with the other side masked off by a layer of lacquer. The finished cathode was washed with distilled water, dried and stored in a desiccator for the overlay plating at a later stage.

3.3.2 Ni-Sn Alloy

The Ni-Sn plating bath was prepared on a composition recommended by Brenner [115] for deposition of 65^w/o Sn - 35^w/o Ni alloy. The composition and the operating conditions are given in Table 7. The thickness of the deposit obtained after 5 minutes was about 5 μm; it was smooth and adherent. A plate of pure analytical grade lead was used as anode, having the same area as the cathode. The distance between the two electrodes was maintained at approximately three centimetres.

3.3.3 Cu-P Alloy

Copper-phosphorus alloy was deposited using two baths; (i) cupric chloride bath and (ii) cupric sulphate bath; both containing

TABLE 6. Bath Composition and Operating Condition for Electroplating Iron (After Brenner, Ref 115)

Ferrous Ammonium Sulphate, $FeSO_4(NH_4)_2SO_4.6H_2O(s)$	350 g dm^{-3}
Temperature	25^oC
pH at 25^oC	2.8 - 3.4
Cathode Current Density	2 A dm^{-2}

TABLE 7. Composition and Operating Conidition for $65^w/o$ Sn - $35^w/o$ Ni Alloy Electrodeposition (After Brenner, Ref 115)

Nickel Chloride, $NiCl_2.6H_2O(s)$	250 g dm^{-3}
Stannous Choride, $SnCl_2.2H_2O(s)$	50 g dm^{-3}
Ammonium Fluoride, $NH_4F(s)$	33 g dm^{-3}
Sodium Fluoride, NaF(s)	20 g dm^{-3}
Temperature	50 - 70^oC
pH at 25^oC	6.0
Cathode Current Density	2 A dm^{-2}

phosphoric and phosphorous acids. (See Tables 8 and 9). Both the baths compositions are listed in the patent applications for the overlay bearings diffusion barriers.

The anodes used were high conductivity copper of the same grade as the cathodes. In early experiments it was found that the deposit obtained by using the chloride bath (Table 8) was loose and non-adherent. Later it was discovered that the quality of the deposit could be improved by using the "live entry" method, where the cathode is connected to the power supply before inserting into the bath. The poor adhesion was caused by a hydrated chloride film formed on the surface of the cathode on immersion in the bath. X-ray analysis has shown that the film consisted of $CuCl_2$.

The sulphate bath (Table 9) gave a smooth and adherent deposit at the mentioned range of current densities. Outside the above range the deposits became loose and non-adherent. In both cases the barrier was deposited for eight minutes and the thickness obtained was approximately 5 μm. Some of the samples were used in chemical analysis to estimate the phosphorus content of the deposit. The procedure of the analysis is given in Section 3.6.

3.3.4 Cu-B Alloy

Copper-boron alloy was electrodeposited using a cupric sulphate bath containing boric acid (H_3BO_3). The bath composition is given in Table 10.

TABLE 8. Bath Composition and Operating Conditions for Electroplating Cu-P Alloy (Chloride Bath) (to work)

Cupric Chloride, $CuCl_2.2H_2O(s)$	65 g dm^{-3}
Phosphorous Acid, $H_3PO_3(s)$	12.5 g dm^{-3}
Orthophosphoric Acid, $H_3PO_4(\ell)$ (density 1.75 g cm^{-3})	45 g dm^{-3}
Temperature	40 - 45°C
pH at 25°C	1 - 0.5
Current Density	0.3 - 1.5 A dm^{-2}
Anode/Cathode Area Ratio	1:1
Anode	Pure Copper

TABLE 9. Bath Composition and Operating Conditions for Electroplating Cu-P Alloy.(Sulphate Bath) (to work)

Cupric Sulphate, $CuSO_4.5H_2O(s)$	30 g dm^{-3}
Phosphoric Acid, $H_3PO_4(\ell)$	45 g dm^{-3}
Phosphorus Acid, $H_3PO_3(s)$	12.5 g dm^{-3}
Temperature	40 - 45° C
pH at 25°C	1 - 0.5
Cathode Current Density	0.3 - 1.5 A dm^{-2}
Anode/Cathode Area Ratio	1:1
Anode	Pure Copper

TABLE 10. Bath Composition and Operating Conditions for Electroplating Cu-B Alloy (This work)

Cupric Sulphate, $CuSO_4 5H_2O(s)$	30 g dm^{-3}
Boric Acid, $H_3BO_3(s)$	40 g dm^{-3}
Temperature	20 - 25°C
Cathode Current Density	0.5 - 1.0 A dm^{-2}
Anode/Cathode area ratio	1:1
Anode	Pure Copper

TABLE 11. Bath Composition and Operating Conditions for Electroplating Cu-S Alloy (This work)

Cupric Sulphate, $CuSO_4.5H_2O(s)$	200 g dm^{-3}
Sodium Thiosulphate, $Na_2S_2O_3(s)$	20 g dm^{-3}
Temperature	25°C
pH at 25°C	4
Cathode Current Density	1.5 A dm^{-2}
Anode/Cathode Area Ratio	1:1
Anode	Pure Copper

Samples were electroplated at a range of current densities varying from 0.5 A dm^{-2} to 1.5 A dm^{-2} . The deposits obtained above 1 A dm^{-2} were found to be not efficient as diffusion barriers, although they looked adherent and smooth. Attempts made to analyse this deposit to estimate the boron content was not successful. The microprobe analyser could not detect boron in the deposit as expected. Although detection of boron in the deposit was not possible, it was evident that the deposits contained some boron, as discussed later.

3.3.5 Cu-S Alloy

After a few unsuccessful attempts, a Cu-S alloy was deposited successfully using a cupric sulphate bath containing sodium thiosulphate. The composition of the plating solution is given in Table 11.

The deposit was grey in colour and was well adherent. The samples were plated for 10 minutes, and then lead-tin alloy overlay plated for 25 minutes as in all the other experiments.

3.4 ELECTROLESS PROCESSES FOR BARRIER PLATING

Two types of barriers, obtained by electroless plating, were tested in the experiments. They were produced by electroless-plating of nickel, and by chromating the copper surface. The samples used were the same as in earlier experiments (high conductivity copper of BS2870 C101).

Electroless nickel was plated using a bath composition [130] given in Table 12.

TABLE 12. Bath for Electroless Nickel Plating. (After Graham, Ref 130)

Nickel Chloride, $NiCl_2.6H_2O(s)$	45 g dm^{-3}
Sodium Hypophosphite, $NaH_2PO_2.H_2O(s)$	11 g dm^{-3}
Tri-Sodium Citrate, $Na_3C_6H_5O_7.2H_2O(s)$	100 g dm^{-3}
Ammonium Chloride, $NH_4Cl(s)$	50 g dm^{-3}
pH at 25°C	4.6
Temperature	95 - 100°C

TABLE 13. Bath for Chromating. (After Graham, Ref 130)

Sodium Dichromate, $Na_2Cr_2O_7.2H_2O(s)$	30 g dm^{-3}
Nitric Acid, HNO_3(conc) (ℓ)	130 g dm^{-3}
Acetic Acid, CH_3COOH (ℓ)	150 g dm^{-3}
Sodium Chloride, NaCl(s)	52 g dm^{-3}
Temperature	25°C

A 500 cm^3 portion of the solution was prepared and heated up to 100°C. The sample was then kept immersed for about 15 minutes. An adherent smooth coating, approximately 5 μm in thickness, was obtained.

A solution of sodium chromate, nitric acid, acetic acid and sodium chloride was used for chromating the copper surface. The composition of the bath is given in Table 13.

The samples were immersed in the above solution at room temperature for three minutes and after washing in distilled water plated with lead-tin overlay.

3.5 OVERLAY PLATING

The Pb-Sn overlay was deposited on each of the samples previously barrier-plated as described above, and stored in desiccator for less than two days. The bath used for plating the Pb-Sn overlay had stannous tin and lead metal in the ratio of approximately 1:9, roughly in the same proportion as the deposit composition, which had about 10 $^{w}/_{o}$ Sn. The composition of the bath used is given in Table 14.

After deposition of the overlay the specimens were washed, dried and cut into smaller pieces. These were then heat-treated in non-oxidising silicone oil at temperatures 100, 115, 125, 135, 145 and 160°C for periods up to 20 days, and in some cases, up to 90 days. The heat-treated samples were mounted in cold mounting resin and examined under the optical microscope as mentioned earlier.

TABLE 14. Bath Composition and Operating Conditions for Electroplating Pb-10^{w}/o Sn Alloy (Ref 136)

Basic Lead Carbonate, $PbCO_3.Pb(OH)_2$ (s)	130 g dm^{-3}
Fluoboric Acid, HBF_4 42% (ℓ)	350 g dm^{-3}
Gelatin	2 g dm^{-3}
Stannous Fluoborate	25 ml dm^{-3}
Temperature	25°C
Cathode Current Density	1.5 A dm^{-2}
Anode/Cathode Area Ratio	1:1
Anodes	Cast Pb-10^{w}/o Sn Alloy

3.6 CHEMICAL ANALYSIS FOR PHOSPHORUS IN THE Cu-P ELECTRODEPOSIT[157]

A few of the Cu-P alloy plated samples were used for the chemical analyses of phosphorus. About 2g of accurately weighed Cu-P alloy was dissolved in about 50 cm^3 of 1:1 HNO_3, the weight of the alloy being the difference in weight of the sample before and after electroplating. The nitrous acid fumes were boiled off.

2 $^w/_o$ $KMnO_4$ solution was added dropwise until a stable precipitate was formed in order to convert any HPO_3 to H_3PO_4 . The precipitate and the solution was boiled for a few minutes and then dissolved by adding H_2SO_3 dropwise. Boiling was continued to expel the excess of SO_2 .

The solution was then diluted to about 50 cm^3 and cooled to about 50°C. While stirring, a solution of 50% NaOH was added until a slight permanent hydroxide precipitate persisted. This was redissolved with a minimum quantity of dilute HNO_3 .

The temperature of the solution was adjusted to approximately 50°C, and while stirring vigorously, 50 cm^3 of freshly filtered ammonium-nitromolybdate solution was added. Stirring was continued until precipitation began and then left to settle for about 2 hours.

The phosphorus-bearing yellow precipitate was then filtered off, washed several times with 2 $^v/_o$ HNO_3 and finally with 0.2 $^w/_o$ KNO_3 until the filtrate washings were acid free when tested with methyl orange. The yellow precipitate was then transferred along with the

filter paper to the original acid free beaker and then a known amount of 0.01 mol dm^{-3} NaOH solution was added to dissolve the precipitate and to give a small excess. This solution was then diluted with 50 cm^3 of cold, boiled, distilled water. The solution was then back titrated with standard 0.01 mol dm^{-3} HNO_3 using phenolphthalein as an indicator. The percentage of phosphorus was obtained using the following calculation:

$$1\ cm^3 \text{ of consumed } 0.01 \text{ mol } dm^{-3} \text{ NaOH} = 1.349 \times 10^{-5} \text{ g of P} \qquad (3.1)$$

$$\text{Percentage of P in deposit } [P] = \frac{x.\ 1349 \times 10^{-5}\ 100}{\text{Mass of deposit}}$$

where x = number of cm^3 of 0.01 mol dm^{-3} NaOH consumed to dissolve the yellow precipitate.

3.7 QUALITATIVE MEASUREMENT OF ADHESION OF BARRIER PLATED OVERLAYS

Mittal[151] describes quantitative and qualitative methods of measuring adhesion of electrodeposited coatings. Special instruments are needed for the quantitative tests. Some of the qualitative tests recommended for Pb-Sn electrodeposits could be performed without using special apparatus. The qualitative tests recommended by the above author for Pb-Sn deposits are: burnishing, drawing, heating and quenching, and peeling. These tests are also recommended for copper deposits.

The Cu-P and Cu-B barriered and overlay plated specimens were degreased in trichloroethylene vapour. Two specimens of 1 cm

by 4 cm were bonded together on the overlay plates sides with an epoxy resin, so that an area of 1 cm x 2 cm of each specimen was in contact with a similar area of its neighbour. After leaving overnight for the araldite resin to set, holding one specimen in a vice with the free end, the free end of the other specimen was bent with a pair of pliers as illustrated in Figure 8b.

In another test, the specimens were heated in an oil bath up to 160^{o}C and quenched in water. This heating and quenching was repeated five times and then the test described above performed on the specimens.

The specimens were buffed with a rotating wire brush in a third test.

3.8 ELECTRONPROBE MICROANALYSIS AND X-RAY EXAMINATION

The specimens prepared for metallographic examinations were used, in unetched condition, for microanalysis work. The instrument used was an Electronprobe X-ray Microanalyser Type JXA 3A, with facilities for taking photographs.

X-ray photographs were taken on the specimens in the area of the overlay and the interface with the substrate. These photographs show the distribution of each element. The specimens were then line-scanned for each element, to obtain concentration profiles across the specimens.

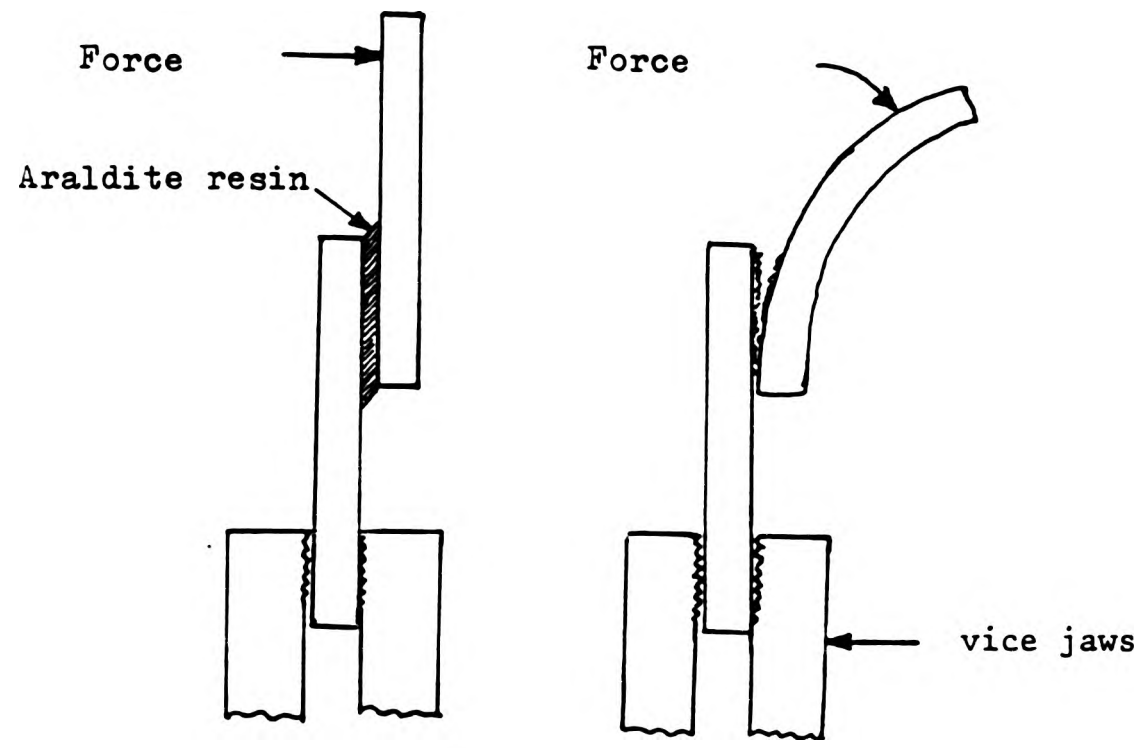

Figure 8b. Adhesion test

For X-ray diffractometry experiments the unmounted specimens of about 1 cm square were used. For the identification of intermetallic compounds, the overlay was carefully removed by dissolution in acetic acid. Leaving the specimens dipped in the acid overnight was found adequate to dissolve the overlay completely. The instrument used was Philips Powder Diffractometer PW 1353 with Philips X-ray Generator PW 1010 using copper K_α X-rays with a nickel filter.

4. RESULTS

4.1 INTRODUCTION

In the case of the copper substrate, plated with Pb-10 $^{w}/_{o}$ Sn overlay, at first a grey Cu-Sn intermetallic compound is formed. This later transformed into another Cu-Sn compound, having a higher copper content and a darker colour. The first compound was identified by X-ray analysis as Cu_6Sn_5 and the second one as Cu_3Sn. It was observed that the whole of the Cu_6Sn_5 transformed into Cu_3Sn after a certain lapse of time, the duration of which decreased with the increase of the heat treatment temperature. However, samples stored at room temperature did not show the presence of a Cu_3Sn layer. For calculation of interdiffusion coefficients, the growth of the total thickness of the compounds was used. It was not possible to take any meaningful results from the change in thickness of the Cu_6Sn_5 layer, since it grew for a while and then diminished after the onset of the growth of Cu_3Sn. In the case of overlay plated samples with nickel barrier, the compound formed was Ni_3Sn_4 .

The relationship of the thickness of the diffusion layer, the diffusion coefficient and the interval of time at a given temperature is given by the Einstein-Smoluchowski equation (equation 2.7 Section 2.3.3). The temperature dependence of the diffusion coefficient is given by the Arrhenius equation (equation 2.16, Section 2.3.4).

In order to deduce which species was rate controlling in the growth of the intermetallic compound, modified Arrhenius equation [56] (equation 2.23) was employed. The graph of x^2 versus t is linear only up to a heat treatment time of about 20 days, after which the

overlay becomes completely depleted of tin. Diffusion coefficients were calculated from the slope of the linear portion of the plot. In order to obtain reproducible results an average of 20 readings of x was taken. Growth kinetic of intermetallic compounds of copper-tin and nickel-tin were obtained, and no attempts were made to calculate kinetics parameters of the reactions involved in barrier plated systems where intermetallic compounds were formed.* Photomicrographs have been obtained in all the barrier plated samples, and formation of intermetallic compounds can be seen in them. In the systems with Cu-P barriers, the photomicrographs do not show compound growth at any temperature. However, in some of the samples which have a phosphorus content in the barrier less than a critical amount, a thin layer of a compound was detected. Similar observations have been made in samples with Cu-B barrier.

Microprobe analysis of the samples of lead-tin on copper have shown that there are two intermetallic compounds formed between the overlay and the substrate. In the case of samples with Ni barrier, only one compound was detected. In both of the above systems, there was no evidence of the presence of copper or nickel in the overlay after heat treatment. In the case of Cu-P and Cu-B barrier plated specimens copper has diffused into the overlay, but no intermetallic compound formation could be detected. A gradient of copper concentration in the overlay could be seen.

Diffusion of phosphorus into the overlay, even after a few hours of heat treatment has been observed. Diffusivity of phosphorus in the Pb-Sn overlay was calculated from microprobe traces.

*except in Ni barriered samples

4.2 INVESTIGATION OF THE Pb - 10 ^{w}/o Sn OVERLAY BEARINGS ON DIFFERENT SUBSTRATES

4.2.1 Metallography

4.2.1.1 Copper. Photomicrographs in Figures 9 and 10 show the formation of intermetallic compounds after heat treatment. Figure 9a shows the layer of compound Cu_6Sn_5 between the overlay and the substrate, after heat treatment at 100^{o}C for two days. At this time the second layer of Cu_3Sn is not visible. The duplex layer of Cu_6Sn_5 and Cu_3Sn can be seen in Figure 9b, where the sample has been heat treated at a higher temperature and for a longer time. The duplex layer transformed into a single layer of Cu_3Sn after further heat treatment and is shown in Figure 9c.

The line scans of copper, lead and tin of the specimens in Figures 9a, 9b and 9c are shown in Figures 10a, 10b and 10c, respectively.

X-ray diffractiometric experiments show that the first formed copper-tin compound is Cu_6Sn_5 which is metastable, and the stable phase formed subsequently is Cu_3Sn.

4.2.1.2 Nickel Barrier. The microstructures and the nickel, lead and tin line scans are shown in Figures 11a and 11b. X-ray diffractometric experiments show that the first compound formed is Ni_3Sn_4 (Figure 11c). Formation of the compound Ni_3Sn_2 could not be detected at the Pb - 10 ^{w}/o Sn composition of the overlay employed.

4.2.1.3 Nickel-Tin Barrier. This barrier was found to be uneffective No attempts were made to measure the rates of growth of the layers or

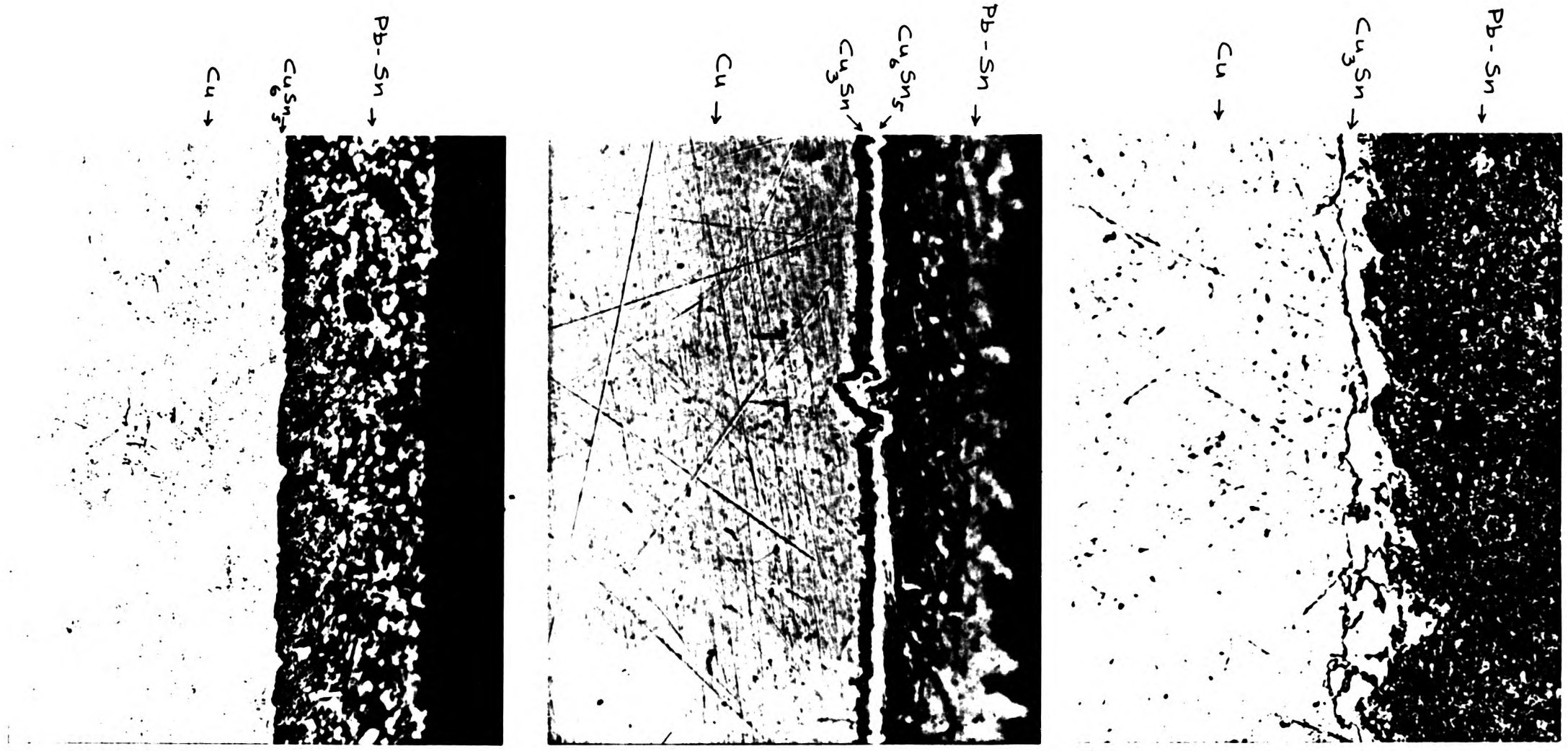

(a) Single Layer of Cu_6Sn_5 (Specimen annealed at 100°C for 1 day) × 400

(b) Duplex layer of Cu_6Sn_5/Cu_3Sn (Specimen annealed at 120°C for 10 days) × 400

(c) Single layer of Cu_3Sn (Specimen annealed at 120°C for 20 days) × 600

Figure 9. Photomicrographs of Pb-Sn on Cu system showing Cu-Sn intermetallic compounds.

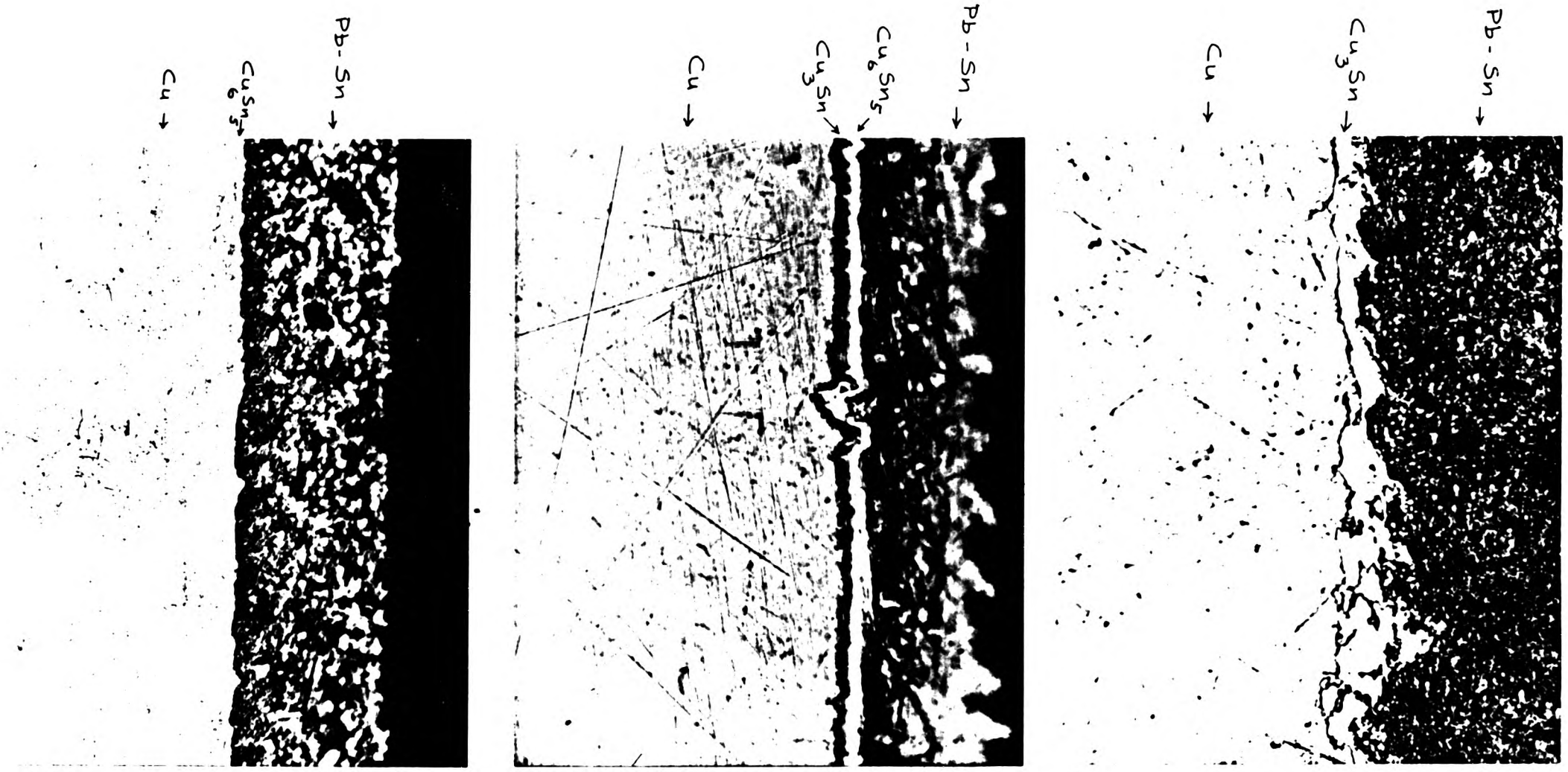

(a) Single Layer of Cu_6Sn_5 (Specimen annealed at 100°C for 1 day) × 400

(b) Duplex layer of Cu_6Sn_5/Cu_3Sn (Specimen annealed at 120°C for 10 days) × 400

(c) Single layer of Cu_3Sn (Specimen annealed at 120°C for 20 days) × 600

Figure 9. Photomicrographs of Pb-Sn on Cu system showing Cu-Sn intermetallic compounds.

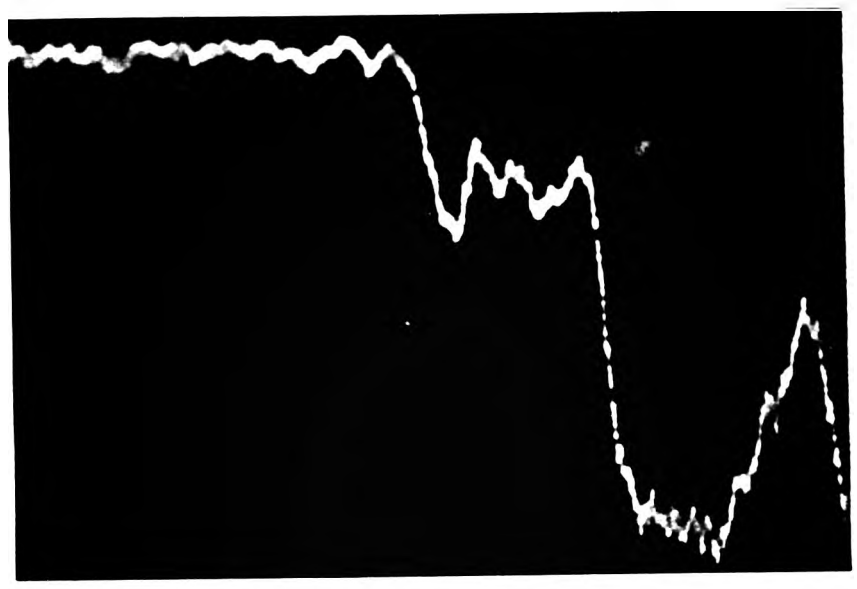

Cu

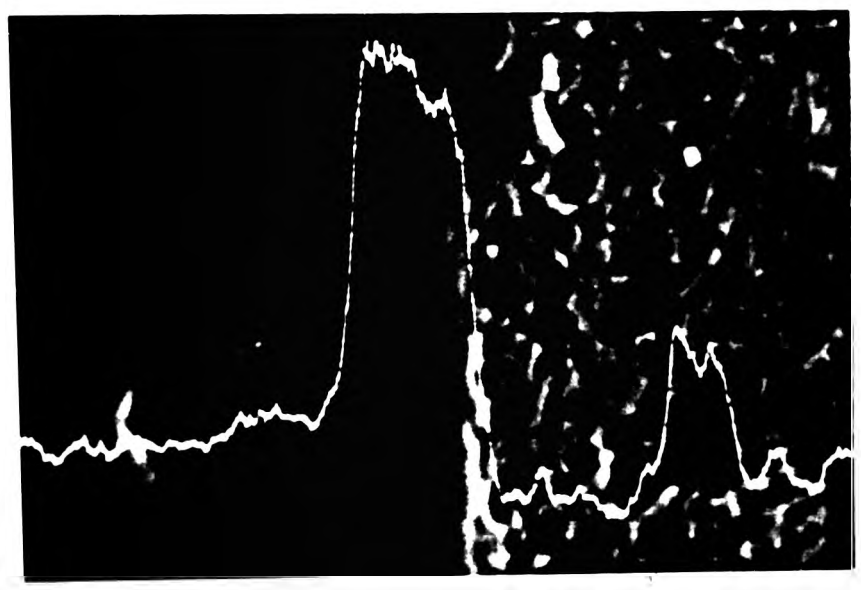

Sn

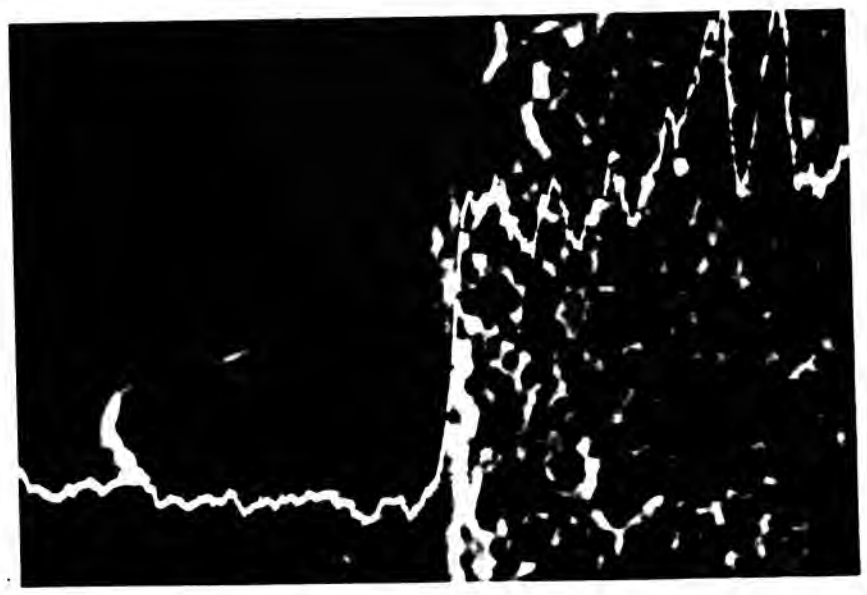

Pb

Figure 10a. X-ray/concentration profiles across the interface of Cu/Pb-Sn in sample in Figure 9a.

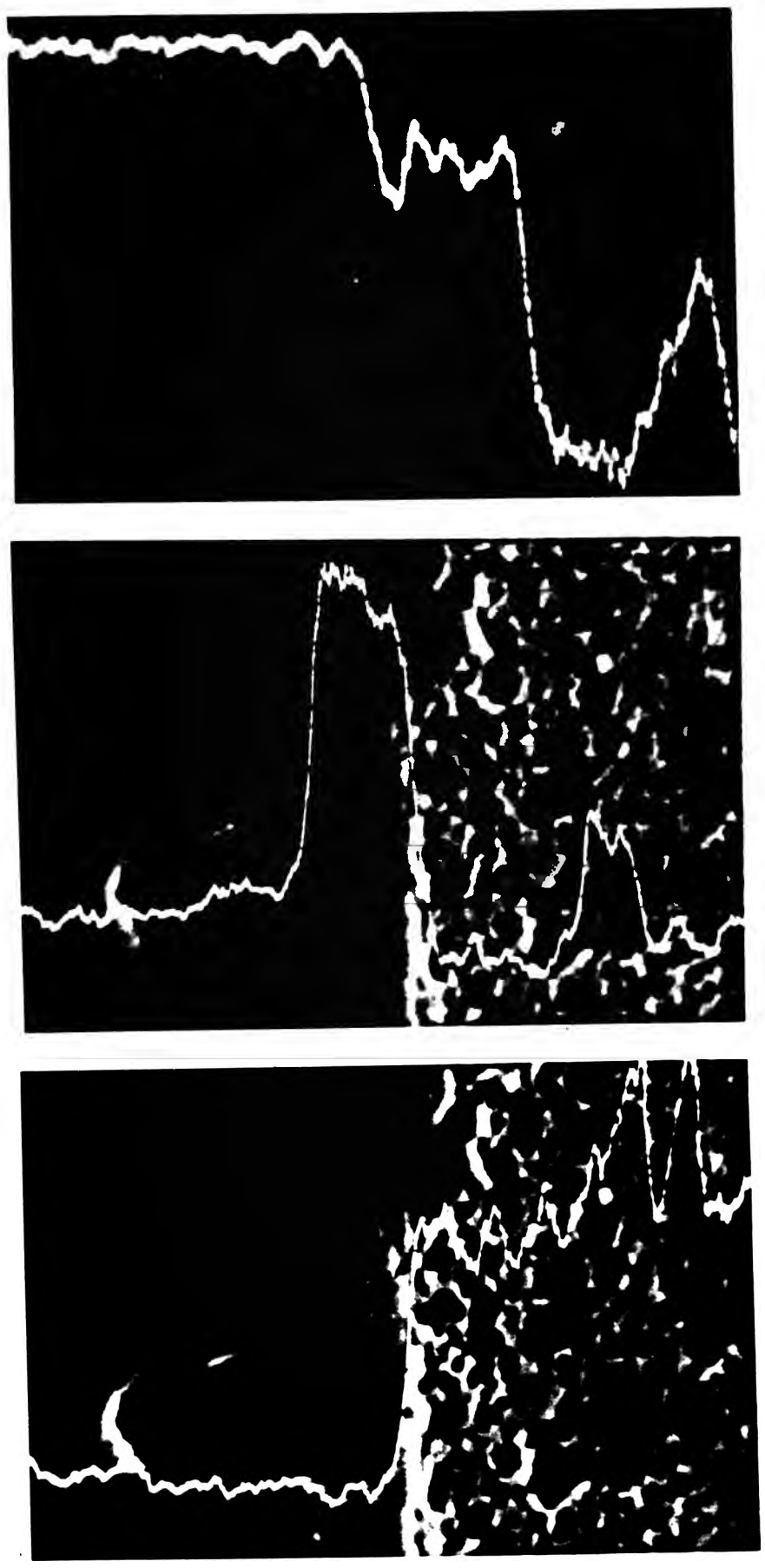

Figure 10a. X-ray/concentration profiles across the interface of Cu/Pb-Sn in sample in Figure 9a.

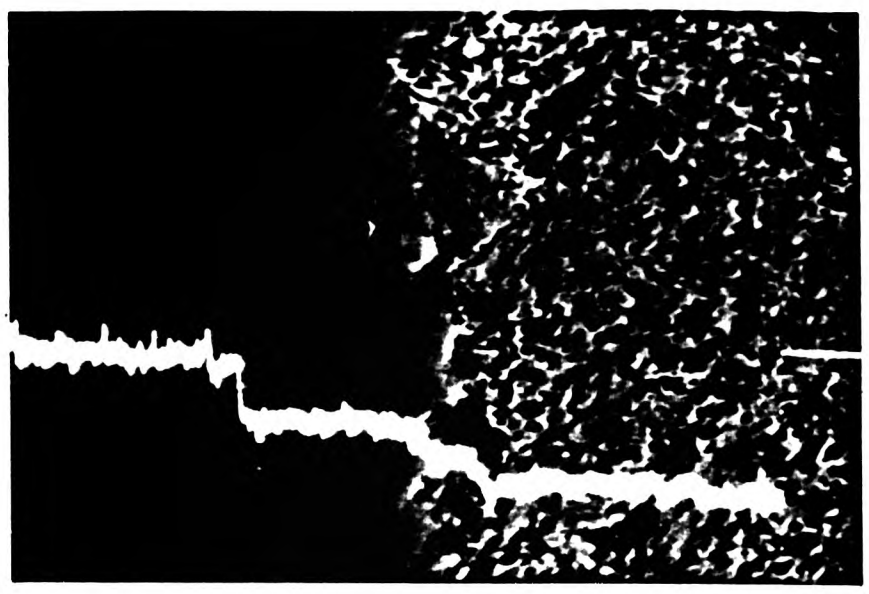

Cu

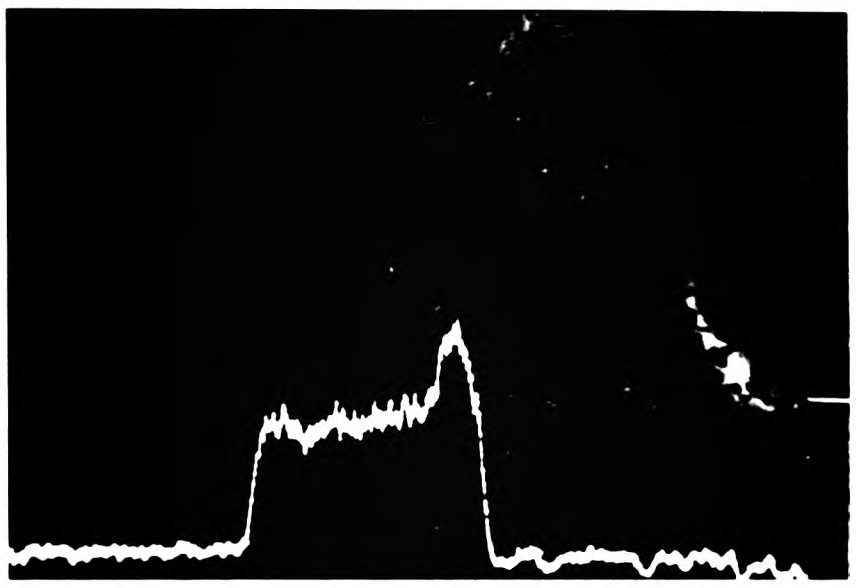

Sn

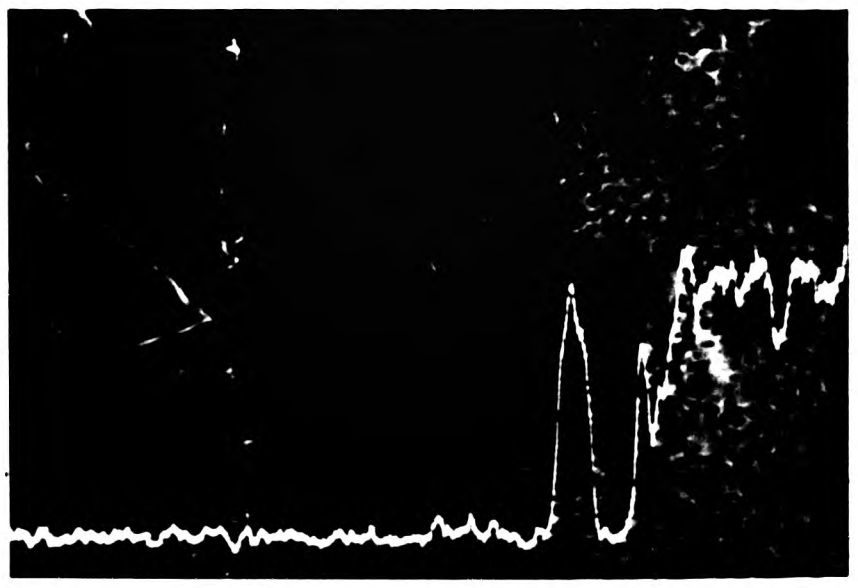

Pb

Figure 10b. X-ray/concentration profiles across the interface of Cu/Pb-Sn in sample in Figure 9b.

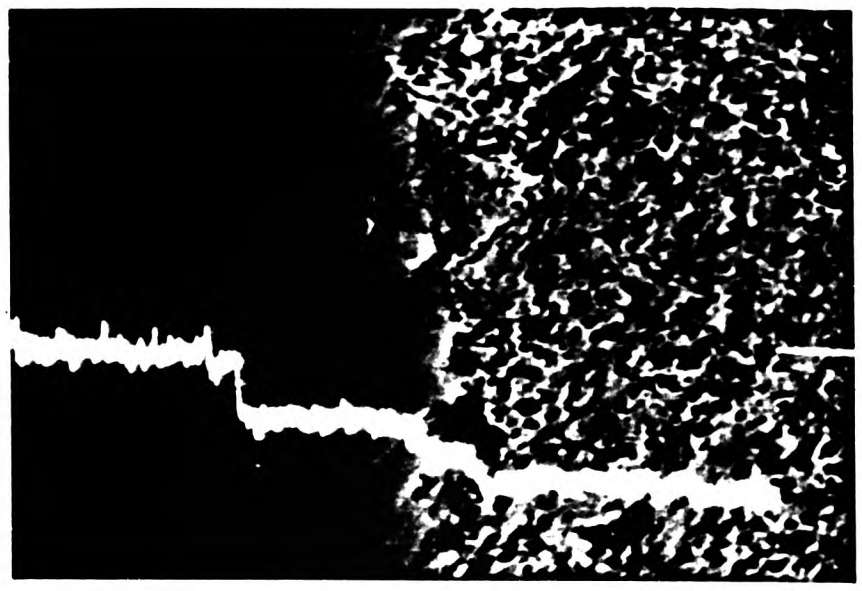

Cu

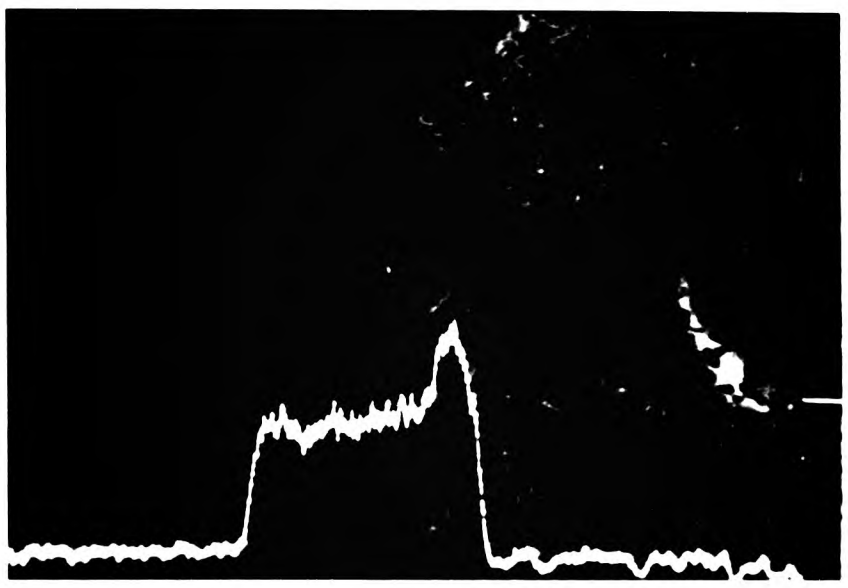

Sn

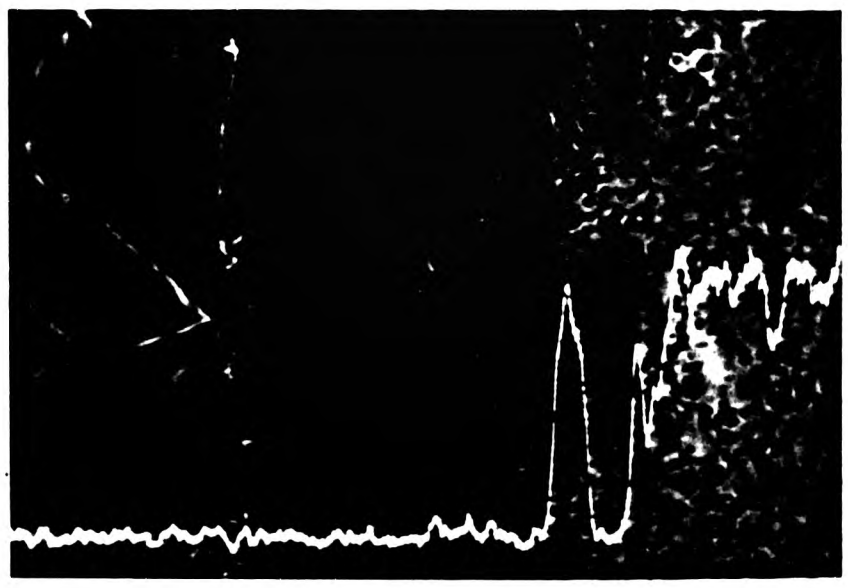

Pb

Figure 10b. X-ray/concentration profiles across the interface of Cu/Pb-Sn in sample in Figure 9b.

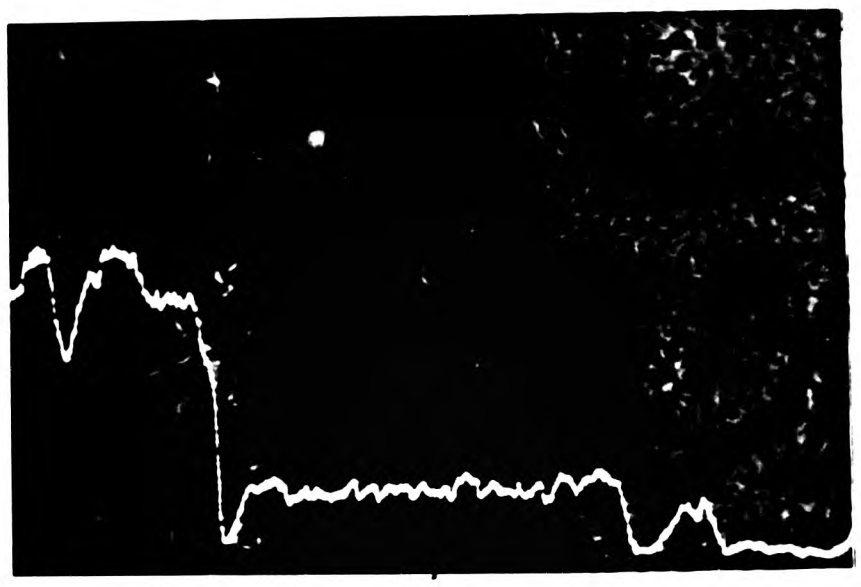

Cu

Sn

Pb

Figure 10c. X-ray/concentration profiles across the interface of Cu/Pb-Sn in sample in Figure 9c.

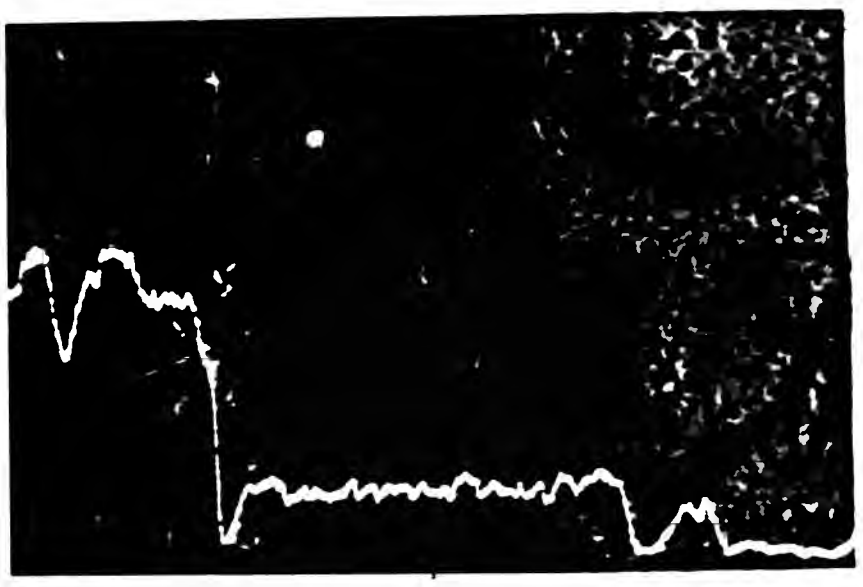

Figure 10c. X-ray/concentration profiles across the interface of Cu/Pb-Sn in sample in Figure 9c.

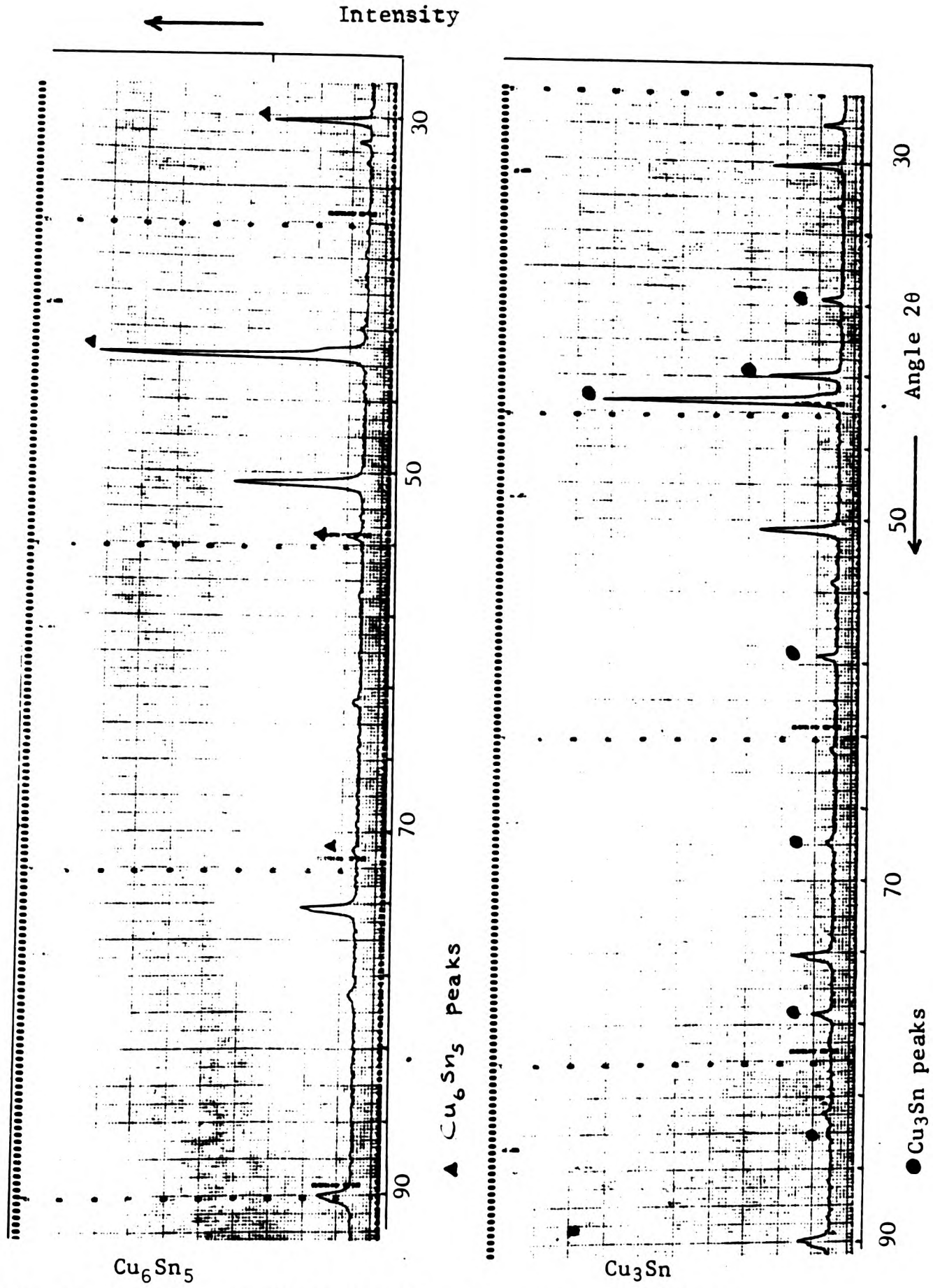

Figure 10d. X-ray (Cu Kα) diffraction traces of Cu_6Sn_5 and Cu_3Sn intermetallic compounds.

Figure 11a. Micrograph of Pb-Sn overlay on a Ni barrier showing Ni-Sn intermetallic compound. Specimen annealed at 120°C for 10 days.

Figure 11b. Ni and Sn X-ray/concentration profiles at the Ni/Pb-Sn interface of the sample in Figure 11a.

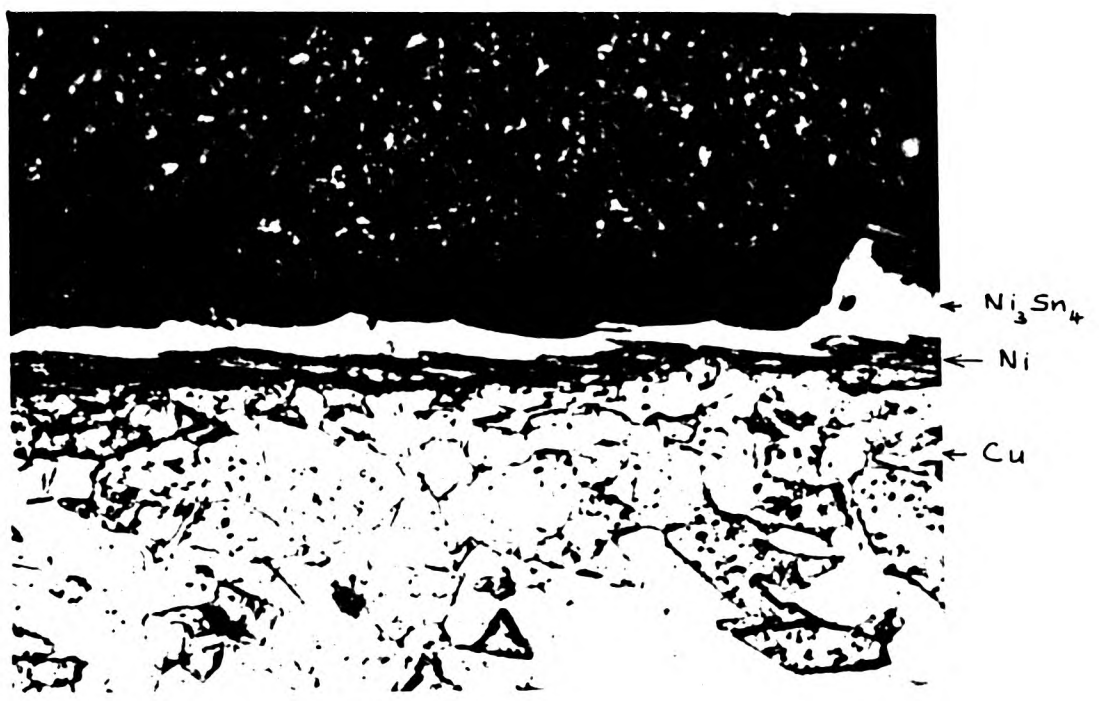

Figure 11a. Micrograph of Pb-Sn overlay on a Ni barrier showing Ni-Sn intermetallic compound. Specimen annealed at 120°C for 10 days.

Figure 11b. Ni and Sn X-ray/concentration profiles at the Ni/Pb-Sn interface of the sample in Figure 11a.

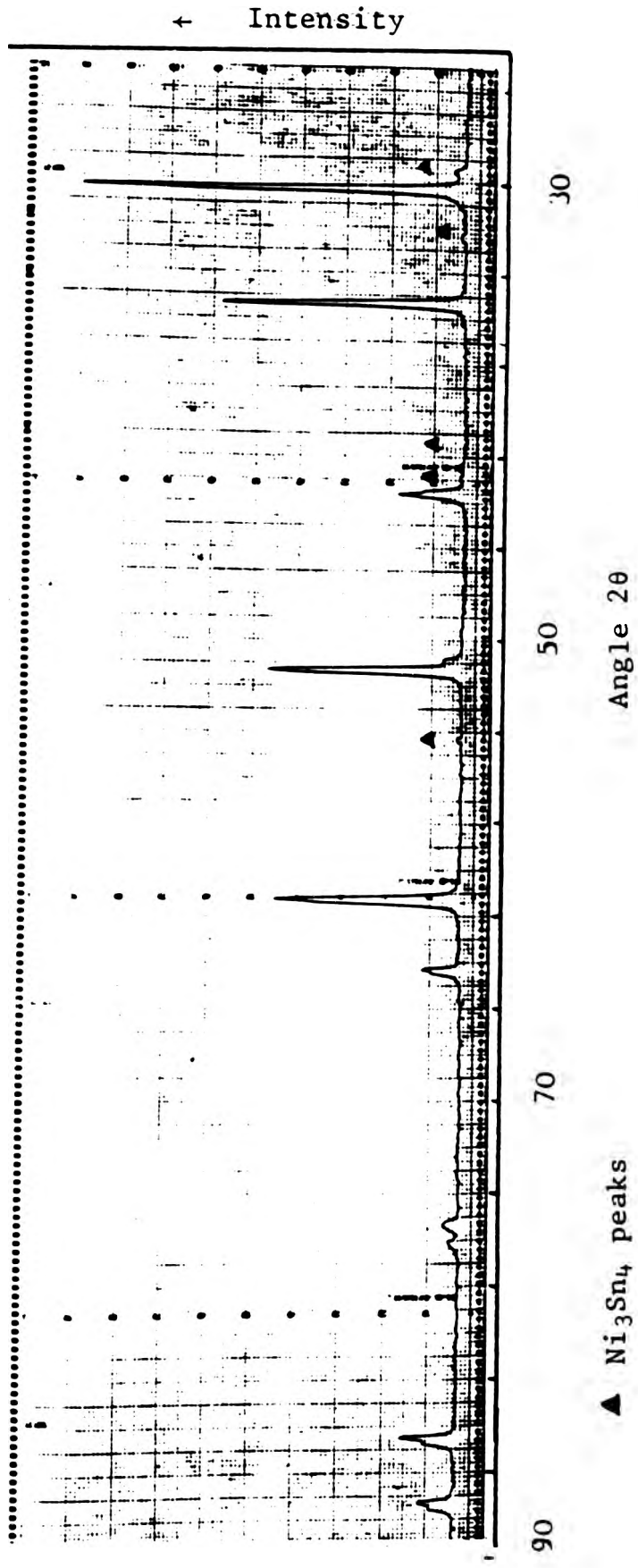

Ni_3Sn_4

Figure 11c. X-ray (Cu Kα) diffraction traces of Ni_3Sn_4 intermetallic compound.

to identify the diffusion compounds formed. A typical microstructure is shown in Figure 12.

4.2.1.4 Iron Barrier. Iron barrier was also found to be ineffective. It was clear that an iron-tin compound was formed with an iron barrier although the growth rate was not measured. Figure 13 shows the diffusion layer formed after heat treatment.

4.2.2 Growth Kinetics of Diffusion Compound

4.2.2.1 Copper-tin. Using equation 2.7 and plotting x^2 versus t (Table 15) at temperatures of 100, 115, 125, 135, 145 and 160°C, the interdiffusion coefficients were obtained (Figure 14). The values obtained at the above six temperatures are listed in Table 16 and the Arrhenius plot for the system is given in Figure 15. The slope of the Arrhenius plot is $- 3.92 \times 10^{-3}$ and,

$$Q_D = 75.11 \text{ kJ mol}^{-1} \qquad (4.1)$$

Using equation (2.18),

$$\log D_o = - 17.15 + 3.92 \times 2.50 \qquad (4.2)$$

$$D_o = 4.54 \times 10^{-8} \text{ m}^2 \text{ s}^{-1}$$

The Arrhenius expression for the diffusion process is

$$D = 4.54 \times 10^{-8} \exp\left(- \frac{75.11 \text{ kJ mol}^{-1}}{RT}\right) \text{m}^2 \text{ s}^{-1} \qquad (4.3)$$

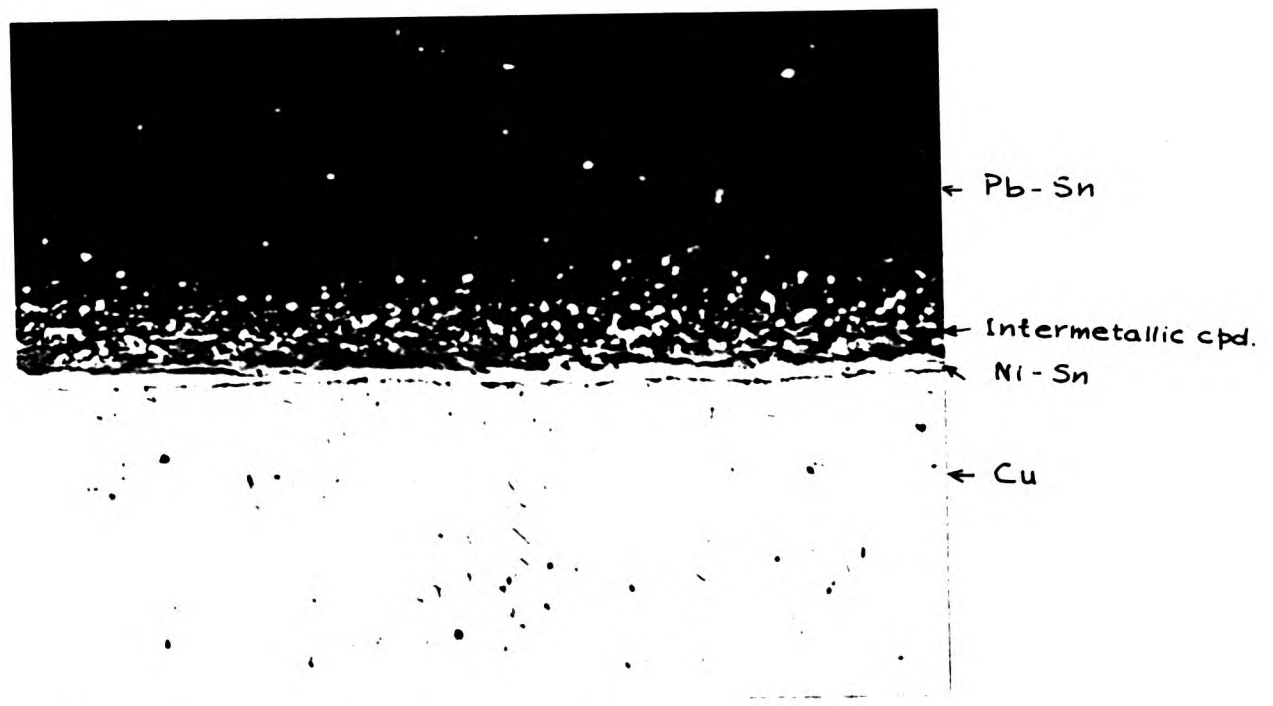

Figure 12. Micrograph of Pb-Sn overlay on a Ni Sn alloy barrier. Formation of diffusion compounds between the overlay and the barrier can be seen. Specimen annealed at 120°C for 10 days.

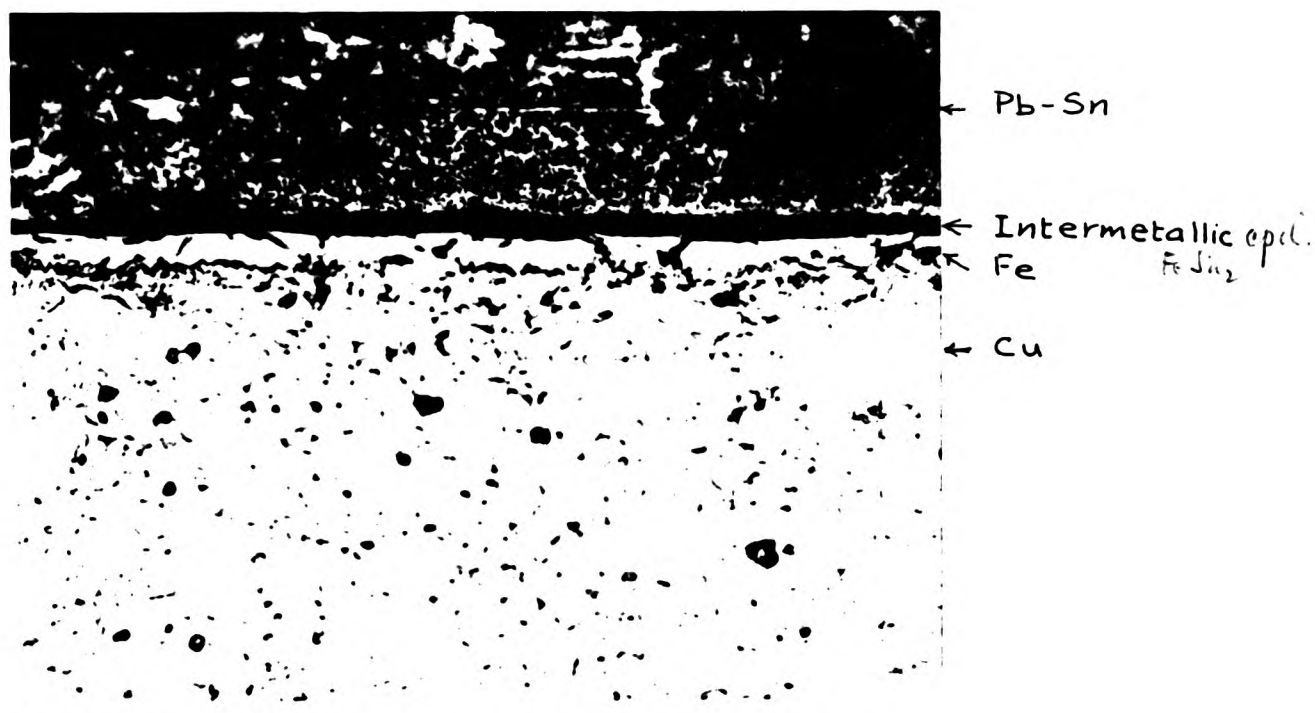

Figure 13. Micrograph of Pb-Sn overlay with Fe barrier. Fe-Sn intermetallic compound has formed between the barrier and the overlay. Specimen annealed at 120°C for 10 days.

TABLE 15. Growth of Diffusion Layer in Cu/Pb 10 w/o Sn System at Different Temperatures

Time		Thickness x at Temperature/°C											
		100		115		125		135		145		160	
t/h	$t/10^5$ s	$x/10^{-6}$ m	$x^2/10^{-12}$ m^2	$x/10^{-6}$ m	$x^2/10^{-12}$ m^2	$x/10^{-6}$ m	$x^2/10^{-12}$ m^2	$x/10^{-6}$ m	$x^2/10^{-12}$ m^2	$x/10^{-6}$ m	$x^2/10^{-12}$ m^2	$x/10^{-6}$ m	$x^2/10^{-12}$ m^2
48	1.73	0.67	0.45	1.14	1.30	1.40	1.98	1.98	3.92	2.34	5.47	3.84	14.80
96	3.45	1.01	1.00	1.48	2.19	1.95	3.82	2.92	8.52	3.52	12.39	5.20	27.04
192	6.91	1.39	1.93	1.95	3.80	2.74	7.52	4.04	16.32	4.92	24.20	5.82	33.87
240	8.64	1.60	2.56	2.24	5.02	3.09	9.54	4.60	21.16	5.25	27.56	6.02	36.24
288	10.37	1.81	3.27	2.43	5.95	3.43	11.78	4.98	24.80	5.72	32.71	6.24	38.93
336	12.09	1.90	3.84	2.64	6.98	3.62	13.10	5.16	26.62	-	-	-	-
432	15.52	2.19	4.79	3.07	9.42	4.18	17.47	5.28	27.87	-	-	-	-
480	17.28	2.28	5.19	3.16	9.98	4.25	18.06	-	-	-	-	-	-

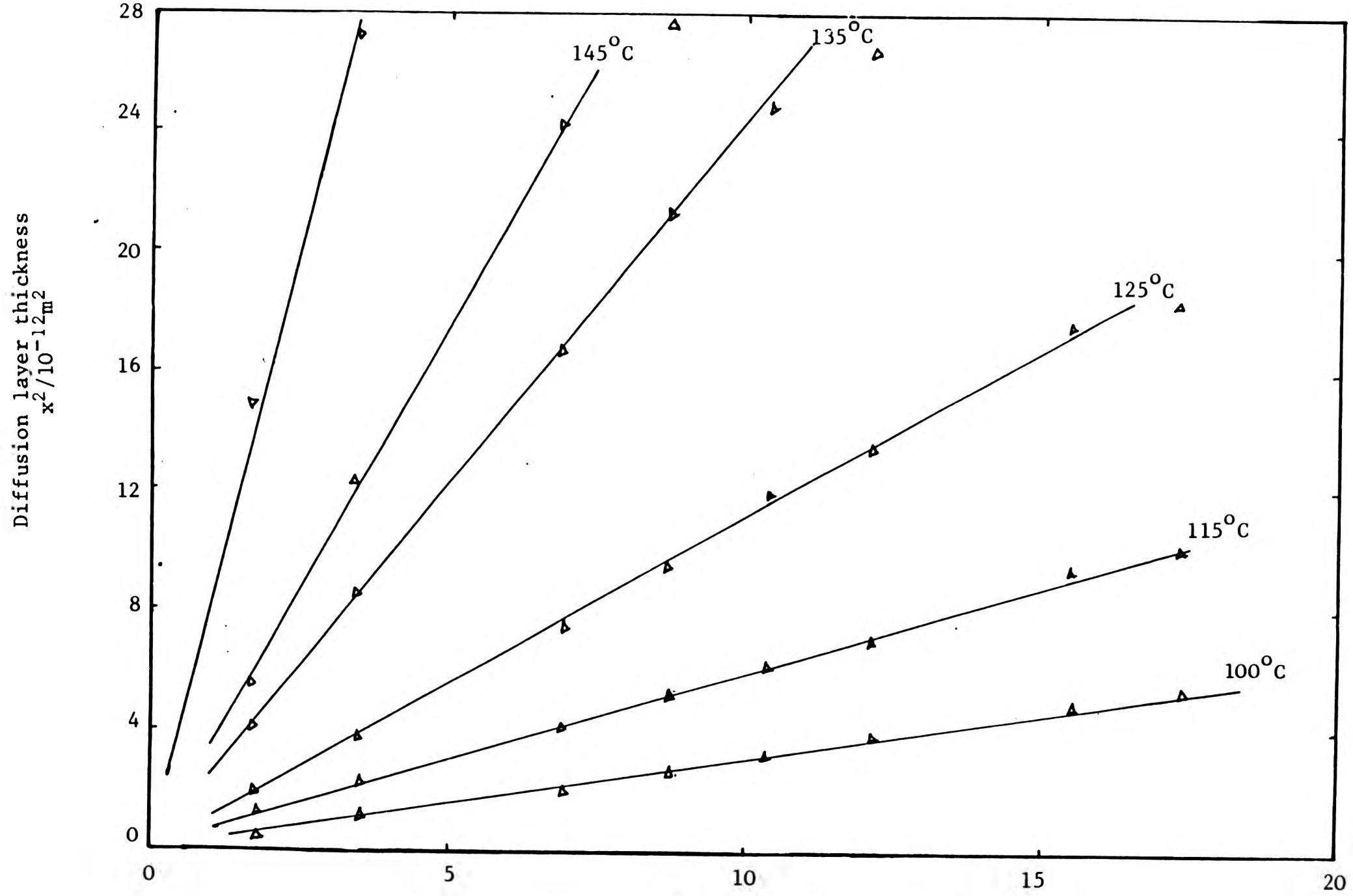

Figure 14. Diffusion layer growth in Cu/Pb-10^{w}/o Sn system

TABLE 16. Interdiffusion Coefficients of Cu-Sn (Cu-Pb-10 w/o Sn) System at Different Temperatures

T/°C	T/K	$T^{-1}/10^{-3}K^{-1}$	D/m^2s^{-1}	$lg(D/m^2s^{-1})$
100	373	2.680	1.5×10^{-18}	- 17.82
115	388	2.577	2.9×10^{-18}	- 17.53
125	398	2.512	5.6×10^{-18}	- 17.25
135	408	2.451	1.23×10^{-17}	- 16.91
145	418	2.392	1.77×10^{-17}	- 16.75
160	433	2.309	4.16×10^{-17}	- 16.38

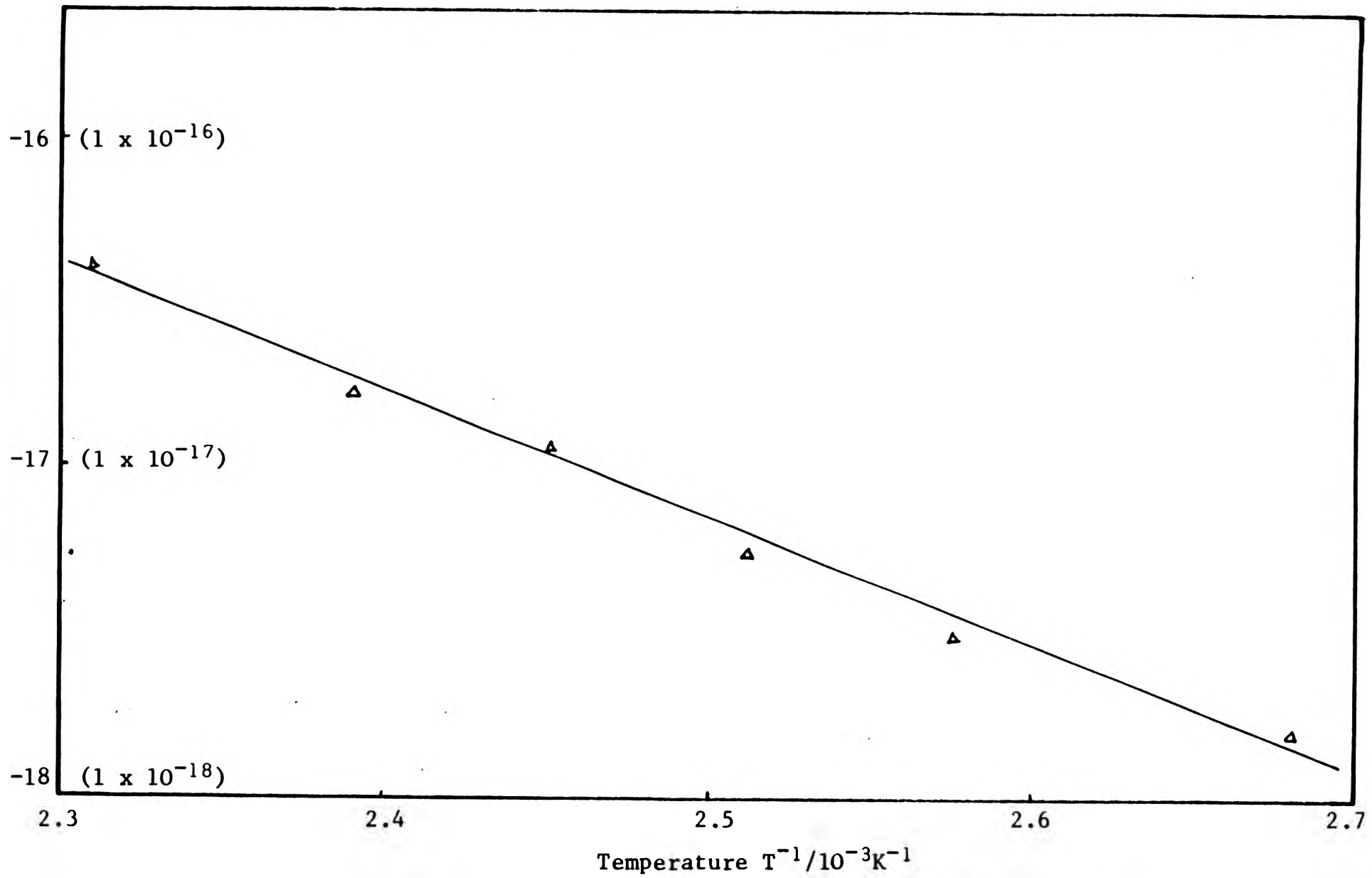

Figure 15. Arrhenius Plot for Cu/Pb - 10 w/o Sn system (growth of Cu-Sn compound layer)

Using equation (2.23),

$$D = D_\theta \exp \frac{Q_D}{R} \left(\frac{1}{\theta} - \frac{1}{T}\right) \qquad (2.23)$$

and substituting D_θ and θ values for Sn and Cu (Table 2), values of Q_D for the two species are obtained.

For Cu, θ = 1880 K, and $D_\theta = 5.00 \times 10^{-10}$ m^2 s^{-1} . At T = 373 K, $D = 1.5 \times 10^{-18}$ m^2 s^{-1} . Hence, Q_D for Cu, $Q_{Cu} = 75.95$ kJ mol^{-1} . For Sn, θ = 870 K, $D_\theta = 2.66 \times 10^{-10}$ m^2 s^{-1} and as above. Q_D for Sn, $Q_{Sn} = 103.10$ kJ mol^{-1} . Thus it can be seen that the activation energy for the process is similar to that of Cu and much less than that of Sn.

4.2.2.2 Nickel-Tin. For this system, x versus t values (Table 17) are plotted in Figure 16. Table 18 lists the interdiffusion coefficients at 100, 115, 125, 135, 145 and 160°C. The Arrhenius plot is displayed in Figure 17. The slope of Arrhenius plot is - 4.0×10^3 and,

$$Q_D = 76.57 \text{ kJ mol}^{-1} \qquad (4.4)$$

$$D_o = 1.45 \times 10^{-8} \text{ m}^2 \text{ s}^{-1} \qquad (4.5)$$

The general expression for the process is

$$D = 1.45 \times 10^{-8} \exp\left(-\frac{76.57 \text{ kJ mol}^{-1}}{RT}\right) \text{ m}^2 \text{ s}^{-1} \qquad (4.6)$$

Using equation (2.23) and substituting values of θ and D_θ for Ni and Sn (Table 2), Q_D values of the two species are obtained.

TABLE 17. Growth of Diffusion Layer in Ni/Pb-10 w/o Sn Systems at Different Temperatures

Time		Thickness x at Temperature/°C											
		100		115		125		135		145		160	
t/h	$t/10^5$ s	$x/10^{-6}$ m	$x^2/10^{-12}$ m^2	$x/10^{-6}$ m	$x^2/10^{-12}$ m^2	$x/10^{-6}$ m	$x^2/10^{-12}$ m^2	$x/10^{-6}$ m	$x^2/10^{-12}$ m^2	$x/10^{-6}$ m	$x^2/10^{-12}$ m^2	$x/10^{-6}$ m	$x^2/10^{-12}$ m^2
48	1.73	0.52	0.27	0.62	0.38	0.68	0.46	0.82	0.67	1.34	1.79	1.86	3.45
96	3.45	0.62	0.38	0.72	0.51	0.98	0.96	1.52	2.31	1.88	3.53	2.76	7.61
192	6.91	0.70	0.49	1.09	1.18	1.34	1.79	1.67	2.78	2.74	7.50	3.84	14.74
240	8.64	0.82	0.67	1.18	1.39	1.48	2.19	1.96	3.84	3.10	9.61	4.32	18.66
288	10.37	0.90	0.81	1.18	1.39	1.58	2.49	2.10	4.41	3.32	11.02	4.68	21.90
336	12.09	1.01	1.02	1.34	1.79	1.78	3.16	2.22	4.92	3.72	13.83	4.88	23.81
432	15.52	1.02	1.04	1.54	2.37	1.88	3.53	2.48	6.15	4.10	16.81	5.10	26.01
480	17.28	1.09	1.18	1.62	2.62	2.00	4.00	2.64	6.96	4.28	18.31	5.22	27.24

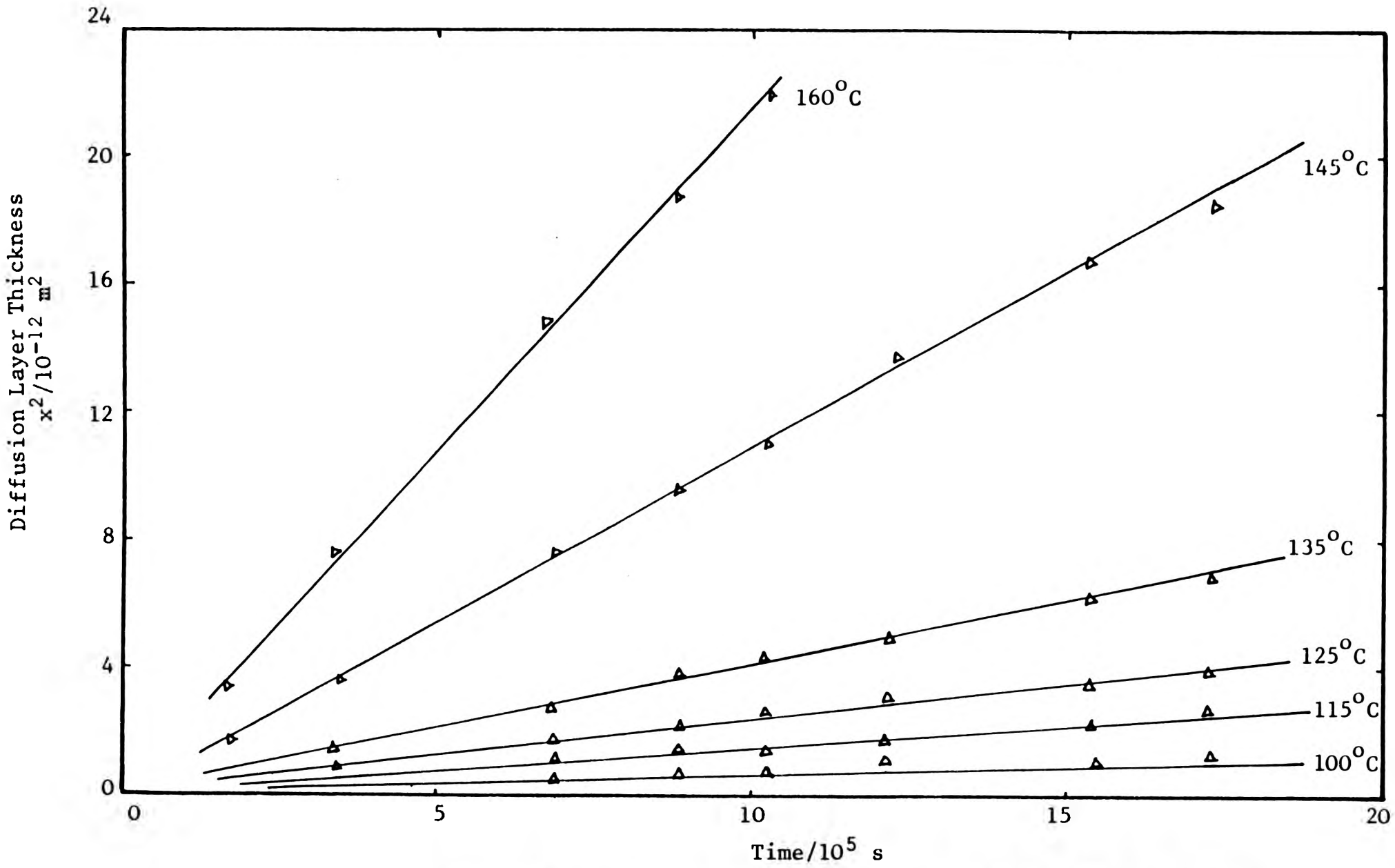

Figure 16. Diffusion layer growth in Ni/Pb - 10^{w}/o Sn system.

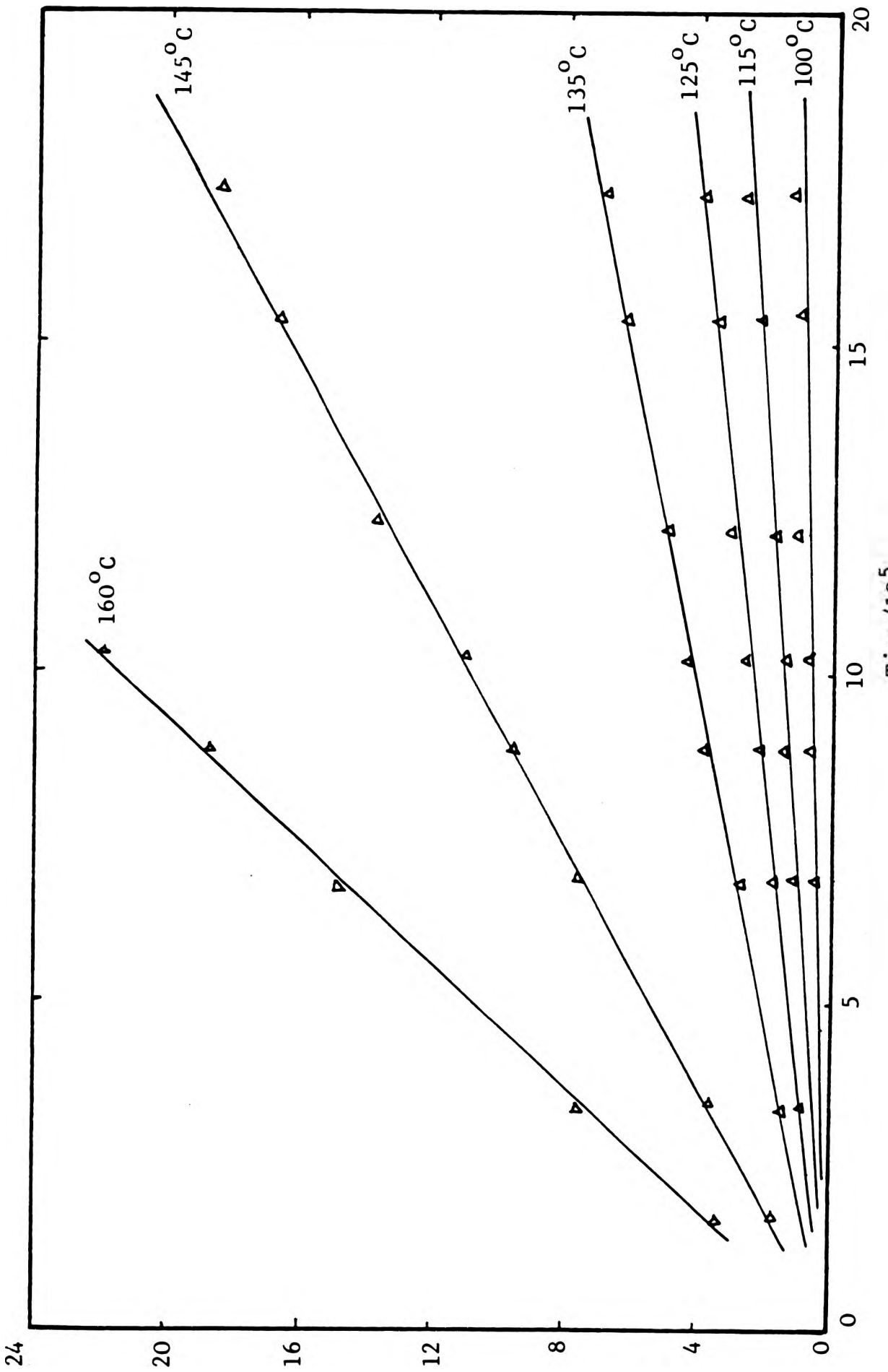

Figure 16. Diffusion layer growth in Ni/Pb - 10 w/o Sn system.

TABLE 18. Interdiffusion Coefficients of Ni-Sn (Ni/Pb-10 $^{w}/_{o}$ Sn) System at Different Temperatures

$T/^{o}C$	T/K	$T^{-1}/10^{-3}K^{-1}$	D/m^2s^{-1}	$lg(D/m^2s^{-1})$
100	373	2.680	2.82×10^{-19}	- 18.55
115	388	2.577	7.50×10^{-19}	- 18.12
125	398	2.512	1.20×10^{-18}	- 17.92
135	408	2.451	2.00×10^{-18}	- 17.60
145	418	2.392	5.57×10^{-18}	- 17.25
160	433	2.309	1.09×10^{-17}	- 16.96

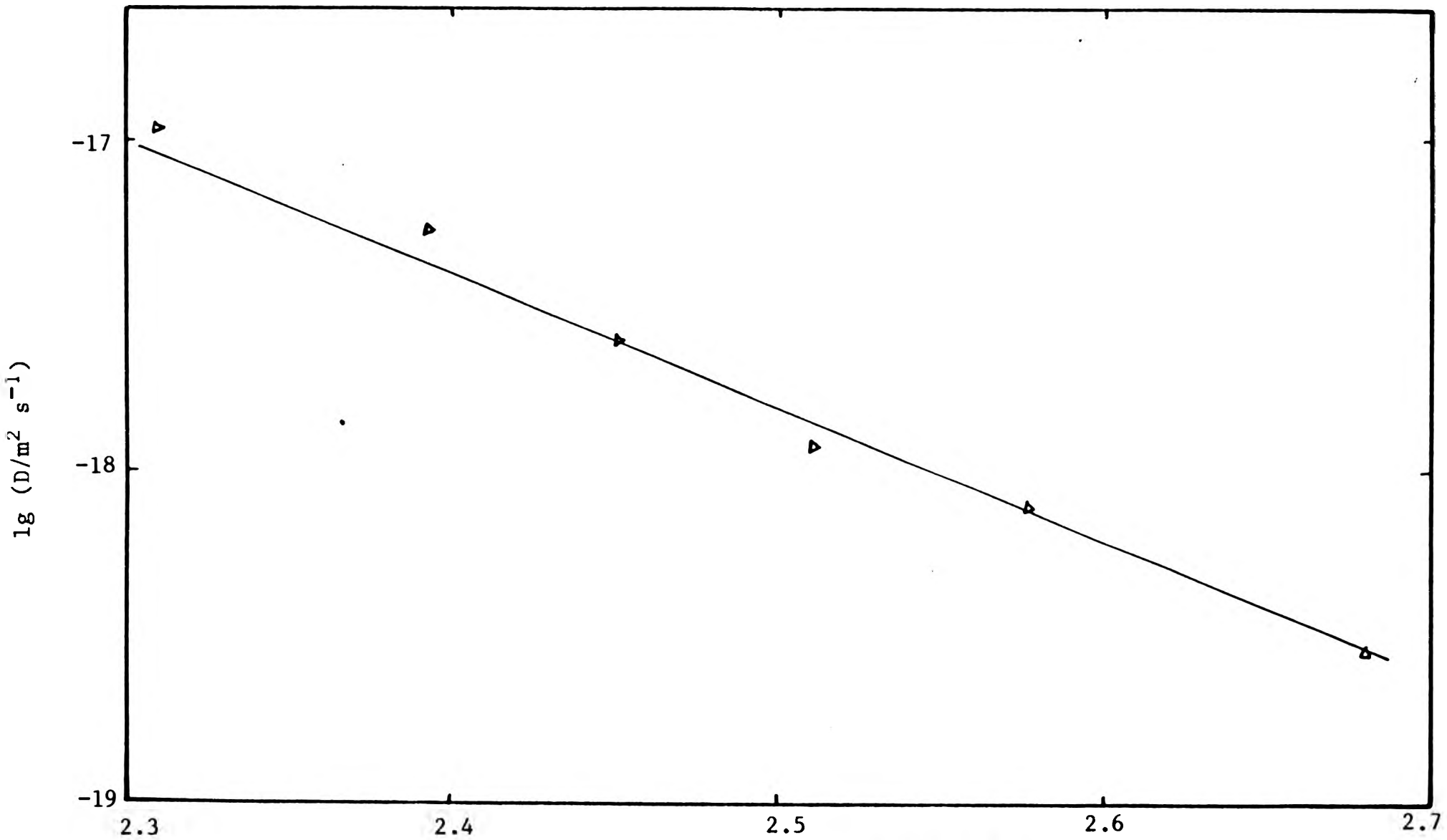

Figure 17. Arrhenius Plot for Ni/Pb - 10 w/o Sn system.
(growth of Ni - Sn compound)

At 373 K, $D = 2.8 \times 10^{-19}$ m^2 s^{-1} .

Hence, Q_D for Sn, $Q_{Sn} = 112.22$ kJ mol^{-1} ;

Q_D for Ni, $Q_{Ni} = 76.75$ kJ mol^{-1} .

In this case also, the observed activation energy for the diffusion process is similar to calculated value of Ni species, and is much lower than that of Sn.

4.3 EXAMINATION OF THE Pb - 10 w/o Sn OVERLAY BEARINGS WITH IMPROVED BARRIERS.

4.3.1 Metallography

4.3.1.1 Copper-Phosphorus Electrodeposit. The photomicrographs of overlay plated specimens provided with Cu-P alloy barrier, plated at current densities of 0.5 - 1.5 A dm^{-2}, after heat treatment do not show any diffusion compounds formed at the interface of the overlay and the substrate. Figures 18a, 18b and 18c show a photomicrograph and line scans of Cu, P, Sn and Pb across a sample heat treated at 160°C for 40 days. These clearly show that phosphorus has diffused outwards into the overlay and the tin has remained totally in the overlay during the heat treatment process. Copper has diffused into the overlay and a concentration gradient across the overlay is clearly seen.

Microscopic examination as well as X-ray diffractometry did not show the presence of phosphides or borides in the alloy layers or in the overlay after heat treatment. Macroscopically and micros-

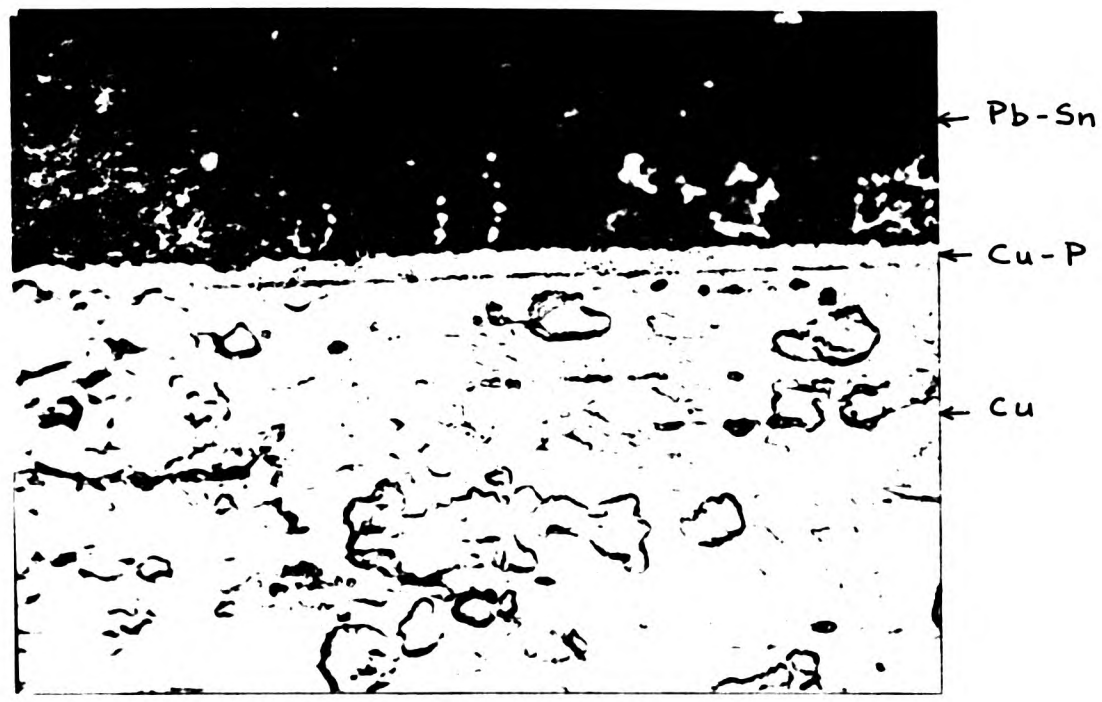

Figure 18a. Micrograph of Pb-10 w/o Sn overlay with Cu-P alloy barrier. Intermetallic compounds are not formed. Specimen annealed at 160°C for 40 days.

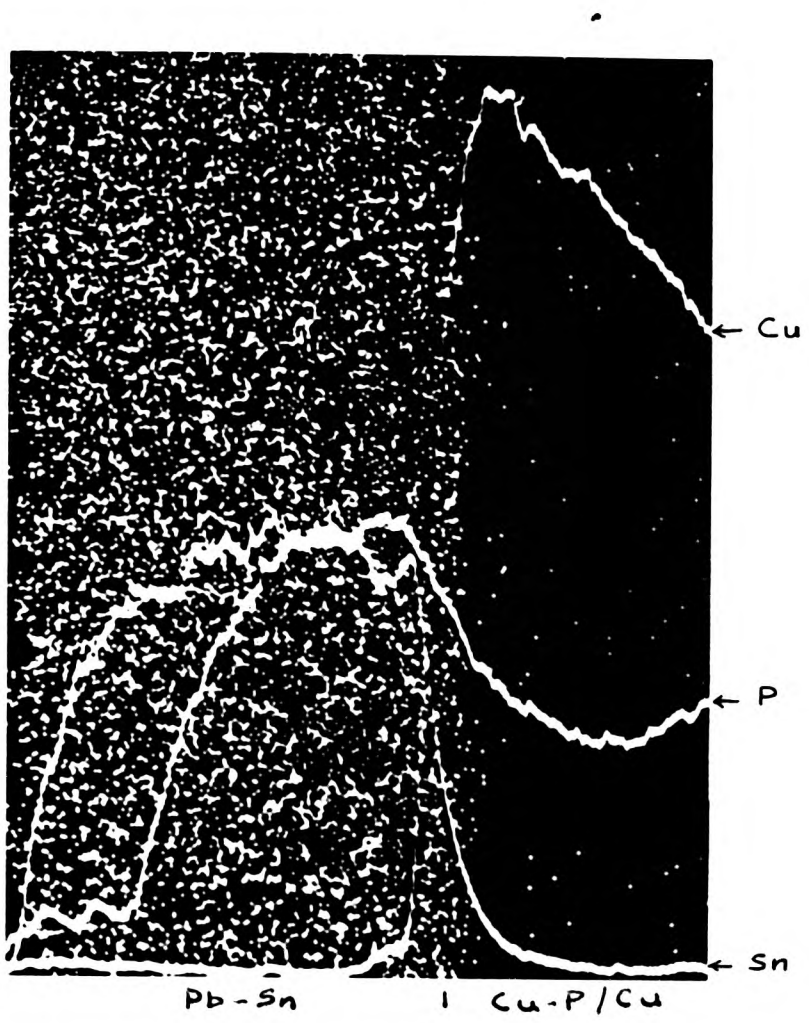

Figure 18b. X-ray/concentration profiles of Cu, P and Sn across the sample in Figure 18a.

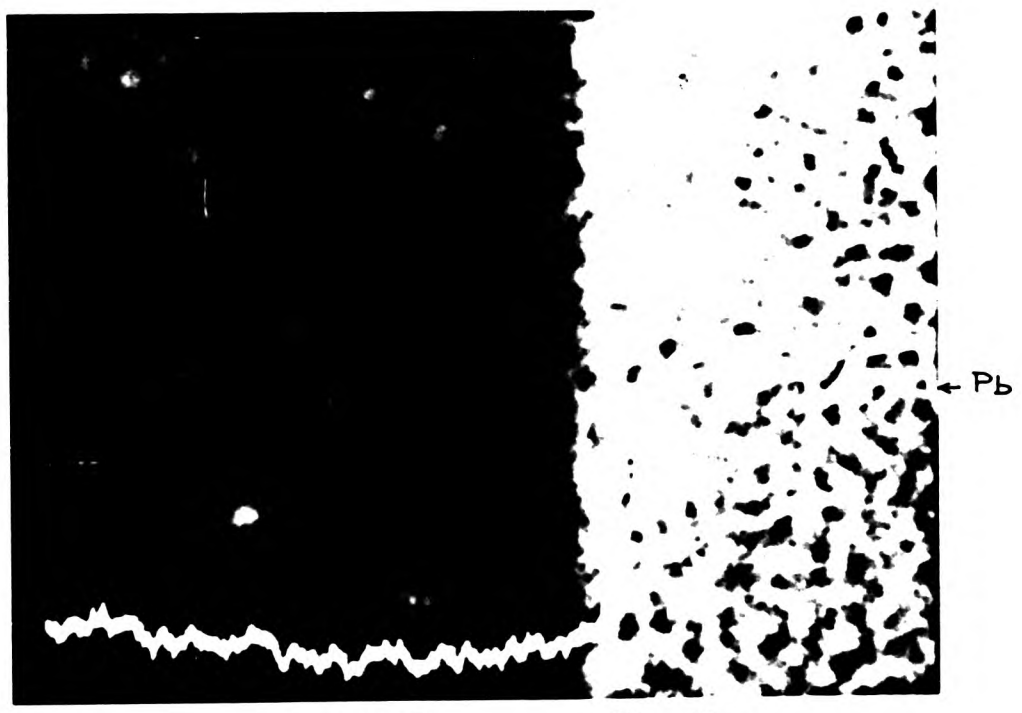

Figure 18c. X-ray/concentration profile of Pb across the sample in Figure 18a.

copically both the alloy layers were very adhesive to the substrate. Due to the absence of levelling agents in the plating solutions of the alloy layers, the alloy deposits were not bright, hence some "keying effect" of the overlay could be observed.

4.3.1.2 Copper-Boron Electrodeposit. The microprobe analyser is not capable of detecting boron in the specimens due to its low atomic number. Attempts to estimate the boron content in the deposit by chemical analysis was not successful. However, there was clear evidence that in specimens with Cu-B barriers plated at current densities ranging from about 0.8 to 1.5 A dm^{-2} , no visible diffusion compounds were formed at the interface. Figures 19a and 19b show photomicrographs of samples with Cu-B alloy barriers heat treated at 160^{o}C for 40 days. Figure 19a is from a specimen with Cu-B alloy plated at a current density of 0.5 A dm^{-2} and 19b at 1 A dm^{-2} . The former shows some diffusion compound whereas in the latter there is hardly any evidence of presence of a compound. This may be an indication that a lower current density deposits a lower percentage of boron as opposed to the case with phosphorus, where a higher percentage is associated with a lower current density.

4.3.1.3 Copper-Sulphur Electrodeposit. The Cu-S alloy electrodeposit obtained from a cupric sulphate bath was brittle and dark-coloured. This was found to be ineffective as a diffusion barrier. Compound started forming after a short period of heat treatment even at 100^{o}C.

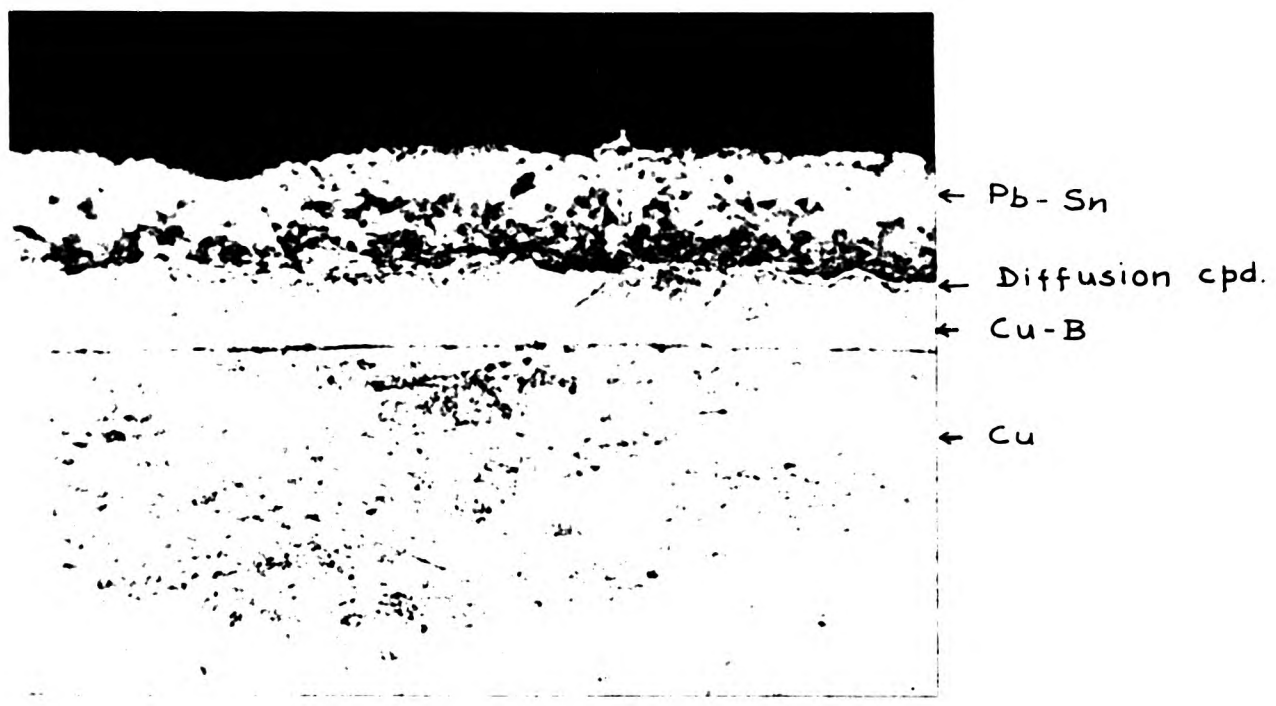

Figure 19a. Micrograph of Pb-10^{w}/o Sn overlay with Cu-B barrier electrodeposited at a current density of 0.5 A dm^{-2}. Small quantity of diffusion compound has formed. Specimen annealed at 140^{o}C for 40 days. × 400.

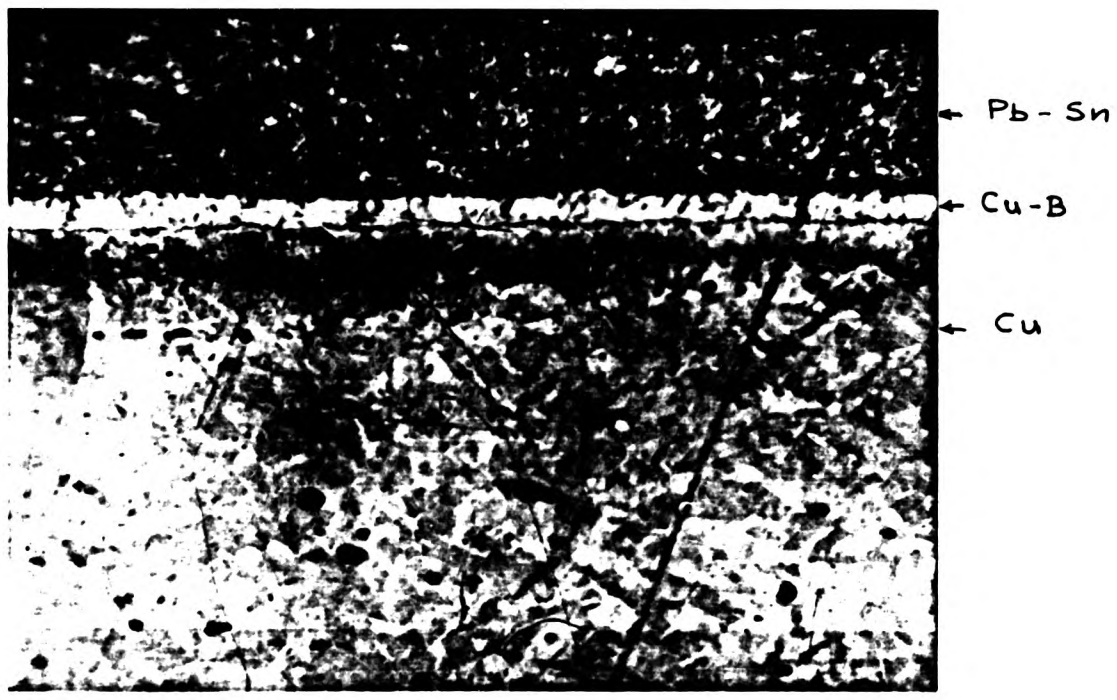

Figure 19b. Micrograph of Pb-10^{w}/o Sn overlay with Cu-B barrier electrodeposited at 1 A dm^{-2}. No diffusion compounds are visible. Specimen annealed at 140^{o}C for 40 days. × 400.

4.3.1.4 Nickel-Phosphorus Electroless Deposit. This barrier was also found to be ineffective. Formation of a compound similar to that found with the nickel barrier was observed. The identification of this phase and its kinetic characteristics were not considered important since diffusion process occurred rapidly.

4.3.1.5 Chromate Coating. Heat treatment of the chromated specimens resulted in formation of a diffusion compound between the chromate layer and the overlay (Figure 20). This phase appeared to be Cu_6Sn_5 as in the case of Pb-Sn alloy in contact with copper. Thus, the chromate layer may be regarded as a marker which allows the copper atoms to pass through. The width of this layer remained unchanged during the heat treatment.

4.3.2 Studies on Diffusion Barriers

4.3.2.1 Copper-Phosphorus. Electronprobe microanalysis of the annealed samples with Cu-P barriers showed that copper and phosphorus had diffused into the overlay. The presence of Cu-Sn compounds could not be detected in this composite system, either by probe analysis or by optical examination. However, on prolonged annealing (more than thirty days) at temperatures above $100^{o}C$, the overlay became slightly copper-coloured, but both the methods of examination did not show copper-tin compounds. In the case of copper a gradient in concentration was observed, and the microprobe concentration profile, as shown in Figures 21a and 21b, may be approximated to an error function. This profile was used to calculate the diffusion coefficient

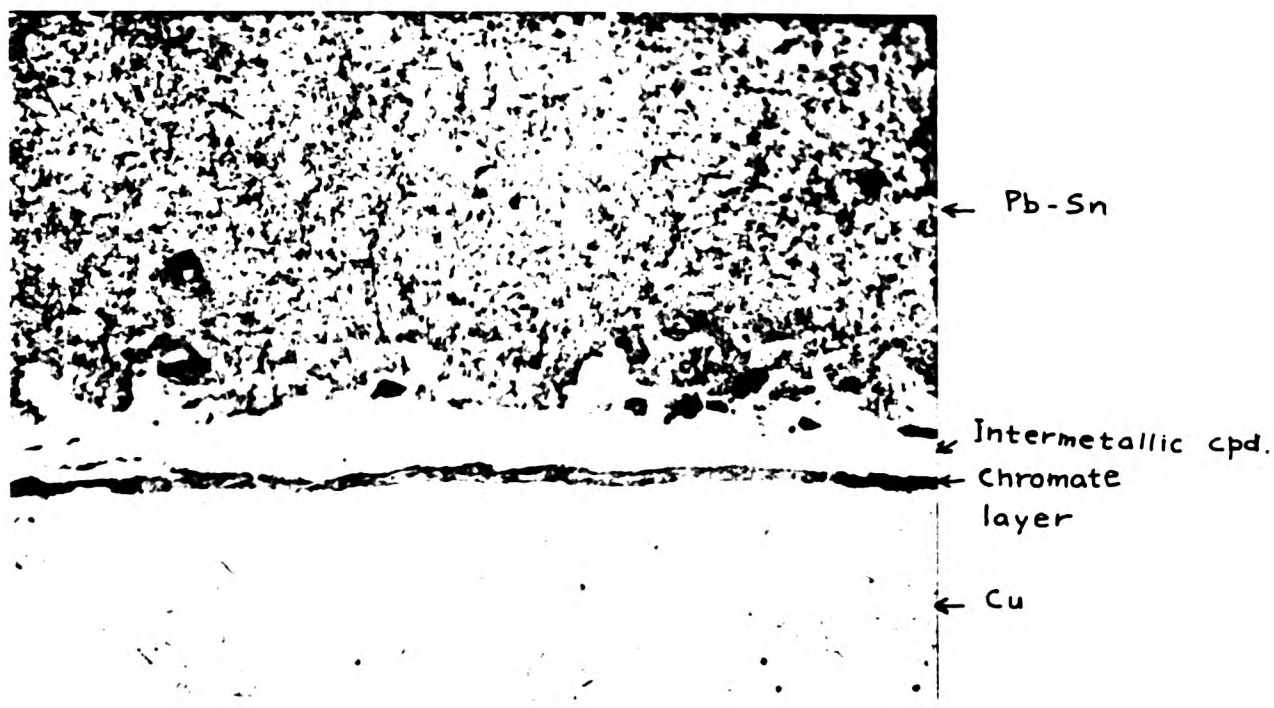

Figure 20. Micrograph of Pb-10^{w}/o Sn overlay deposited on a chromated surface of a Cu substrate. Intermetallic compound has formed between the chromate layer and the overlay. × 800.

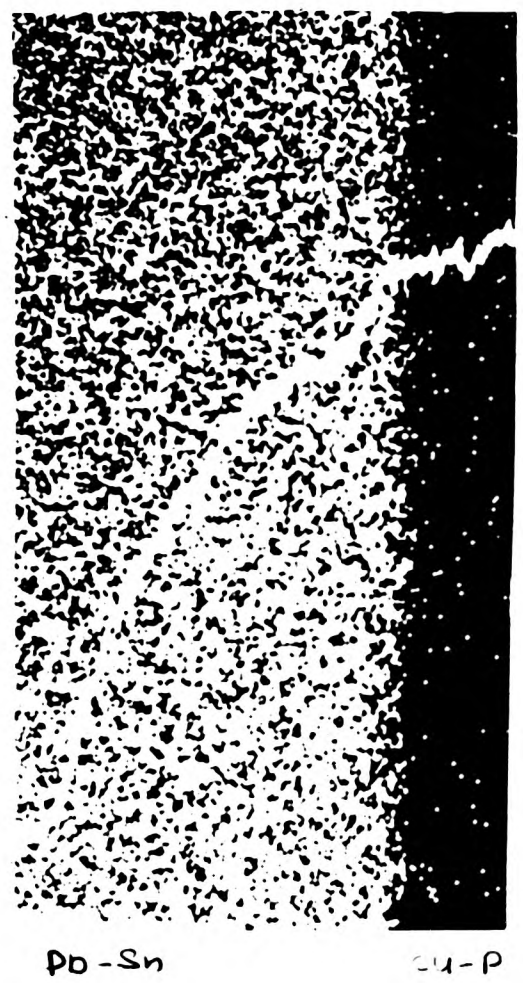

Figure 21a. X-ray/concentration profile of Cu, after annealing for 80 min at 140°C. Copper diffused into Pb-10 w/o Sn overlay from Cu-P

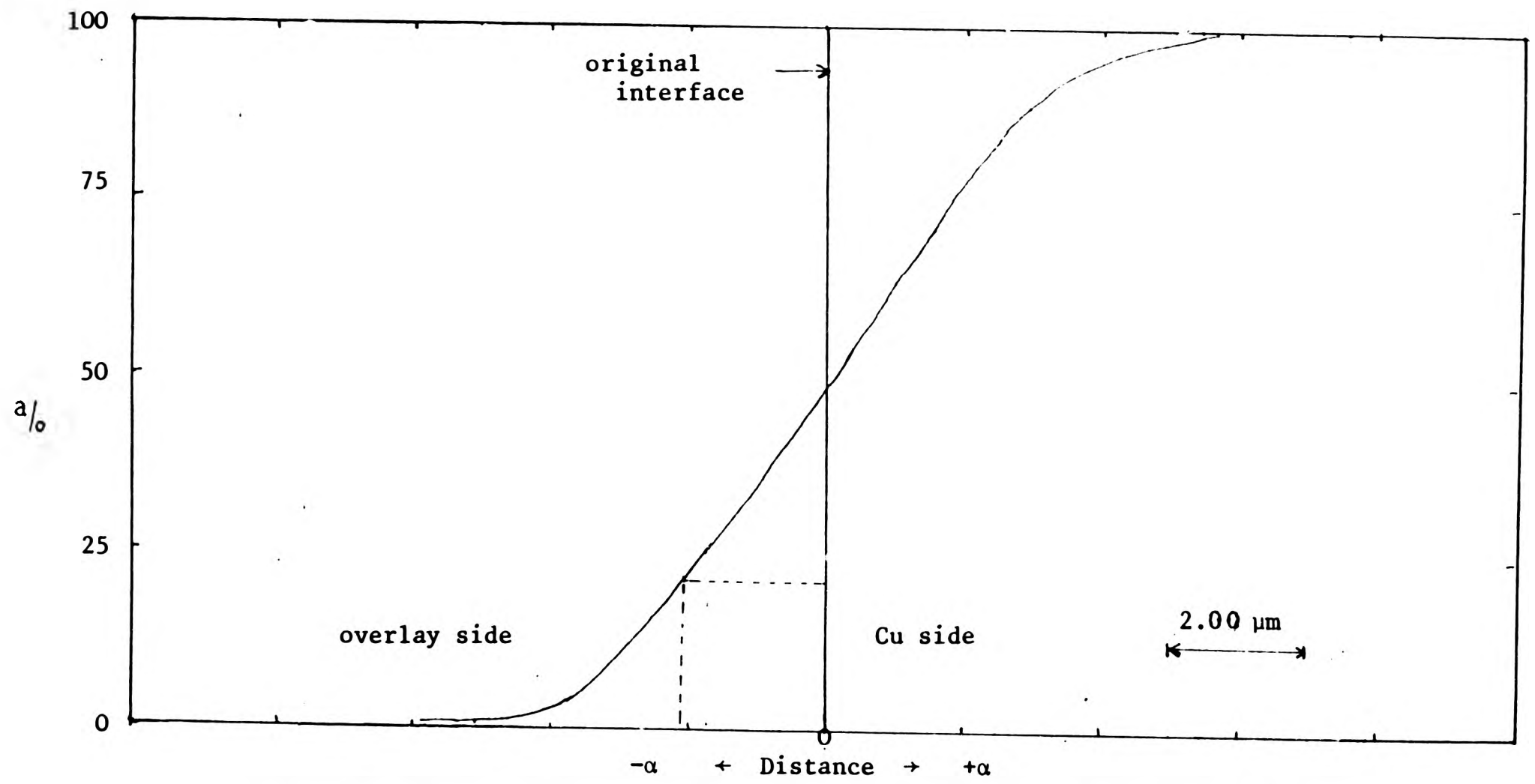

Figure 21b. Copper concentration profile in Pb-10 w/o Sn overlay at t = 4800s and 140°C (deduced from Figure 21a).

of copper in the overlay. The concentration profile of phosphorus was somewhat different as it resembled the growth of a finite phase, and was similar to that of oxide growth. The phosphorus profile, as shown in Figure 21c, does not show a gradient in concentration, except at the barrier/overlay interface and the diffusing phosphorus front but both the peripheral gradients may be due to instrumental inaccuracies. Transport of phosphorus in the overlay was found to be very fast. The diffusion coefficient of phosphorus in the overlay was calculated from the profile using Einstein-Smoluchowski equation (equation 2.7)

Figure 21a is the concentration profile of copper after annealing for 80 min at 140°C. Using equation 2.5 (section 2.3.3) for a value of x = - 2.13 μm, c = 22.5 a/o and from the plot

$$c = c_s - \tfrac{1}{2}(c_s - c_o)\ \mathrm{erf}\ \frac{x}{2\sqrt{Dt}} \qquad (2.5)$$

$$22.5 = 50\ (1 - \mathrm{erf}\ \frac{2.13 \times 1 \times 10^{-6}}{2 \times D^{\frac{1}{2}} \times (80 \times 60)^{\frac{1}{2}}}\ ) \qquad (4.7)$$

$$D = 8.15 \times 10^{-16}\ m^2\ s^{-1} \qquad (4.8)$$

The above value is the diffusivity of copper at 140°C in an electroplated Pb-10 w/o Sn alloy containing about 0.02 w/o P. Using D_θ and θ values for copper (Table 2) and equation (2.23) the activation energy for the diffusion process can be calculated,

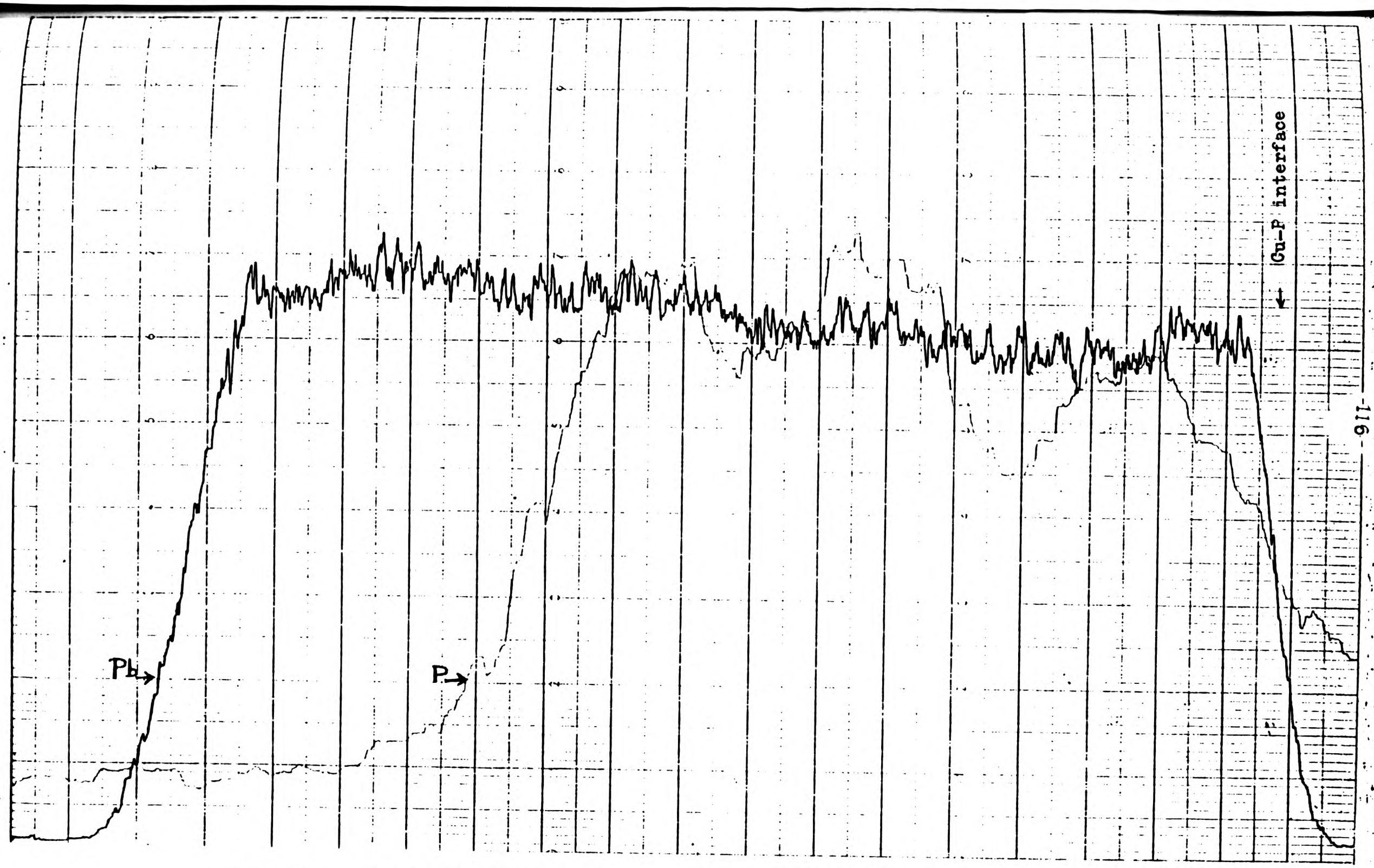

Figure 21c. X-ray/concentration profile of P in Pb-10 w/o Sn. P diffused from Cu-P alloy. Specimen annealed at 140°C for 80 minutes.

for copper: $D = 5.0 \times 10^{-10}\ m^2\ s^{-1}$, $\theta = 1880\ K$

$$D_{140^oC} = D_\theta \exp \frac{Q_D}{8.314} \left(\frac{1}{1800} - \frac{1}{413} \right) \qquad (4.9)$$

$$Q_D = 58.64\ kJ\ mol^{-1} \qquad (4.10)$$

The concentration profile of phosphorus in the overlay (Figure 21c), is similar to that expected for the growth of a compound where there is not change in concentration in the diffused area. Hence the Einstein-Smoluchowski equation (equation 2.7) can be used to calculate the diffusivity. From the profile at temperature 140^oC and time 20 min, the diffused distance x is 27.5 μm. Using equation (2.7),

$$x^2 = 2\ Dt \qquad (2.7)$$

$$D_{140^oC} = \frac{(2.75 \times 10^{-5})^2}{2 \times 20 \times 60} \qquad (4.11)$$

$$= 3.15 \times 10^{-13}\ m^2\ s^{-1}$$

Substituting values of $D_\theta = 1.024 \times 10^{-9}\ m^2\ s^{-1}$ and $\theta = 1150$ K values for phosphorus, and $D_{140^oC} = 3.15 \times 10^{-13}\ m^2\ s^{-1}$, in equation (2.23), the activation energy for the diffusion of phosphorus is calculated as:

$$Q_D = \frac{8.314\ \ln (3.15 \times 10^{-13}/1.02 \times 10^{-9})}{\frac{1}{1150} - \frac{1}{413}} \qquad (4.12)$$

$$= 43.33\ kJ\ mol^{-1}$$

for copper: $D = 5.0 \times 10^{-10}\ m^2\ s^{-1}$, $\theta = 1880\ K$

$$D_{140^oC} = D_\theta \exp \frac{Q_D}{8.314} \left(\frac{1}{1800} - \frac{1}{413} \right) \qquad (4.9)$$

$$Q_D = 58.64\ kJ\ mol^{-1} \qquad (4.10)$$

The concentration profile of phosphorus in the overlay (Figure 21c), is similar to that expected for the growth of a compound where there is not change in concentration in the diffused area. Hence the Einstein-Smoluchowski equation (equation 2.7) can be used to calculate the diffusivity. From the profile at temperature 140^oC and time 20 min, the diffused distance x is 27.5 μm. Using equation (2.7),

$$x^2 = 2\ Dt \qquad (2.7)$$

$$D_{140^oC} = \frac{(2.75 \times 10^{-5})^2}{2 \times 20 \times 60} \qquad (4.11)$$

$$= 3.15 \times 10^{-13}\ m^2\ s^{-1}$$

Substituting values of $D_\theta = 1.024 \times 10^{-9}\ m^2\ s^{-1}$ and $\theta = 1150$ K values for phosphorus, and $D_{140^oC} = 3.15 \times 10^{-13}\ m^2\ s^{-1}$, in equation (2.23), the activation energy for the diffusion of phosphorus is calculated as:

$$Q_D = \frac{8.314\ \ln (3.15 \times 10^{-13}/1.02 \times 10^{-9})}{\frac{1}{1150} - \frac{1}{413}} \qquad (4.12)$$

$$= 43.33\ kJ\ mol^{-1}$$

4.3.2.2 Chemical Analysis for Phosphorus in the Cu-P Electrodeposit.

The results of the chemical analysis for phosphorus in a Cu-P alloy electrodeposited from a sulphate bath are listed in Table 19. The phosphorus content was calculated using equation (3.1) (Section 3.6). The appearance of the Cu-P alloys becomes darker as the current density of deposition is decreased due to the increase in the phosphorus content. The alloys deposited at, and lower than, 0.2 A dm^{-2} were brittle and non-adhesive.

4.3.2.3 Effect of Current Density on P-Content of the Cu-P Electrodeposit.

As shown in Figure 22 there is an exponential relationship between the current density of deposition, in the range 0.2 - 1.5 A dm^{-2} , and the phosphorus in the alloy. The best fit obtained using a computer program [131] , is given by the equation:

$$[P] = 0.088 - 0.059 \ln (i/A\ dm^{-2}) \qquad (4.13)$$

where, [P] = Phosphorus content in $^{w}/o$

i = Current density in A dm^{-2}

4.3.2.4 Adhesion Tests for the Overlays and Composite Coatings.

The qualitative tests mentioned in Section 3.7 indicated good adhesion of both the Cu alloy and the overlay. In every test of the glued specimens when forced to separate, no peeling off of

TABLE 19. Phosphorus Content of Cu-P Alloys Deposited from a Sulphate Bath (TABLE 9) at Different Current Densities and at 40°C

i/A dm^{-2}	wt of Cu-P deposit/g	consumed 0.01 mol dm^{-3} NaOH vol/ml	w/o P
* 0.2	0.8560	118.7	0.187
0.3	0.5360	60.9	0.153
0.5	1.6355	148.7	0.122
1.0	1.7030	126.0	0.099
1.5	1.1182	48.5	0.058
2.0	1.2110	42.2	0.047

* Brittle deposit.

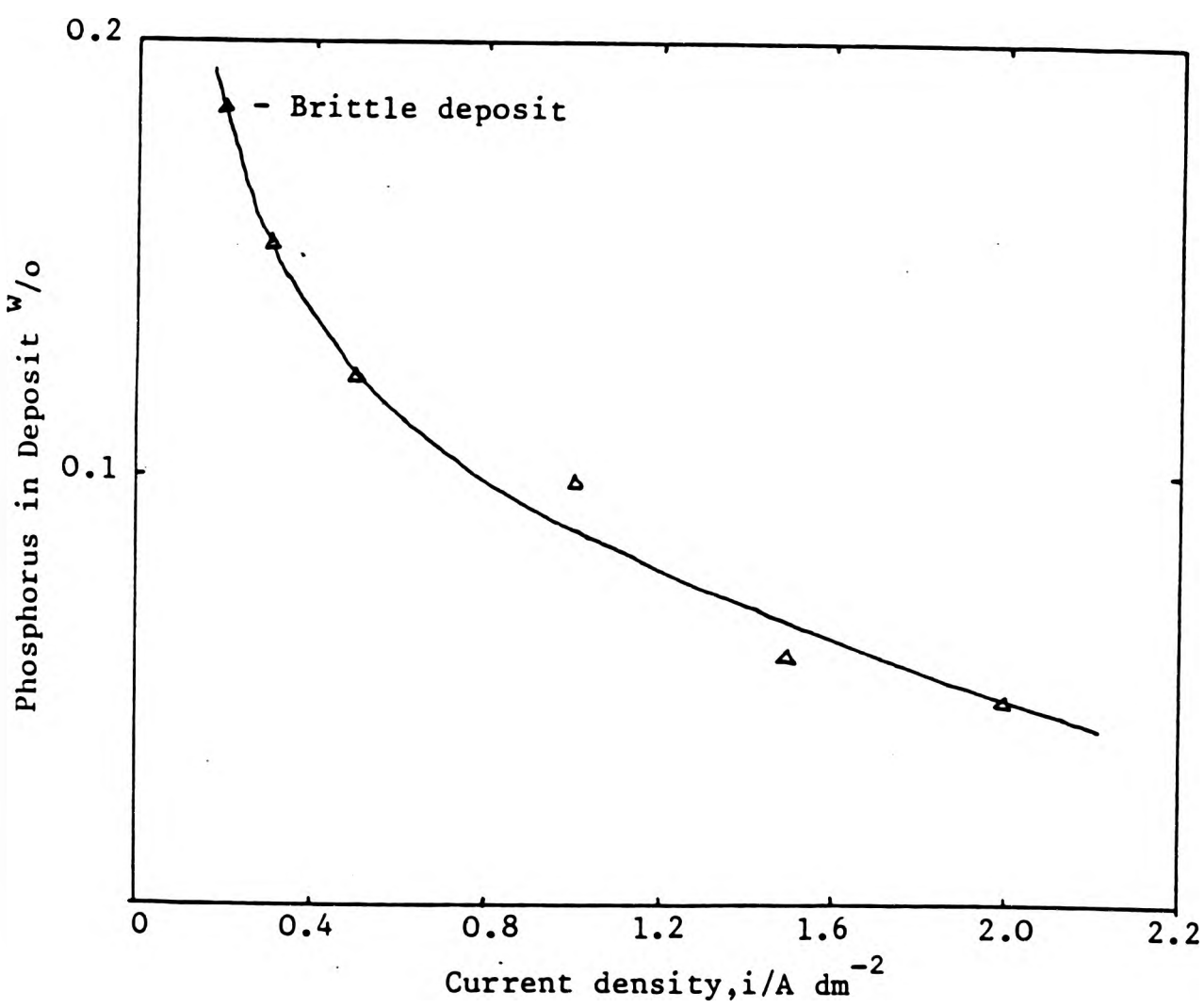

Figure 22. Effect of current density on the Phosphorus content of Electrodeposited Cu-P alloys. Bath composition in Table 9.

the electrodeposits were observed. Thermocycling made no difference to the quality of adhesion of the deposits. Microscopic examination of the sectioned surface showed no sign of separation from the electroplated interfaces.

4.4 PHOTOSENSITIVITY OF CURPOUS CHLORIDE DEPOSIT

When a copper cathode was immersed into the chloride bath (Table 8), prepared for depositing the Cu-P alloy, before connecting it to the electricity supply, a transparent film was formed on the surface. On 'live entry' this was not noticed. This film was later analysed using X-ray diffractometry and was found to contain cuprous chloride, which is soluble in water. The deposited layer became darker and eventually turned black on exposure to sunlight or white light. X-rays did not have a noticeable effect on this deposit. It was later discovered that such a photosensitive deposit could be obtained by dipping a clean copper surface in any cupric chloride solution.

4.5 RELATED CALCULATIONS

4.5.1. Solubility of Phosphous in Copper

Using the Arrhenius equation (equation 4.14), solubility of phosphorus at any temperature can be calculated, substituting published values of solubility and temperature, assuming that the activation energy is constant over the temperature range.

$$C = A \exp\left(-\frac{Q_c}{RT}\right) \qquad (4.14)$$

where, c = solubility; mol m^{-3}

Q_c = activation energy for solubility; J mol^{-1}

T = temperature; K

A = pre-exponential factor having the units of solubility

Re-arranging equation (4.14), in the following form:

$$\ln c = \ln A - \left(\frac{Q_c}{R} \cdot \frac{1}{T} \right) \qquad (4.15)$$

and plotting ln c versus T^{-1}/K^{-1} , and extrapolating as necessary, solubility values at the temperatures concerned can be obtained. Using the values in Hansen [130] , the plot in Figure 23 and Table 20, were constructed. The slope of the graph in Figure 23 is $-1462\ K^{-1}$ and from the intercept, $A = 9.76 \times 10^3$ mol m^{-3} .

4.5.2 Heat of Mixing and Excess Entropy of Mixing of Phosphorus in Copper

The heat of mixing and excess entropy of mixing of phosphorus in copper can be obtained using equation (2.41)(Section 2.4).

$$\ln N = \frac{\Delta S_{xs}}{R} - \frac{\Delta H_{xs}}{RT} \qquad (2.41)$$

By plotting $\ln N_p$ (mole fraction) versus T^{-1}/K^{-1} the gradian is (figure 24) -1440 and the intercept on y-axis is -1.9. Using equation (2.41) the heat of mixing $\Delta H_{xs} = 11972$ J mol^{-1} and excess entropy of mixing $\Delta S_{xs} = -15.79$ J mol^{-1} K^{-1} .

TABLE 20. Solubility of P in Cu in the temperature range 25-700 °C. (After Hansen. Ref 138).

T/°C	$T^{-1}/10^{-3}K^{-1}$	S_p/w/o	$x_p/10^{-2}$	ln x_p	$C_p/10^3$ mol m^{-3}	ln(C_p/mol m^{-3}
* 25	3.330	0.04	0.093	-6.98	0.079	4.380
* 140	2.420	0.20	0.404	-5.51	0.275	5.620
200	2.114	0.33	0.636	-5.02	0.460	6.131
300	1.745	0.60	1.192	-4.42	0.840	6.733
400	1.485	0.85	1.700	-4.07	1.190	7.081
500	1.290	1.10	2.200	-3.81	1.540	7.340
600	1.145	1.40	2.783	-3.58	1.960	7.580
700	1.050	1.70	3.400	-3.38	2.380	7.774

* Solubility values obtained from extrapolation.

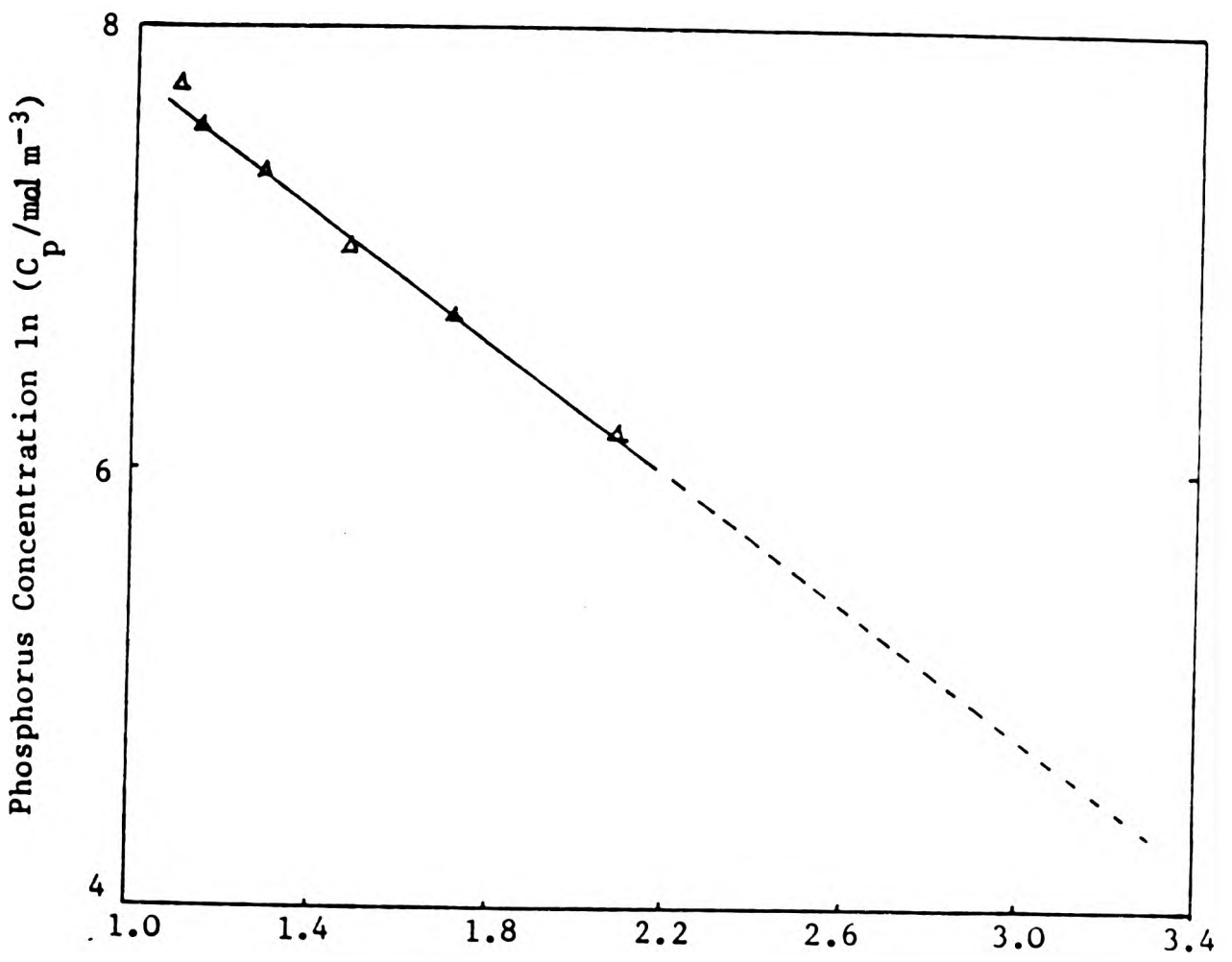

Figure 23. Solubility of Phosphorus in Copper. (After Hansen Ref 138).

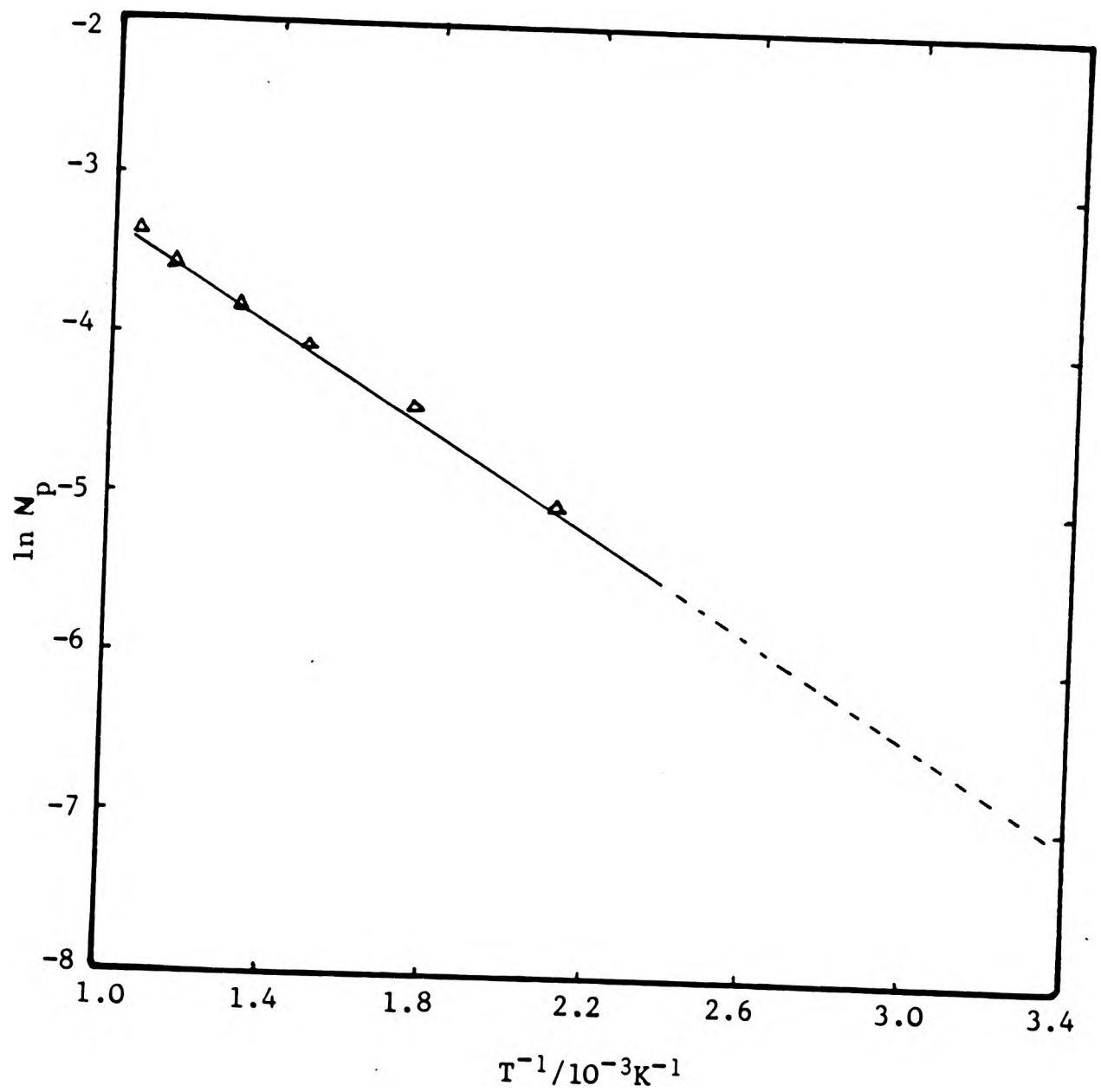

Figure 24. Solubility of Phosphorus in Copper
ln N_p (mole fraction) versus T^{-1}.

4.5.3 Diffusion of Phosphorus into Lead from an Electroless Ni-P Deposit

Using a concentration profile of phosphorus diffusing into an electrodeposit of Pb from an electroless nickel deposit [142], the diffusivity of phosphorus in lead was calculated. The concentration profile does not give the absolute values but only the intensity of radiations, which is proportional to the concentration. From the concentration profile (Figure 25), the values of $\ln \frac{I - I_b}{I_o - I_b}$ at different distances, x, were obtained and tabulated (Table 21). These values were plotted (Figure 26) and the slope of the graph gives $-\frac{1}{4Dt} = -3.39 \times 10^{11}$ (equation 2.9 and 2.10, Section 2.3.2).

$$-\frac{1}{4Dt} = -3.39 \times 10^{11} \qquad (4.15)$$

at $t = 3600s$,

$$D_{220^oC} = 2.04 \times 10^{-16}\ m^2\ s^{-1} \qquad (4.16)$$

Substituting D_θ and θ values for phosphorus (Table 2) and D_{220^oC} in equation (2.21), the activation energy and diffusion coefficient at 140^oC is calculated.

$$Q_D = \ln\left(\frac{2.04 \times 10^{-16}}{1.024 \times 10^{-9}}\right) \Big/ \frac{1}{8.314}\left(\frac{1}{1150} - \frac{1}{493}\right) \qquad (4.17)$$

$$= 110.67\ kJ\ mol^{-1}$$

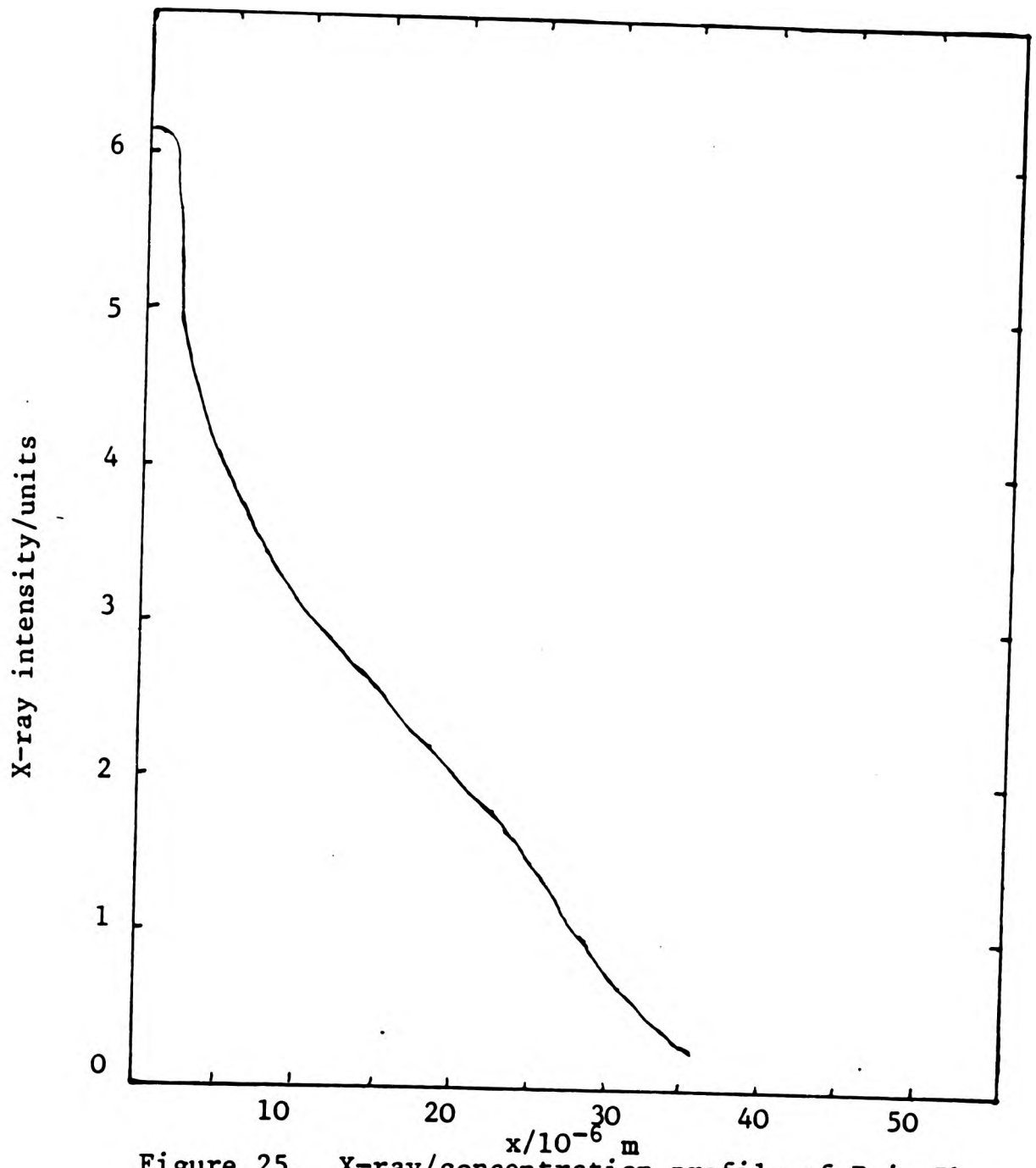

Figure 25. X-ray/concentration profile of P in Pb. Phosphorus diffused from a Ni-P electroless deposit at 220°C for 1 hr.

TABLE 21. Phosphorus concentration in lead at different distances from the interface at Ni-P alloy and Pb layer.
(Annealing time 1 hr at 220°C)

Distance $x/10^{6}m$	$x^2/10^{-12}m^2$	$I-I_b$ units	I_o-I_b units	$\ln(I-I_b/I_o-I_b)$
5	25	3.9	6.1	- 0.45
10	100	3.0	6.1	- 0.71
15	225	2.5	6.1	- 0.89
20	400	2.0	6.1	- 1.12
27	729	1.05	6.1	- 1.76
30	900	0.7	6.1	- 2.16

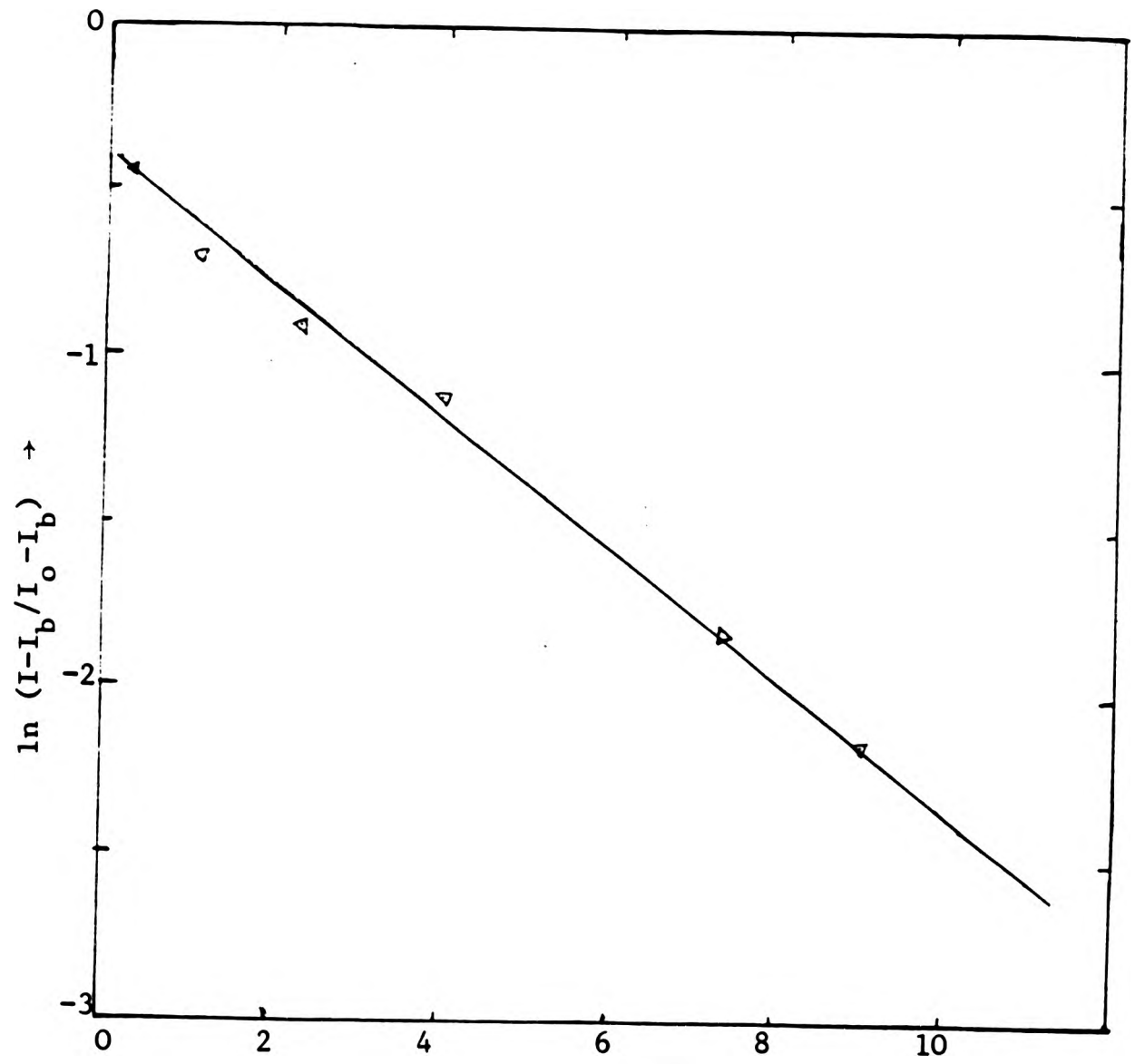

Figure 26. Plot of the distribution of phosphorus concentration in lead after annealing for 1 hr at 220°C. X-ray intensity $I-I_b/I_o-I_b$, is directly proportional to concentration. Phosphorus diffused from a Ni-P deposit to a lead layer.

and, $$D_{140^{\circ}C} = 1.024 \times 10^{-9} \exp \frac{110670}{8.314} \left(\frac{1}{1150} - \frac{1}{418} \right) \qquad (4.18)$$

$$= 1.09 \times 10^{-18} \ m^2 \ s^{-1}$$

4.5.4 Analysis of Diffusion Data.

Diffusion coefficients of the relevant metals in different matrices were calculated from the available published data and the experimental findings of the present investigation. The Arrhenius equation (equation 2.12) was used for the calculations where the activation energy and pre-exponential factor are available. In other instances, Wach's equation (equation 2.17) was used with the θ and D_θ values of the corresponding elements. Diffusivities of phosphorus in Cu, Sn and Pb were calculated using equation (2.17) with θ and D_θ values [57,140] of phosphorus and average activation energy values for the three matrices. These calculated values are listed in Table 22.

4.6 CORROSION RESISTANCE OF THE Pb-10 w/o Sn OVERLAY WITH IMPROVED BARRIERS

Qualitative evaluation of the rates of corrosion of the overlays provided with Cu-P or Cu-B barriers were not carried out in this project. However, some specimens with improved barriers and some without, were annealed, in a multigrade lubricating oil (SAE 30-50) used in petrol engines, at 160°C for 14 days. After this period the lubricating oil had completely deteriorated far beyond serviceability, and had transformed into a very dark, highly viscous substance with a bitumin appearance. The specimens without the barriers had completely lost the overlay, while the specimens with the Cu-P and Cu-B barriers retained most of the overlay.

TABLE 22 Diffusion coefficients.

Diffusant	Solvent	Q_D/kJ mol^{-1}	D_o/m^2 s^{-1}	D_{140^oC}/m^2 s^{-1}	Notes and References
Cu(self)	Cu	210.67	7.8×10^{-5}	2.7×10^{-31}	Ref 139; Arrhenius eq.
Cu(tracer)	Sn	33.02	2.4×10^{-7}	1.58×10^{-11}	" "
Cu(tracer)	Pb			3.7×10^{-11}	" "
Cu/Sn(interdiff)	Cu_3Sn	130.50	4.8×10^{-1}	(1.50×10^{-17} (6.58×10^{-23} (5.71×10^{-19}	" " " ;Wach eq. with θ_{Cu} and $D_{\theta(Cu)}$ " " " " θ_{Sn} and $D_{\theta(Sn)}$
" "	Cu_6Sn_5	127.20	1.25×10^{-1}	(1.02×10^{-17} (1.39×10^{-22} (9.48×10^{-19}	" ; Arrhenius eq. " ; Wach's eq.with θ_{Cu} and $D_{\theta(cu)}$ " " " "
" "	Cu_3Sn	95	-	-	Ref 80.
" "	Cu_6Sn_5/Cu_3Sn	75.11	4.54×10^{-8}	1.51×10^{-17}	Expt. values; see Section 4.2.2.1.
" "	"	39	-	-	Ref 63.
Cu	Pb/Sn/P	58.64	-	8.15×10^{-16}	Expt. values; see Section 4.3.2.1.
Sn(self)	Sn	107.00	8.2×10^{-4}	2.32×10^{-17}	Ref 139; Arrhenius eq.
Sn	Pb/Sn (sol.s)	100.32	4.0×10^{-4}	8.19×10^{-17}	" "
Sn	Pb	-	-	2.46×10^{-18}	Ref 141; Wach's eq. with θ_{Sn} and $D_{\theta(Sn)}$
Pb(self)	Pb	107.21	9.95×10^{-5}	2.74×10^{-18}	Ref 139; Arrhenius eq.
P(self)	P	114.53	$(3.6 \pm 1.4)10^{-4}$	1.85×10^{-18}	" "
P	Cu	204.4	-	2.64×10^{-26}	Av. Q of Ref 139 for Cu Matrix; Wach's eq. θ_P and $D_{\theta(P)}$
P	Sn	84.23	-	1.5×10^{-16}	" " " " "
P	Pb	73.87	-	1.05×10^{-15}	" " " " "
P	Pb	110.67	-	1.09×10^{-18}	Diffusion from Ni-P; see Section 4.5.3.
P	Pb/Sn	43.33	-	3.15×10^{-13}	Expt. values; see Section 4.3.2.1.
Ni/Sn(interdiff)	Ni_3Sn_4	76.57	1.45×10^{-8}	3.00×10^{-18}	Expt. values; see Section 4.2.2.2.
" "	"	37	-	-	Ref 63
" "	"	13-17	-	-	Ref 150

5. DISCUSSION

5.1 INTRODUCTION

The present investigation on lead-tin bearing overlays was carried out in order to find a solution to the problem of diffusion which caused premature failure of bearings. It has been demonstrated in the foregoing experiments that in the presence of an electrolytically deposited copper-phosphorus or a copper-boron alloy barrier, between overlay and the substrate, the problem of diffusion can be overcome. The process of electrodepositing the barriers has been recognised as commercially significant, and patents have been granted for the processes in view of future commercial exploitation by Shell Research Limited. It was thought that the above processes of depositing barriers may find use in the printed circuit board industry. Patent applications are appended at the end of the thesis.

It is understood that some work is being carried out in Japan to produce petrol and diesel engines using ceramic materials to run at temperatures much higher than in conventional engines. Improved bearings may find use in the new generation of engines and possibly in aircraft engines.

Literature searches, including patents, have revealed no reference to any work carried out with copper-phosphorus or copper-boron alloy diffusion barriers. Inclusion of some phosphorus in copper electrodeposits obtained from pyrophosphate baths have been observed by Sorkin et al [126] and Furlani et al [128], but the authors have not investigated the properties of such deposits.

A possible mechanism leading to the prevention of Cu-Sn intermetallic compound formation by phosphorus and boron is also presented.

5.2 INTERMETALLIC COMPOUNDS

Metallographic examination shows that copper forms two intermetallic compounds with tin. Using X-ray diffractometry, the first formed compound was identified as Cu_6Sn_5 and the second as Cu_3Sn (Figures 11a and 11b). Formation of Cu_6Sn_5 has been detected even at room temperature, with a well discernible layer of Cu_6Sn_5 formed after storing for about 30 days. At temperatures over 100^oC, Cu_6Sn_5 is transformed into Cu_3Sn, resulting in a duplex layer (Figure 9b). After the overlay is exhausted of its tin content, the Cu_6Sn_5 is totally transformed into the copper rich Cu_3Sn.

In the Ni-Sn system, only one compound, identified as Ni_3Sn_4, has been observed in the foregoing experiments, (Figure 11c). Two more compounds, Ni_3Sn_2 and Ni_3Sn have been identified by other workers [63,64] in cases where nickel has been in contact with tin alone, rather than a lead-tin alloy. Ni_3Sn_4 has the lowest free energy of formation (-312 kJ mol^{-1}), while Ni_3Sn_2 and Ni_3Sn have energies of -244 and -142 kJ mol^{-1} respectively.

From the copper-tin equilibrium diagram (Figure 27a) it can be seen that only two intermetallic phases (η and ε) exist at temperatures below about 200^oC. The η(and η') phase which has a hexagonal crystal structure, corresponds to the composition [149] Cu_6Sn_5 and the ε phase, with an orthorhombic crystal structure,

Equilibrium Diagrams

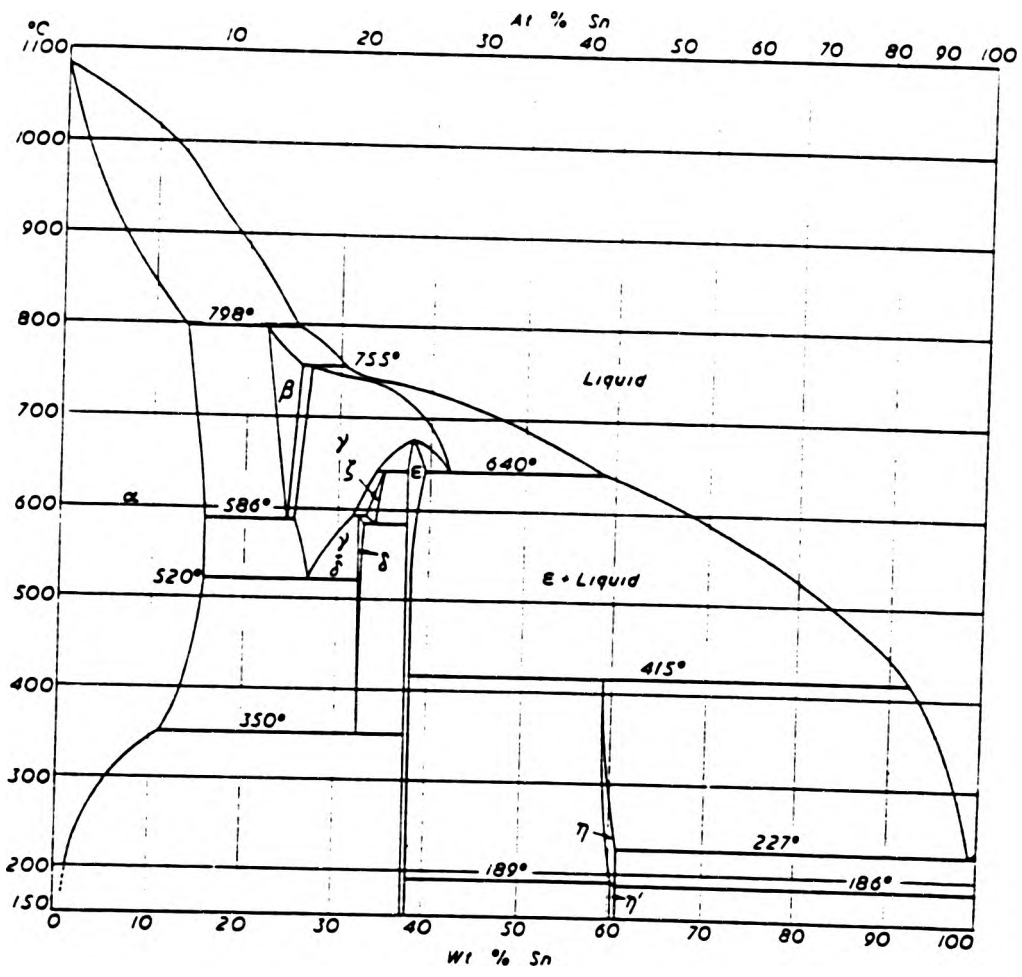

Cu-Sn

Figure 27a.

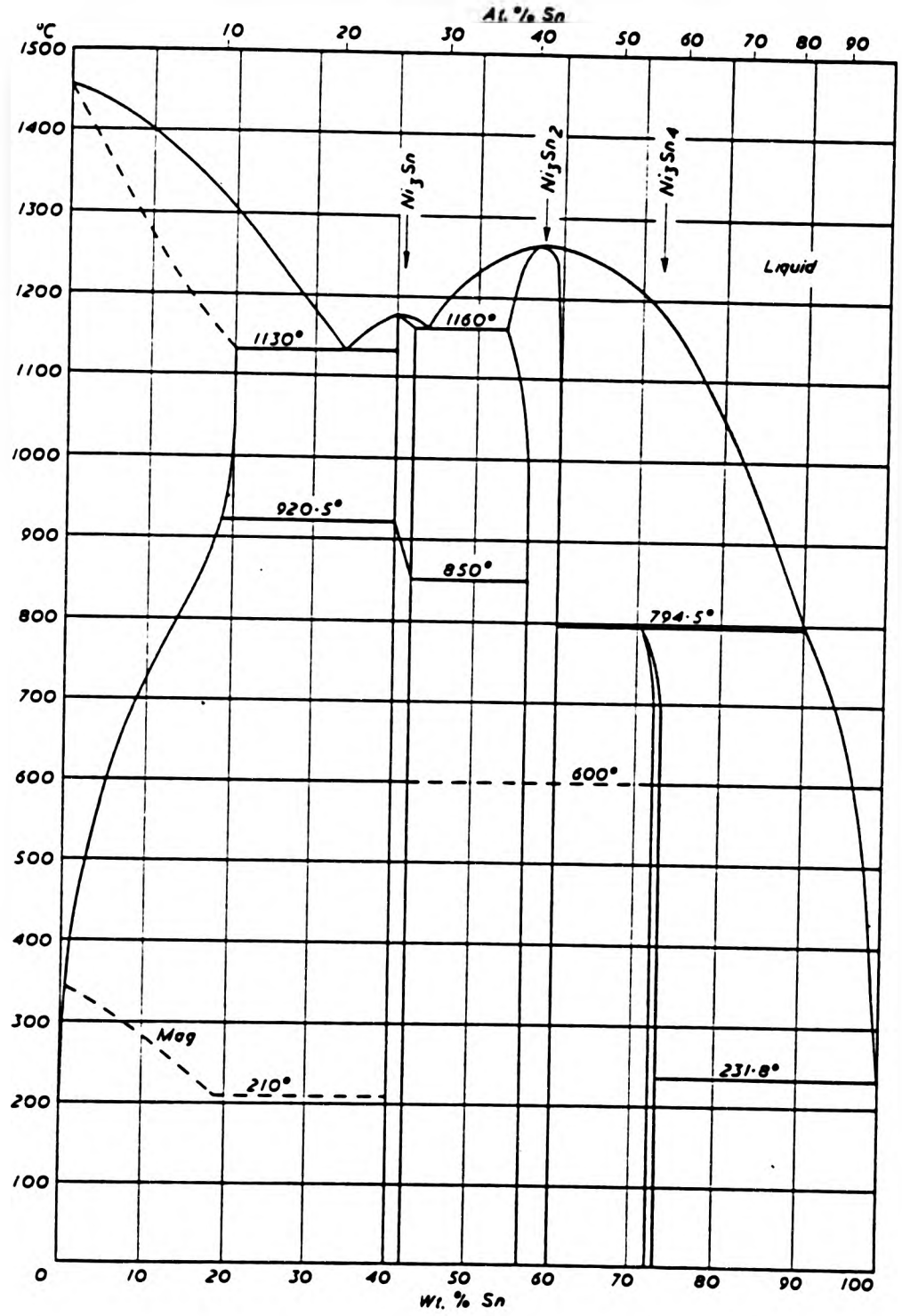

Ni-Sn

Figure 27b.

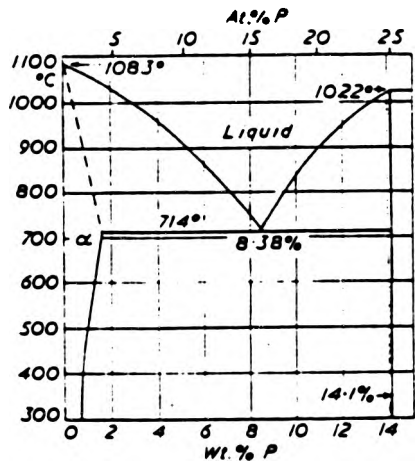

Cu-P

Figure 27c.

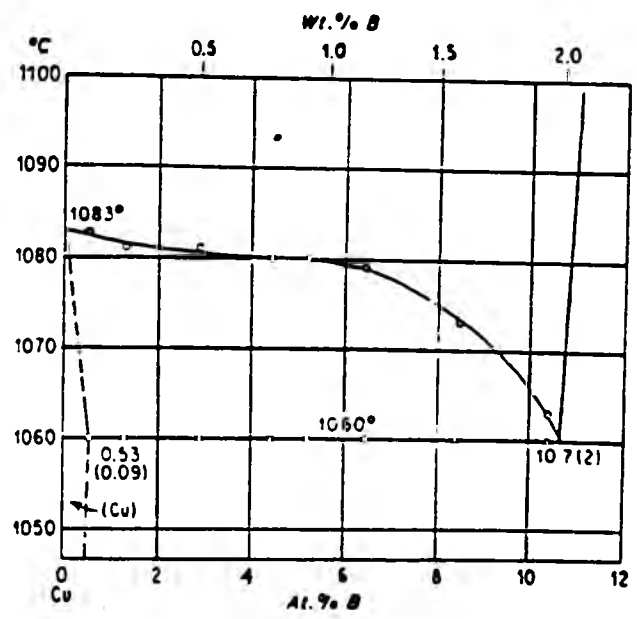

B-Cu

Figure 27d.

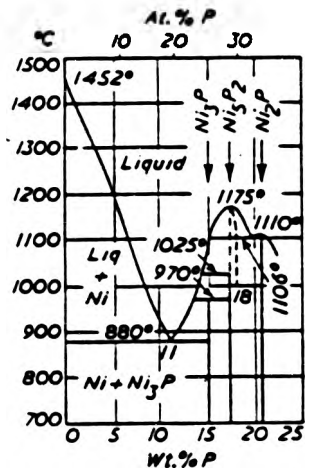

Ni-P

Figure 27e.

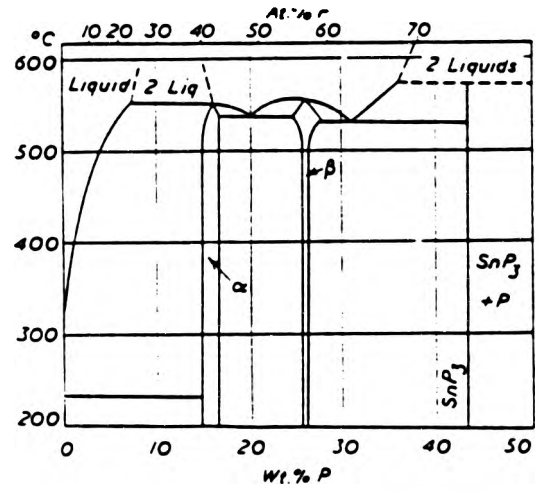

P-Sn

Figure 27f.

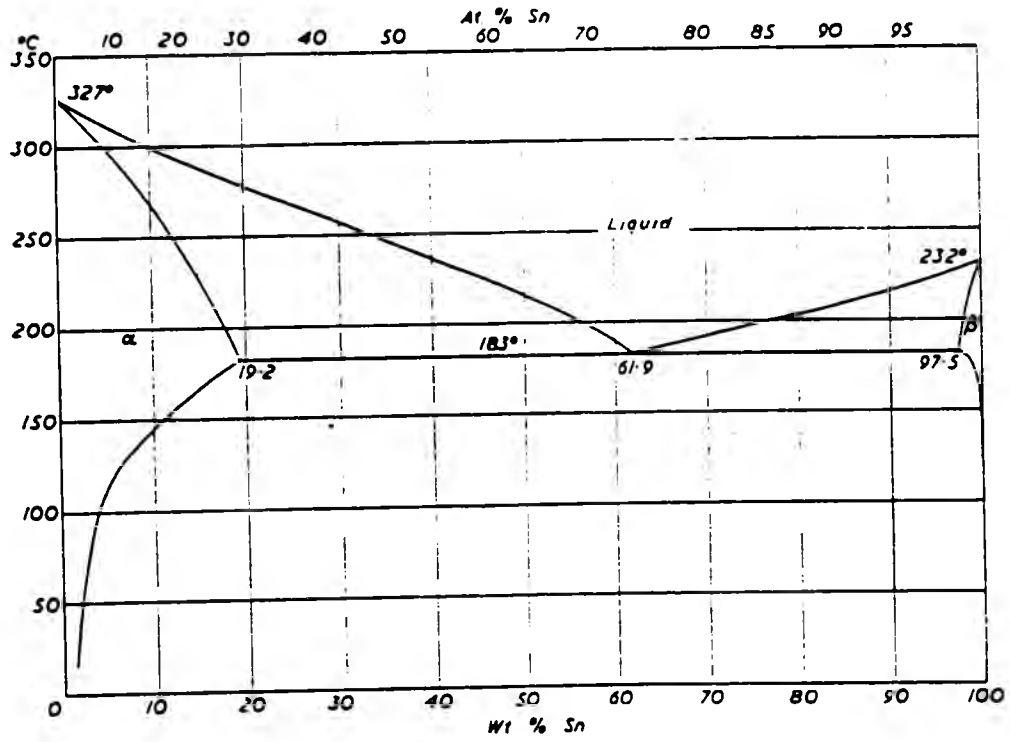

Pb-Sn

Figure 27g.

corresponds to the composition [149] Cu_3Sn. The Ni-Sn equilibrium diagram (Figure 27b) shows three intermetallic phases stable below about 200°C: Ni_3Sn_4, Ni_3Sn_2 and Ni_3Sn.

The formation of tin-rich compounds initially is in itself an evidence that the mass transport of copper and nickel in the compounds are rate controlling in their growth. This fact has also been established by Tu and Thompson [80] using a marker technique. The chromate layer and the CuS layer deposited on Cu in the present investigation (Sections 3.3.5 and 3.4) served as convenient markers. These showed that the compounds are formed between the marker layer and the overlay, confirming that the transport of copper atoms through the compound controls the growth process.

When a Ni-Sn alloy barrier (Section 4.2.1.3) was interposed, instead of a pure Ni barrier, between the copper substrate and the lead-tin overlay, the formation of a compound, most likely to be Ni_3Sn_4, was observed. The exact composition of this compound was not established. The formation of the compound showed the ineffectiveness of a Ni-Sn alloy layer as a diffusion barrier.

An electrodeposited layer of iron, interposed between the copper substrate and the overlay (Section 3.3.1), also formed a diffusion compound, not identified in this work. It can only be surmised that this compound was $FeSn_2$, which has been established by Castell-Evans [82], to form on steel, plated with tin.

5.3 KINETICS OF INTERMETALLIC COMPOUND FORMATION

5.3.1 Copper-tin System

The initial growth rate of the total compound was found to be parabolic as shown by the linearity of the plot of x^2 versus t (Figure 14). In the thickness measurements of the compound (Table 15) the total compound growth was considered rather than the growth of separate layers. Therefore the activation energy calculated from such results represents an average activation energy value for the growth of the two compounds. Kay and Mackay [63,64] adopted a similar method to calculate the overall activation energy for the process. However other workers [139] found that the activation energy values for the growth of Cu_6Sn_5 and Cu_3Sn were similar. Therefore the error involved in calculating an overall activation energy from the total compound thickness is relatively small.

Due to the exhaustion of tin in the overlay, the linearity of the x^2 versus t plot was limited to the initial few days, as can be seen in Figure 14. For this reason, only the initial linear parts of the plots were taken into account for the calculation of the diffusion coefficients (Section 4.2.2.1). The activation energy calculated from the diffusivity results for the copper-tin compound growth is 75.11 kJ mol^{-1} (Section 4.2.2.1). Kay and Mackay [63] obtained an activation energy of about half of the above values (39 kJ mol^{-1}). The difference is due to the fact that the authors used a relationship $x = (2Dt)^{\frac{1}{2}}$, whereas Einstein-Smoluchowski equation (equation 2.7) $x^2 = 2Dt$ was used in the present investigation. The value for the

activation energy obtained by Tu and Thompson [80] for the growth of Cu_3Sn is 95.0 kJ mol^{-1} and other workers [139] obtained 130.50 and 127.20 kJ mol^{-1} for the diffusion mechanisms of Cu_3Sn and Cu_6Sn_5 respectively. The discrepancy in the values of activation energy can be attributed to the different methods used by the authors. The higher activation energy for the growth of Cu_3Sn obtained by the authors, results from the lower activity of tin deposited by the electron gun [80], whereas an active electrolytic Pb-Sn alloy was employed in the present investigation and in that of Kay and Mackay. However, it is interesting to note that the values of interdiffusion coefficients at 140°C calculated in the present work (1.51×10^{-17} m^2 s^{-1}) and that of reference 139 (1.50×10^{-17} m^2 s^{-1} for Cu_3Sn and 1.02×10^{-17} m^2 s^{-1} for Cu_6Sn_5) are very similar (Table 22). Most likely this is due to the coincidence of the two growth rates at the temperature.

Kay and Mackay [63,64] claim that Arrhenius plots of copper-tin intermetallic compound growth from Pb-Sn coatings of different compositions (varying from 40-100 $^{W}/_{o}Sn$) give slightly different activation energies. However, an examination of the Arrhenius plots obtained by the authors from just four experimental results does not show a marked difference of the slopes and correspondingly of the Q_D values. This again can be regarded as another evidence for the transport of the copper being rate controlling in the diffusion process leading to the formation of Cu-Sn intermetallic compounds.

Using Wach's equation (equation (2.23) also, it can be shown that the diffusion of copper, rather than tin, controls the growth of the Cu-Sn intermetallic compounds. The value of Q_D calculated using θ and D_θ values for Sn from an experimentally obtained diffusion coefficient, is 103.10 kJ mol^{-1} and the corresponding value of Q_D for Cu is 75.95 kJ mol^{-1} (Section 4.2.2.1). The value for Cu is lower and is very similar to the activation energy obtained experimentally using Arrhenius equation (equation 2.17), and Figure 15. It is well recognised that for the growth of compounds, controlled by diffusion, the component exhibiting the lowest activation energy is rate controlling. Thus the mass transport of copper, rather than tin, controls the overall growth. This mechanism of growth of intermetallic compounds of copper and tin has been predicted by Tu and Thompson [80].

5.3.2 Nickel-tin System

As in the case of Cu-Sn compound growth, the growth of Ni_3Sn_4 was initially parabolic, as indicated by the straight line relationship of x^2 to t (Figure 16). Due to the exhaustion of tin the linear relationship was only limited to an initial period, the duration of which decreased with the increase in temperature. Diffusion coefficients were calculated from the initial gradients of the x^2 versus t plots (Section 4.2.2.2). The activation energy calculated from an Arrhenius plot of the diffusivities for the process is 76.57 kJ mol^{-1}. The value obtained by Kay and Mackay[63,64] using the relationship $x = kt^{\frac{1}{2}}$ is 37 kJ mol^{-1}. The factor of 2 difference in magnitude between the two values comes from the fact that the rate constant $k = (2D)^{\frac{1}{2}}$. The values of activation

energies for different stages in the interdiffusion of liquid tin and solid nickel, obtained by Kang and Ramachandran [150] vary from 13.0 to 17.1 kJ mol^{-1}. The authors have used the relationship $x = Dt^n$ (n = 0.54, 0.62 and 0.63 for initial, intermediate and final stages respectively) in the growth process. At the temperatures employed by the authors in their experiments (300 - 520°C), two more nickel-tin intermetallic phases (Ni_3Sn_2 and Ni_3Sn) have been observed in addition to Ni_3Sn_4. The authors conclude that the rate controlling step is the diffusion of nickel in liquid tin, since their values are in agreement with the value of activation energy for the diffusion of nickel in liquid reported by Ma and Swalin [152].

Wach's equation (equation 2.23), in this case also, as shown in Section 4.2.2.2, can be used as a further evidence of Ni being the rate controlling species in the growth of Ni-Sn compounds. The calculated Q_D value is 76.75 KJ mol^{-1} which is very similar to the experimentally obtained value (76.57 kJ mol^{-1}) from an Arrhenius plot. The activation energy for Sn, calculated using equation (2.23), is much higher (112.22 kJ mol^{-1}), hence Ni, with a lower activation energy, controls the growth of Ni_3Sn_4.

5.4 Cu-P AND Cu-B ALLOY PLATING SOLUTIONS

It has been demonstrated in the foregoing experiments that phosphorus and boron can be successfully co-deposited with copper In order for two metals to codeposit these must be in an electrolyte that provides a cathodic film in which the individual deposition potentials should be similar. In an alloy plating bath, the static electrode potential E_s of a metal is given by:

$$E_s = E^{\ominus} + \frac{RT}{nF} \ln a_{M^{z+}} \qquad (5.1)$$

The equation is applicable for conditions of reversibility. Since electrodeposition is obtained under the irreversible conditions, equation 5.1 cannot indicate the true deposition potential, which is a dynamic value associated with the discharge of cations at a definite rate. The deposition potential, given by equation (5.2), includes a term E_i, which gives the difference of the static and the deposition potential.

$$E_d = E^{\ominus} + \frac{RT}{nF} \ln a_{M^{z+}} + E_i \qquad (5.2)$$

In both the equations (5.1 and 5.2), $a_{M^{z+}}$ is the activity of the depositing cation in the cathode film. $E^{\ominus}$ is the standard equilibrium electrode potential, and E_i denotes a rate factor, expressed as the extra potential required to keep the deposition going at the given speed under the prevailing experimental conditions.

The deposition of phosphorus, copper and boron can occur according to one, or more, of the reactions of equilibrium [155,156] given in Table 23. The $E^{\ominus}$ values of phosphorus and boron are far apart from those of copper, and codeposition prospects appear to be remote. For codeposition to take place the E_d value of the copper cation should be lowered to the E_d values of phosphorus or boron. This can be achieved by lowering the activity of copper cations by reducing the concentration of copper ions in the vicinity of the cathode. The concentration of copper in the baths developed to deposit Cu-P and Cu-B alloys (Tables 8-10) is much lower than the concentrations of copper in conventional baths used to electroplate the copper

metal. It may also be possible that in the presence of phosphate and phosphite ions copper forms a complex ion which reduces the copper ion activity resulting in a lower deposition potential.

Milazzo and Caroli [156] give two reactions of reduction of $CuHPO_4$ and $Cu(H_2PO_4)_2$ to copper and neither of them has an $E^{\ominus}$ value as low as that of phosphorus or boron deposition (Table 23). Considering an $E^{\ominus}$ value of 0.34V for Cu and −0.51V for P, it is seen that (Table 23) the activity of the copper cations should be as low as 1×10^{-5}, in order that the deposition potential of Cu is lowered to that of phosphorus. The concentration of Cu^{2+} in the bath in Tables 9 and 10 is about $0.2 mol dm^{-3}$ and the activity of Cu^{2+} cannot be expected to be much less than 1×10^{-2}. It may be assumed that the remaining potential drop comes from the concentration over-potentials. To a degree this is contradicted in practice since higher phosphorus content in the deposit is obtained at lower current densities, hence at a lower concentration polarisation (Figure 22).

The cupric sulphate bath (Table 9) developed to deposit Cu-P alloy was superior to the chloride bath (Table 8), since the former was more controllable. The deposit obtained from the chloride bath without 'live entry' was less adhesive due to the formation of cuprous chloride film. The reduction of cupric chloride to cuprous chloride in the presence of metallic copper can occur by the reaction in equation (5.3)

$$Cu_{(s)} + CuCl_{2(aq)} = 2CuCl_{(s)} \qquad (5.3)$$

The photosensitivity of cuprous chloride may be due to the formation of black cupric oxide in the presence of oxygen catalysed

by light, perhaps according to the equation (5.4)

$$Cu_2Cl + O_2 + Cu = 2CuO + CuCl \qquad (5.4)$$

In the deposition of Ni-P and Cu-P alloys studied by Brenner [115], and in the study of Cu-P alloys deposition from pyrophosphate baths by Sorkin et al [126], it has been observed that a lower current density deposits a higher concentration of phosphorus. The results of the experiments (Section 4.3.2.2) in the present work established that the current density bears an exponential relationship to the concentration of phosphorus in the deposited alloy, as given by equation (4.13).

$$[P] = 0.088 - 0.059 \ln (i/A\ dm^{-2}) \qquad (4.13)$$

The relationship is not quoted in the published literature. The above relationship may be applicable only within the current density range of 0.2 - 2.0 A dm^{-2} (Figure 22). The deposits obtained at current densities less than 0.2 A dm^{-2} were loose, non adherent and brittle. The corresponding phosphorus content to a current density 0.20 A dm^{-2} is 0.187 w/o. As shown in Table 19, adhesive epitaxial deposits contain 0.187 - 0.047 w/o P. A further observation from this experiment is that adhesive epitaxial deposits of Cu-P contain a maximum of approximately 0.18 w/o P, which can be deposited at a current density of 0.2 A dm^{-2} .

In the case of boron, assuming the boron deposition potential is -0.87 V, the activity of copper ions should be lowered to 1×10^{-21} for codeposition to be possible. No reference could be found on Cu-B electrodeposition in the published literature. The laboratory equipment, and analytical techniques used, were not

TABLE 23 Standard Electrode Potentials at 298K Relevant to Cu-P and Cu-B Alloy Deposition

Electrode Reaction	$E^{\ominus}$/V
(1) $H_3PO_4(aq) + 2H^+(aq) + 2e^- \rightleftharpoons H_3PO_3(aq) + H_2O(\ell)$	−0.28
(2) $H_3PO_3(aq) + 2H^+(aq) + 2e^- \rightleftharpoons H_3PO_2(aq) + H_2O(\ell)$	−0.50
(3) $H_3PO_2(aq) + H^+(aq) + e^- \rightleftharpoons P(s) + 2H_2O(\ell)$	−0.51
(4) $Cu^{2+}(aq) + 2e^- \rightleftharpoons Cu(s)$	+0.34
(5) $Cu^+(aq) + e^- \rightleftharpoons Cu(s)$	+0.52
(6) $Cu(H_2PO_4) + 2e^- \rightleftharpoons Cu(s) + 2H_2PO_4^-(aq)$	+0.20
(7) $CuHPO_4 + 2e^- \rightleftharpoons Cu(s) + HPO_4^{2-}(aq)$	+0.17
(8) $H_3BO_3(aq) + 3H^+(aq) + 3e^- \rightleftharpoons B(s) + 3H_2O(\ell)$	−0.87
(9) $HBO_3^{2}(aq) + 5H^+(aq) + 3e^- \rightleftharpoons B(s) + 3H_2O(\ell)$	−0.43
(10) $H_2BO_3^- + 4H^+(aq) + 3e^- \rightleftharpoons B(s) + 3H_2O(\ell)$	−0.68

able to evaluate the boron content deposited in the electroplating process described in Section 3.3.4. However, the deposits obtained at a current density in the range 0.8 to 1.5 A dm^{-2} , served as efficient diffusion barriers retarding, if not preventing altogether, the formation of Cu-Sn intermetallic compounds. As mentioned in Section 4.3.1.2, the Cu-B alloy deposited at 0.5 A dm^{-2} was not as efficient as those deposited at higher current densities. That may be an indication that lower current densities produce alloys of lower boron content in contrast to the findings with the Cu-P alloys deposition. In this case the argument of concentration polarisation contribution to lower the copper ion activity appears to be plausible.

5.5 EFFICACY OF THE Cu-P AND Cu-B ALLOY DIFFUSION BARRIERS

No evidence has been cited in the published literature, including patent literature, concerning the function of Cu-P and Cu-B diffusion barriers. The presence of some phosphorus in copper-electrodeposits from pyrophosphate baths has been observed by Sorkin et al [128] . The authors have not investigated the properties of such deposits.

Microscopic examinations show that these new barriers are extremely efficient as to the prevention of intermetallic compound formation, and hence depletion of tin from the overlay, below the critical value of 2^{w}/o Sn, in the lead-tin overlay in order to forestall lead dissolution in oxidised hot oils leading to bearing degradation.

After annealing the Cu-P alloy barried samples phosphorus and some copper had diffused intothe overlay without any interface compound formation. There appears to be a quaternary effect in that the solubility of Cu in the Pb-Sn overlay is increased by the presence of phosphorus in the overlay. The presence of Cu in Pb-Sn overlays is known to enhance their mechanical performance. Therefore a process of Cu diffusion into the bearings overlays in service may serve the purpose of self-healing during unusually severe service conditions. Some conventional bearing materials contain as much as $2^{w}/o$ Cu as mentioned in Section 1.

The diffusivity of phosphorus in the overlay at $140^{o}C$ was calculated as 3.15×10^{-13} m^2 s^{-1} and that of Cu as 8.15×10^{-16} m^2 s^{-1} (Section 4.3.2.1). Therefore, although the formation of Cu-Sn compounds is prevented by the Cu-P diffusion barrier, some of the bearing properties of Pb-$10^{w}/o$ Sn overlay may have changed due to the presence of small quantities of phosphorus and copper, after annealing. It was not possible to calculate the exact concentration of phosphorus present in the overlay after reaching equilibrium, since the X-ray profile is not a true representation of the concentration. However, since the original concentration of P in the Cu-P barrier is around $0.1^{w}/o$ and the width of the barrier is 20% of the composite overlay, havingadensity about 1½ times that of Cu, even if all the P were transferred from the barrier to the overlay the maximum concentration of phosphorus at equilibrium would be less than about $0.01^{w}/o$. The percentage of copper in the overlay at equilibrium was not assessed.

At equilibrium the activities of phosphorus in the overlay and the Cu-P alloy are the same. Wach [103,137] shows that the activity of a species is given by the quantity $D^{\frac{1}{2}}c$. The estimated value of 0.01 w/o P at equilibrium in the overlay can be used together with the diffusivity of phosphorus in the overlay and the original concentration of phosphorus in the Cu-P alloy to estimate the diffusivity of P in the Cu-P alloy.

$$D_1^{\frac{1}{2}} c_1 = D_2^{\frac{1}{2}} c_2 \qquad (5.5)$$

$$D_2 = \frac{3.15 \times 10^{-13} \times (0.01)^2}{(0.1)^2} = 3.1 \times 10^{-15}\ m^2\ s^{-1} \qquad (5.6)$$

This estimated value is about $3.1 \times 10^{-15}\ m^2\ s^{-1}$. This value is much higher than the diffusivity of P in the copper matrix ($2.6 \times 10^{-26} m^2\ s^{-1}$) estimated from average activation energy for the copper matrix and θ and D_θ values for phosphorus (Table 22). This shows that electrodeposits are more active in regard to mass transport and that data obtained from other sources do not readily lend themselves to the interpretation of interdiffusion of active electrodeposits.

5.6 ADVANTAGES OF THE Cu-P AND Cu-B ALLOY BARRIERS OVER THE CONVENTIONAL BARRIERS.

Nickel is the most widely used barrier in the plain bearings industry. Iron and cobalt also have been suggested for the purpose by some workers [64]. It is evident that none of the above barriers prevent the formation of intermetallic compounds with tin and hence its depletion from the overlay. An electrodeposit of nickel is sometimes used as a preplate to the overlay for better adhesion to the substrate. The practice would appear to be undesirable and harmful

for the following reasons:

(i) the extra cost of an electroplating operation;

(ii) a hard Ni layer, most likely containing fairly high content of occluded hydrogen, may add to the danger of journal damage in case of overlay failure; and

(iii) the Cu-P and Cu-B barriers give far better performance at a lower cost.

Similar considerations apply to the other metal preplates.

Kay and Mackay [63,64] claim that the reaction of an iron barrier with tin is slower than that of a nickel barrier, and that after annealing at 170°C for 400 days the coating had not fully reacted. As the authors point out, using iron as a preplate material involves iron plating followed by an immediate plating of an adequate coating of tin or lead-tin alloy, to prevent atmospheric corrosion of iron leading to poor adhesion of the overlay. Cu-P and Cu-B alloys preplates, in place of pure Cu, can be profitably employed in the printed circuit board and allied industries where problems are experienced with short shelf life on account of Cu-Sn compound formation and whisker growth which may lead to short circuiting. This would entail only a slight compositional modification of the conventional bath composition and the operating temperature. The Cu-P and Cu-B barriers also provide a better adhesion of the overlay due to the 'keying effect' of the microscopically rough surface contour, which is obtained in the absence of a levelling agent in such baths (Tables 8 - 10). The imposition of efficient Cu-P and Cu-B diffusion barriers may allow the use of Pb-Sn overlays with lower Sn content. However,

the influence of alloy composition modification still remains to be investigated in the light of the findings presented in this work showing that P and Cu enrichment in the overlay takes place in service and could serve the purpose of self healing.

5.7 THE ROLE OF PHOSPHORUS IN THE CONTROL OF DIFFUSION COMPOUND FORMATION

The factor which determines whether the barrier is effective in preventing the formation of diffusion compounds or not is that the alloying element is in excess of a certain minimum level. This level, in the case of phosphorus, is about 0.5 to 0.15 percent by weight. The minimum percentage in the case of boron has not been established. However, by comparison, levels similar to above may be expected. By choosing a current density between 0.5 to 1.5 A dm^{-2} copper-phosphorus alloys of the required composition (0.05 - 0.15 $^{w}/o$ P) can be obtained. In the case of Cu-B alloys the range of current densities which would deposit an efficient barrier is between 0.8 to 1.5 A dm^{-2} .

The solubility of phosphorus in copper at 140^{o}C is 0.20 $^{w}/o$ (Table 20). The alloys, obtained at the current densities mentioned above, are in the solid solution region. The solubility of boron in copper at lower temperatures is not available, but it has a solubility less than that of phosphorus. Since it was not possible to estimate the concentration of boron in the deposit, no inference can be made as to boron being in solid solution or not. The equilibrium diagrams of the systems involved are displayed in Figure 27.

Two important observations have been made concerning annealed Cu-P barriered specimens:

(a) phosphorus has diffused into the overlay at a significantly fast rate:

(b) there is no indication of intermetallic compound formation.

The diffusion coefficient of phosphorus in the overlay at 140°C has been calculated as 3.15×10^{-13} m^2 s^{-1} with an activation energy of 43.33 kJ mol^{-1} (Table 27). This value is the overall activation energy required for the phosphorus atoms to break the Cu-P bonds and diffuse through the Cu lattice and the Pb-Sn lattice of the overlay. When phosphorus atoms diffuse from an electroless nickel deposit into the overlay, the diffusion rate is much lower and the activation energy much higher. The diffusion coefficient in this instance is 1.09×10^{-18} m^2 s^{-1} at 140°C, with an activation energy of 110 kJ mol^{-1} (Table 22) as shown in Section 4.6.3. This high value of overall activation energy shows that it is much more difficult for the phosphorus to break the Ni-P bonds and diffuse through the Ni-P lattice. Electroless nickel deposits are known to have phosphorus in the form of phosphides. It is therefore understandable that the Ni-P bonds are much stronger than those in Cu-P solid solution. The positive heat of solution in the Cu-P system also shows the weak Cu-P bonds. Nickel forms a number of phosphides which shows that the two elements have strong affinity for each other. In addition the solid solubility of phosphorus in nickel is very low as seen in the equilibrium diagram (Figure 27e), whereas an appreciable quantity of phosphorus dissolves in copper (Figure 27c and Table 20).

Tin and phosphorus also have an affinity for each other, which is indicated by the formation of a number of tin phosphides. The equilibrium diagram of Sn and P (Fig 27f) shows that, as in the case of nickel, the solid solubility of phosphorus in tin is very low. Equilibrium data for Pb and P are not available in the published literature. At 140°C the diffusivity of tin in lead, and lead-tin alloys, is 2.46×10^{-18} and 8.19×10^{-17} m^2 s^{-1} respectively (Table 22). Both values are much lower (by 5 orders of magnitude) than the diffusivity of phosphorus in the overlay from a Cu-P matrix. Diffusivity of phosphorus into the overlay from a Ni-P matrix is much lower than that of tin in the lead-tin alloy. At 140°C the diffusivity of copper in the overlay is 8.15×10^{-16} m^2 s^{-1} and is a little higher than that of tin in the overlay.

Vacancies in dilute alloys are known to associate with solute atoms preferentially in solution. This effect is known as the Johnson effect. The binding of vacancies to the impurity atoms increases the effective vacancy concentration near those atoms so that the mean jump rate of the solute atoms or impurity atoms is much increased. This association helps the solute atoms to move through the lattice, but conversely, the speed of migration of the vacancy is reduced because it lingers in the neighbourhood of the solute atom.

Fast movement of the phosphorus atoms from the Cu-P lattice into the vacancies around tin atoms in the overlay, could slow down the diffusivity of tin atoms, effectively 'locking up' the

tin atoms. Thermodynamically this implies that the activity of tin atoms is reduced. Wach [137] associates diffusivity with the activity and states that the quantity $D^{\frac{1}{2}}c$ gives a measure of activity. It may be that it is the lowering of the activity of tin in the overlay which prevents the formation of Cu-Sn intermetallic compounds.

The prevention of corrosion of Pb-Sn overlays by tin contents in excess of 2 w/o is thought to be due to the transport of tin atoms to the surface, and subsequent formation of a protective tin oxide layer [7]. It may be possible that the lowering of the activity of tin in the overlay, as suggested above, may affect its corrosion resistance characteristics. On the other hand, the concentration of tin atoms already 'locked up' in the Pb-Sn alloy may be sufficient to provide a protective oxide film. The latter view is supported by the results of the preliminary qualitative corrosion test (Section 4.6).

5.8 CONCLUSIONS

1. Two intermetallic compounds Cu_6Sn_5 and Cu_3Sn are formed at the copper tin interface. Cu_6Sn_5 is formed first and transforms into Cu_3Sn, at temperatures above 100^oC. At room temperature and up to about 100^oC only Cu_6Sn_5 is formed. The growth of the total compound, $Cu_6Sn_5 + Cu_3Sn$, is parabolic. The overall activation energy for the growth process is 75.11 kJ mol^{-1}. The rate controlling species in the process is copper.

2. In this Ni-Sn system the compound formed in the temperature range 100 - 160^oC is Ni_3Sn_4. The growth of Ni_3Sn_4 in the above temperature range is parabolic. The activation energy for the formation of Ni_3Sn_4 is 76 kJ mol^{-1}, and the rate controlling species with process is nickel.

3. Phosphorus and boron can be codeposited with Cu in acid plating baths. By controlling the current density of deposition Cu-P alloys containing up to 0.15 $^w/_o$ P can be obtained.

4. Electrodeposits of Cu-P and Cu-B alloys are efficient diffusion barriers when interposed between copper substrates and Pb-10 $^w/_o$ Sn electrodeposits, preventing the formation of Cu-Sn intermetallic compounds.

5. The activation energy of diffusion of P from electrodeposited Cu-P alloy into a Pb-10 $^w/_o$ Sn alloy is 43.33 kJ mol^{-1} (Section 4.3.2.1).

5.9 SUGGESTIONS FOR FURTHER WORK

1. The corrosion and degradation resistance of the overlays with the new barriers, under service conditions. (This work is already in progress).

2. Further development of the Cu-P and Cu-B electroplating baths and their operating conditions.

3. The ternary effect of alloying P or B with Pb-Sn and the quaternary effect of alloying P or B with Pb, Sn and Cu, on the intermetallic compound formation.

4. The efficacy of the barriers on pure tin, Pb-Sn alloys with higher tin contents and Pb-In alloys.

5. The corrosion and oxidation resistance and other properties of the Cu-P and Cu-B electrodeposited alloys.

6. The assessment of the boron content in the Cu-B electrodeposits.

7. The solderability of Pb-Sn-Cu-P and Pb-Sn-Cu-B alloys.

REFERENCES

1. D F Wilcock and E R Booser, Bearing Design and Application, (McGraw Hill, N.Y., 1957) p 335.

2. G C Pratt, Internat. Metallurgical Rev., 1973, 18, 62.

3. C J Thwaites, Tribologia e Lubrificazione, 1975, 10, 94.

4. J M Conway-Jones, "Selecting Bearing Materials", Diesel and Gas Turbine Progress (North American edn., June 1974) p 15.

5. R A Geshicher, U.S Pat. 3,650,952, March 21, 1972.

6. H J Andrews Jr., U.S Pat. 3,493,508, Feb 3, 1970.

7. R W Wilson and E B Shone, Anti-corrosion Methods Mat., 1970, 17, (8), 9.

8. M Clarke, Electroplating, City of London Polytechnic, 1973, p 48.

9. C M Loane, "Corrosion by Lubricants", Corrosion Handbook, (ed H H Uhlig; J Wiley, N.Y., 1948) p 559.

10. H H Zuidema, Performance of Lubricating Oils, 2nd edn., (Reinhold, N.Y., 1959) p 29.

11. N Zeigler, Trans.Amer.Inst.Mining Met.Eng., 1932, 100, 267.

12. H H Uhlig, Corrosion and Corrosion Control, (J Wiley, N.Y., 1971) p 292.

13. G Tammann, Lehrbuch der Metallkunde, (L Voss, Leipzig, 4th edn.,1932) p 428.

14. H Preiser and B Tytell, Corrosion, 1959, 15, 596.

15. R Bennedict, Materials Protection, 1965, 4, 36.

16. A R P Ghuman and J I Goldstein, Metall.Trans.,1971, 2, 290.

17. M L Hughes, J.Iron & Steel Inst., 1950, 166, 77.

18. P T Stroup and G A Purdy, Met. Progr., 1950, 57, 59.

19. D O Gittings, D H Rowland and J O Mack, Trans A.S.M., 1951, 43, 587.

20. C P Flynn, Point Defects and Diffusion, (Clarendon, Oxford, 1972) p 19.

21. J R Manning, Diffusion Kinetics for Atoms in Crystals, (Van Nostrand, Princeton, N.J., 1968) p 1.

22. Y Adda and J Philbert, La Diffusia dans les Solides, Vol 1, (Presses Universitaire de France, Paris, 1966) p 20.

23. L A Girifalco, Atomic Migration in Crystals, (Blaisdell, N.Y., 1964) p 26.

24. P G Shewmon, Diffusion in Solids, (McGraw Hill, N.Y.,1964) p 9.

25. S R de Groot and P Mazur, Non Equilibrium Thermodynamics, (North Holland, Amsterdam, 1962) p 15.

26. A D Franklin, Point Defects in Solids, Vol I, (eds. J H Crawford Jr. and L M Slifkin; Plenum Press, N.Y., 1972) p 1.

27. L W Barr and A B Lidiard, Physical Chemistry, Vol 10, (ed W Jost; Academic Press, N.Y., 1970) p 151.

28. N L Peterson, Solid State Physics, Vol 22, (eds F Seitz, D Turnbull and H Ehrenreich; Academic Press, N.Y., 1968) p 409.

29. R E Howard and A B Lidiard, Rep.Progress Physics, 1964, 27, p 161.

30. D Lazarus, Solid State Physics, Vol 10, (eds. F Seitz and D Turnbull; Academic Press, N.Y., 1960) p 71.

31. N L Peterson, "Diffusion", Seminar of the A.S.M., Oct 14 and 15, 1972, (ASM,Metals Park, Ohio) 1973, p 47.

32. T R Anthony, Vacancies and Interstitials in Metals, (eds. A Seeger, D Schumacher, W Schilling and J Diehl; North Holland, Amsterdam, 1970), p 935.

33. A Smigelskas and E Kirkendall, Trans. AIME, 1947, 171, 130.

34. R Feder and A S Nowick, Phys.Rev., 1958, 109, 1959.

35. R O Simmons and R W Baluffi, Phys.Rev., 1960, 117, 52.

36. R O Simmons and R W Baluffi, Phys.Rev., 1963, 129, 1533.

37. R O Simmons and R W Baluffi, Phys.Rev., 1960, 119, 600.

38. R O Simmons and R W Baluffi, Phys.Rev., 1962, 125, 862.

39. R Feder and A S Nowick, Phil.Mag.,1967, 15, 805.

40. R Feder and H P Charbnau, Phys.Rev., 1966, 149, 464.

41. R Feder, Phys.Rev., 1970, 32, 828.

42. R Feder and A S Nowick, Phys.Rev.,1972, B5, 1244.

43. C Janot, D Mallejac and B George, Phys.Rev., 1970, B2, 3088.

44. E L Owen, Properties of Electrodeposits, Their Measurement and Significance, (eds. R Sard, H Leidheiser, Jr. and F Ogburn; The Electrochemical Society, Princeton, N.J.,1975), p 80.

45. D A Porter and K E Easterling, Phase Transformations in Metals and Alloys, (Reinhold, N.Y., 1981) p 60.

46. F Seitz, Fundamental Aspects of Diffusion in Solids, (Pittsburgh, 1948).

47. H Huntington, Phys.Rev., 1940, 58, 143.

48. H Huntington, Phys.Rev., 1942, 61, 325.

49. L S Darken, Trans.Met.Soc., AIME., 1948, 175, 184.

50. L Boltzmann, Am.Phys., Leipzig, 1899, 53, 959.

51. C Matano, Japan J. Phys., 1933, 8, 109.

52. C S Hartley, J.Met., 1962, 14, 95.

53. C P Heizwegen and G J Visser, Scr.Metall., 1973, 7, 223.

54. A D Le Claire, Diffusion in Body Centred Cubic Metals (ASM, Metals Park, Ohio, 1965) p 3.

55. A Seeger and H Mehrer, Vacancies and Interstitials in Metals, (eds. A Seeger, D Schumacher, W Schilling and J Diehl; North Holland, Amsterdam, 1970) p 1.

56. S Wach, Proc. 2nd Int.Cong. on Hydrogen in Metals, Paris, June 1977, (Pergamon, Oxford, 1978) Paper 1A1.

57. S Wach, 9th Int.Symp. "Reactivity of Solids", Krakov, 1-6 September 1980 (Elsevier, 1980) p 221.

58. W O Allread, Plating, 1962, 49, 46.

59. J W Frame, MS Thesis, Lehigh University, 1961.

60. M Creydt and R Fichter, Metall.Wissenshaft u. Technik, 1971, 10, 1124.

61. P J Kay and C A Mackay, Trans.Inst.Met.Finish., 1971, 54, 68.

62. D A Unsworth and C A Mackay, Trans.Inst.Met.Finish., 1973, 51, 85.

63. P J Kay and C A Mackay, Trans.Inst.Met.Finish., 1976, 54, 68.

64. P J Kay and C A Mackay, Trans.Inst.Met.Finish., 1979, 57, 169.

65. N Q Lane, S J Rothman and L J Nowicki, Bull.Amer.Phys. Soc., 1972, 17, 244.

66. D R Gabe, Iron and Steel, 1967, 40, 118.

67. K Kirner, Metall, 1962, 16, 672.

68. P K Dutta and M Clarke, Trans.Inst.Met.Finish.,1960, 37, 108.

69. B E Wynne, J W Edington and G P Rothwell, Metall.Trans., 1972, 3, 301.

70. R A E Hooper, D R Gabe and J M West, Trans.Inst.Met. Finish.,1970, 48, 182.

71. D R Gabe, Proc.Conf. "Physical Metallurgy of Surface Coatings", London 2-3 May 1973, (Iron Steel Inst. - Inst.Metals, 1973) p 1.

72. A R P Ghuman and J I Goldstein, Metall.Trans., 1971, 2,2903.

73. M L Hughes, J.Iron Steel Inst., 1950, 166, 77.

74. P T Stroup and G A Purdy, Met.Progr., 1950, 57, 59.

75. D O Gittings, D H Rowland and J O Mack, Trans. A.S.M., 1951, 43, 487.

76. R W Pawel and T S Lundy, Acta.Met.,1965, 13, 345.

77. R P Agarawala, S P Murarka and M S Anand, Acta.Metall., 1964, 12, 871.

78. J A Morris, Trans.Inst.Met.Finish.,1973, 51, 56.

79. A H Du Rose and D M Hutchinson, Plating, 1953, 40, 470 and 630.

80. K N Tu and R D Thompson, Acta.Metall., 1982, 30, 947.

81. B T K Barry and D Phillips, Electrochem.Technology, 1968, 6, 11 and 394.

82. J V Castell-Evans, Trans.Inst.Met.Finish.,1969, 47, 71.

83. D R Gabe and R J Mort, J.Iron Steel Inst., 1965, 203 , 64.

84. G G Kamm, A R Willey and R E Beese, Mat.Protection, 1964, 3(12), 70.

85. W E Hoare, E S Hedges and B T K Barry, The Technology of Tin Plate (Arnold, 1965) p 125.

86. A J Discombe, D R Gabe and R J Mort, J.Iron Steel Inst., 1965, 203, 1252.

87. D R Gabe, High Temperature Materials Coatings and Surface Interactions, (ed. J B Newkirk; Freund, Switzerland, 1980) p 115.

88. B Lustman and R F Mehl, Trans. A.I.M.E., 1942, 147, 369.

89. D D Van Horn, Trans. A.S.M., 1959, 51, 185.

90. T P Hoar and E A G Croom, J.Iron Steel Inst., 1951, 169, 101.

91. J S Kirkaldy, Can.J.Phys., 1958, 36, 917.

92. E J Daniels, J.Inst.Metals., 1932, 49, 169.

93. N L Peterson and R E Ogilvie, Trans.A.I.M.E., 1960, 218, 439.

94. L S Castleman and L L Seigle, Trans.A.I.M.E., 1958, 212, 589.

95. G P Tiwari and B D Sharma, Nature, 1964, 204, 178.

96. E J Daniels, J.Inst.Metals, 1931, 46, 81.

97. L M Gert and A A Babad-Zakhryapin, Fiz.Met.Metalloved., 1964, 18, 210.

98. J S Kirkaldy, Can.J.Phys., 1958, 36, 899.

99. J S Kirkaldy, Can.J.Phys., 1959, 37, 30.

100. N M Rodigin, Fiz.Met.Metalloved., 1961, 11, 240.

101. R W Pawel and T S Lundy, Acta Metall., 1965, 13, 345.

102. V Z Bugakov, Diffusion in Metals and Alloys, (U.S. Dept. of Commerce, Washington, D.C., 1971) p 85.

103. S Wach, Spring Residential Conf., Environmental Degradation of High Temperature Materials, 31 Mar. - 3 Apr.1980, Douglas, Isle of Man. (Inst.of Metallurgists - Inst.of Corr.Sci. & Tech., Series 3, No 13, Vol 2) paper 1/1.

104. C Wagner, Z.Physik.Chem., 1933, B.21, 25.

105. N B Pilling and R E Bedworth, J.Inst.Metals, 1923, 29, 529.

106. G. Tammann, Z.Anorg.Chem., 1922, 124, 25.

107. G A Kokorin and A I Vitkin, Conf.on Surface Phen.in Met. Processes, 1965, p 211 (from D R Gabe, Ref.87).

108. E J Daniels, Trans.Farads.Soc., 1935, 31, 1277.

109. N S Gorbunov, Diffusion Coatings on Iron and Steel, (U.S.S.R Acad.Sci.,1958; transl.Israel Progr.,1960) p 3.

110. R Drewitt, Corr.Sci., 1969, 9, 823.

111. G A Kokorin, Sb.Trad.Tsent.Nauch.Iss.Inst.Chem.Met., 1963, 32, 118.

112. J E Nicholls, Corr.Tech., 1964, 11, 16.

113. T Heumann and S Dittrich, Z.Metallk., 1959, 50, 617.

114. W R Buck and H Leidheiser Jr., J.Electrochem.Soc., 1965, 112, 243.

115. A Brenner, Electrodeposition of Alloys (Academic Press, 1963) Vol 1, p 4; Vol 2, p 457.

116. A E Carlsen and J M Kane, Monthly Rev.Am.Electroplaters Soc., 1946, 33, 255.

117. J B Mohler, Iron Age, 1950, 166, 92.

118. J S Nachtman, U.S. Patent, 2, 446, 716 (1948).

119. A J Du Rose and J D Little, Lead-Tin Alloy Plating, U.S. Patent, 2, 460, 252 (1949).

120. N Parkinson, J. Electrodepositors' Tech.Soc., 1950, 26, 169.

121. A H Du Rose, Trans.Electrochem.Soc., 1946, 89, 417.

122. H Narcus, Metal Finishing, 1943, 43, 242.

123. T Voyda, Proc.Am.Electroplaters' Soc., 1946, p 33.

124. A Brenner and G E Riddell, J.Research Nat.Bur.Standards, 1946, 37, 31.

125. A Brenner, D E Couch and E K Williams, J.Research Nat.Bur. Standards, 1950, 44, 109.

126. G N Sorkin, Yu G Lavrentev and R Yu Bek, Institute of Physicochemical Principles of Ore Conversion, Translated from Zhurnal Prikladnoi Khimii, 1971 (March), 44, 671.

127. C J Owen, J Jackson and E R York, Plating, 1967, 54, 821.

128. A Furlani, A M Giulani and C Furlani, Atti.Acad.Nazl.Lincei. Rend., Classe Sci.,Fis.Met.Nat., 1964, 37(5), 436.

129. British Patent, 1,335,961, Glacier Metal Co.,17.11.1970.

130. K Graham. Electroplating Engineering Handbook, (Van Nostrand, 1971) p 488.

131. D S Cook, City of London Polytechnic, Private Communication.

132. J O'M Bockris, M A Genshaw and M Fullenwider, Electrochim. Acta, 1970, 15, 47.

133. J Frenkel, Teoriya tverdykh i ghidkikh tel (Theory of Solids and Liquids) GTTI., 1934; Kinetic Theory of Liquids (Dover, 1955), p 48.

134. M Polanyi and E Wigner, Z.Phys.Chem.,(A), 1928, 139, 439.

135. D S Kingsley, Trans.Inst.Metal Finish., 1979, 57, 7.

136. Electrodeposition of Tin-Lead Alloys (International Tin Research Institute) Publication 325, 1961, August.

137. S Wach, "The Compensation Effect in Diffusion and the Energetics of Substances", DIMETA 82 Conf., 30 Aug - 3 Sept 1982, Tihany Hungary (eds. F J Kedves and D L Beke, Trans. Tech Publications, 1973).

138. M Hansen, Constitution of Binary Alloys, 2nd edn.,(McGraw Hill, N.Y., 1958) p 607.

139. J Smithells, Metals Reference Book, 5th edn., (Butterworths, London, 1976) p 867.

140. S Wach, City of London Polytechnic, Private Communication.

141. W Seith and J G Laird, Z.Metallkd.,1932, 24, 193.

142. S Mrowec, Defects and Diffusion in Solids, (Elsevier, 1980) p 361.

143. O Kubaschewski, E Ll Evans and C B Alcock, Metallurgical Thermochemistry, Vol 1, 4th edn., (Pergamon, 1967) p 304.

144. J Bardeen and C Herring, Atom Movements, (A.S.M, Cleveland, 1951) p 87.

145. J Bardeen and C Herring, Imperfections in Nearly Perfect Crystals (J Wiley, N.Y.,1952) p 261.

146. E A Guggenheim, Thermodynamics, (North Holland, Amsterdam, 1949) p 92.

147. J W Christian, Theory of Transformation in Metals and Alloys, 1st edn., Vol 7 (Pergamon, 1965) p 161.

148. A Seeger, J.Less-Common Metals, 1972, 28, 387.

149. Equilibrium Data for Tin Alloys (International Tin Research Institute) 1949.

150. S K Kang and V Ramachandran, Scr.Metall.,1980, 14, 421.

151. K L Mittal, "Properties of Electrodeposits, their Measurement and Significance", (eds. R Sard, H Leidheiser Jr. and F Ogburn; The Electrochem.Soc., Princeton, N.J.,1975) p 273.

152. C H Ma and R A Swalin , Acta Met., 1960, 8, 388.

153. I Barin, O Knacke and O Kubaschewski. Thermochemical Properties of Inorganic Substances, Supplement, (Springer-Verlag, Berlin, 1977) p 486.

154. W B Pearson, Handbook of Lattice Spacings and Structures of Metals, (Pergamon, London, 1958) p 611.

155. L L Shreir, Corrosion, Vol 2, (Newnes-Butterworths, London, 1976) p 21.24.

156. G Millazzo and S Caroli, Tables of Standard Electrode Potentials, (J Wiley, NY, 1978).

157. A I Vogel, A Textbook of Quantitative Inorganic Analysis, 3rd edn. (Longmans, 1964) p 635.

PATENT APPLICATIONS

(12) UK Patent Application (19) GB (11) 2 114 156 A

(21) Application No 8202304
(22) Date of filing 27 Jan 1982
(43) Application published
17 Aug 1983
(51) INT CL³
C25D 3/58 5/10 F16C
33/04
(52) Domestic classification
C7B 120 701 705 721
725 737 749 PC
F2A 100 119 150 174
D44
U1S 1364 2031 C7B F2A
(56) Documents cited
None
(58) Field of search
C7B
C7F
F2A
(71) Applicant
Shell Internationale
Research Maatschappij
BV
(Netherlands),
Carel Van Bylandtlaan 30,
The Hague, The
Netherlands
(72) Inventors
Prematilaka W.
Kalubowila,
Stanislaw P. Wach
(74) Agent and/or Address for
Service
R. C. Rogers,
4 York Road, London
SE1 7NA

(54) Composite antifriction bearing

(57) A composite antifriction bearing comprises a base layer of metal alloy containing at least copper and lead, a surface layer of lead alloyed with an anti-corrosion addition e.g. tin and a diffusion barrier arranged between the surface layer and the base layer, wherein the diffusion barrier comprises copper in combination with phosphorus. The method of applying the diffusion barrier and preferably the surface layer is by means of an electro-deposition process.

GB 2 114 156 A

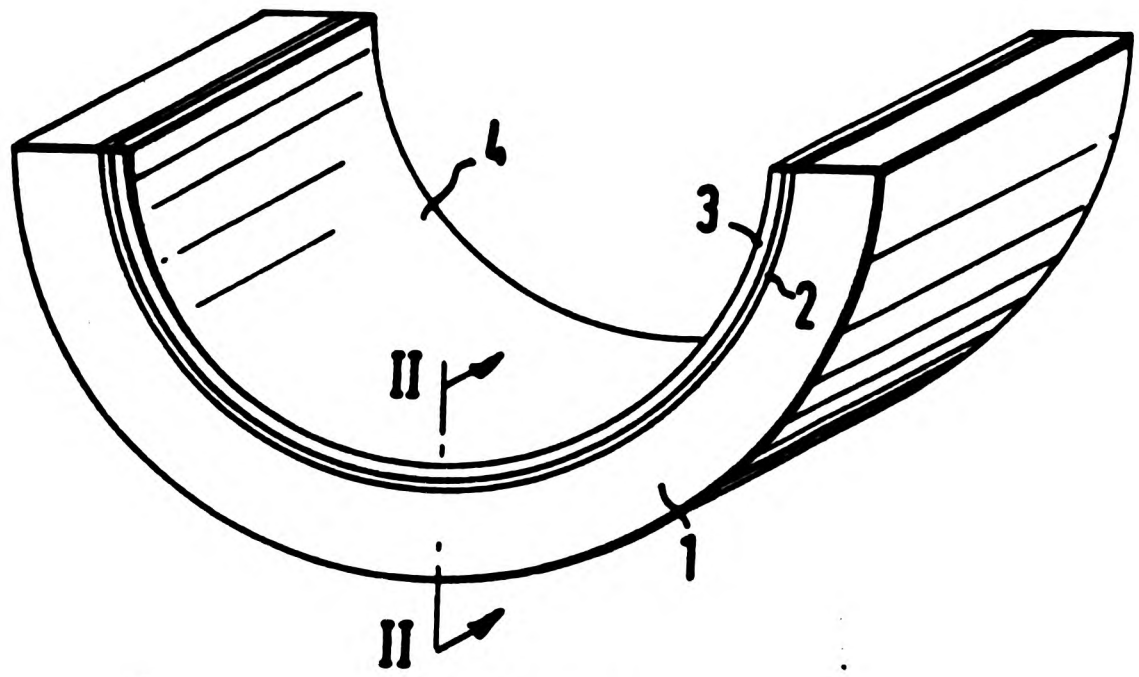

FIG. 1

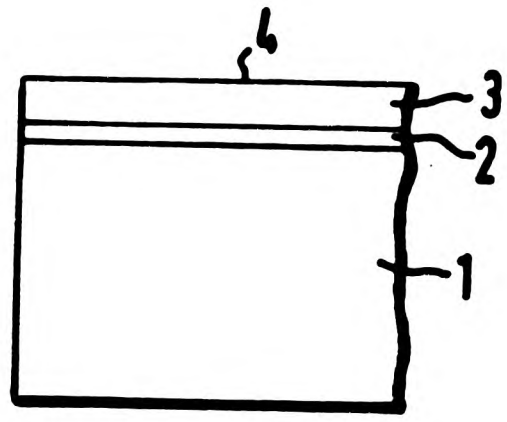

FIG. 2

SPECIFICATION

Composite antifriction bearing

The invention relates to a composite antifriction bearing comprising a base layer of metal alloy containing at least copper and lead, a surface layer of lead alloyed with an anti-corrosion addition and a diffusion barrier arranged between the surface layer and the base layer, wherein the diffusion barrier slows down the reaction rate between the anti-corrosion addition of the surface layer and components of the base layer.

The base layer comprises generally a copper-lead alloy or a lead-bronze alloy.

The purpose of the surface layer is to increase the tolerance of the bearing to misalignment, dirt and wear debris, to enable it to operate against unhardened journals and to protect the bearing against corrosion.

The prime purpose of the anti-corrosion addition in the surface layer is to provide resistance to corrosion by hot-oxidised lubricating oils, or lubricating oils contaminated by partially decomposed fuels. The anti-corrosion addition generally is tin or indium.

From U.S. patent specification No. 3,307,926, a diffusion barrier is known consisting of a tin-nickel alloy for a composite antifriction bearing having a tin containing surface layer.

It is an object of the invention to provide a composite antifriction bearing having an improved diffusion barrier diminishing depletion of the anti-corrosion addition from the surface layer to a greater extent than the known diffusion barriers. For this purpose the composite antifriction bearing according to the invention comprises a base layer of a metal alloy containing at least copper and lead, a surface layer of lead alloyed with an anti-corrosion addition and a diffusion barrier arranged between the surface layer and the base layer, wherein the diffusion barrier comprises copper in combination with phosphorus.

It is another object of the invention to provide a method of manufacturing such a composite antifriction bearing. For this purpose said method comprises applying copper in combination with phosphorus to the base layer by an electrodeposition process, in order to form the diffusion barrier and then applying the surface layer on top of the diffusion barrier.

The invention will now be further explained with reference to the accompanying drawings, wherein

Fig. 1 shows a perspective view of one half of an embodiment of a composite antifriction bearing according to the invention.

Fig. 2 shows a cross-section II—II of the embodiment of Fig. 1.

In the composite antifriction bearing as shown, the base layer is indicated by reference numeral 1, which base layer 1 is a metal alloy containing at least copper and lead, such as a copper-lead alloy or a lead-bronze alloy. The base layer 1 may be supported at the outside periphery by a support body (not shown), for example made of steel. The inner side of the base layer 1 is bonded to a diffusion barrier 2 comprising copper in combination with phosphorus. The inner side of the diffusion barrier 2 is bonded to a surface layer 3. The surface layer 3 may have a thickness in the range of from about 6 μm to 25 μm. The surface layer 3 may be a lead-tin alloy, wherein the quantity of tin is in the range of from about 2% to about 20% by weight. Instead the surface layer 3 may be a lead-indium alloy, wherein the quantity of indium is in the range of from about 3% to about 10% by weight. The inner surface 4 of the surface layer 3 is adapted to cooperate with a journal (not shown), wherein the surface 4 and the journal may be separated by a film of a suitable lubricant.

The bearing according to the invention is manufactured by applying copper in combination with phosphorus to the base layer 1 in order to form the diffusion barrier 2 by an electro-deposition process. In this copper-phosphorus electro-deposition process, an electroplating bath is used having the following composition:

Substance	Concentration in g/dm³ of aqueous solution
Cupric chloride, $CuCl_2 . 2H_2O$ (s)	60—70
Phosphorous acid, H_3PO_3 (s)	10—15
Orthophosphoric acid, H_3PO_4 (1) (density 1.75 g/cm³)	40—50

The operating conditions are as follows:

Temperature	40—45 °C
Current density	0.3—1.5 A/dm²
pH at 22 °C	1—0.5

The resulting product is Cu—P with a phosphorus content of 0.05—0.15% wt.

Finally the surface layer 3 is applied on top of the diffusion barrier 2. This surface layer 3 can for example be applied by an electro-deposition process, which is a process known in the art as such.

CLAIMS

1. A composite antifriction bearing comprising a base layer of a metal alloy containing at least copper and lead, a surface layer of lead alloyed with an anti-corrosion addition and a diffusion barrier arranged between the surface layer and the base layer, wherein the diffusion barrier comprises copper in combination with phosphorus.

2. The antifriction bearing as claimed in claim 1, wherein the anti-corrosion addition is tin.

3. The antifriction bearing as claimed in claim 2, wherein the quantity of tin in the surface layer is in the range of from about 2% to about 20% by weight.

4. The antifriction bearing as claimed in claim 1, wherein the anti-corrosion addition is indium.

5. The composite antifriction bearing as claimed in claim 4, wherein the quantity of indium in the surface layer is in the range of from about 3% to about 10% by weight.

6. The composite antifriction bearing as claimed in any one of the claims 1—5, wherein the thickness of the surface layer is in the range of from about 6 μm to about 25 μm.

7. A method of manufacturing a composite antifriction bearing as claimed in any one of the claims 1 to 6, comprising applying copper in combination with phosphorus to the base layer by an electro-deposition process, in order to form the diffusion barrier, and then applying the surface layer on top of the diffusion barrier.

8. The method as claimed in claim 7, wherein the surface layer is applied by an electro-deposition process.

9. A composite antifriction bearing substantially as described with particular reference to the accompanying drawings.

10. A method of manufacturing a composite antifriction bearing substantially as described.

Printed for Her Majesty's Stationery Office by the Courier Press, Leamington Spa, 1983. Published by the Patent Office, 25 Southampton Buildings, London, WC2A 1AY, from which copies may be obtained.

(12) UK Patent Application (19) GB (11) 2 117 403 A

(21) Application No 8207532
(22) Date of filing 15 Mar 1982
(43) Application published
12 Oct 1983
(51) INT CL³
C25D 7/10 F16C 33/12
(52) Domestic classification
C7B 120 701 721 723
725 737 749 760 PC
F2A 100 114 150 174
D44
U1S 2031 C7B F2A
(56) Documents cited
GB 1600951
GB 0733212
GB 0706672
(58) Field of search
C7A
C7B
C7F

(71) Applicant
Shell Internationale
Research Maatschappij
BV.,
(Netherlands),
Carel Van Bylandtlaan 30,
The Hague,
The Netherlands

(72) Inventors
Prematilaka W.
Kalubowila,
Stanislaw P. Wach,
Michael B. Levens

(74) Agent and/or address for service
R. C. Rogers,
4 York Road,
London,
SE1 7NA

(54) Composite antifriction bearing

(57) A composite antifriction bearing comprises a base layer 1 of metal alloy containing at least copper and lead, a surface layer 3 of lead alloyed with an anti-corrosion addition (e.g. tin or indium) and a diffusion barrer 2 arranged between the surface layer and the base layer, wherein the diffusion barrier comprises copper in combination with boron. The diffusion barrier prevents depletion of the anti-corrosion agent from the surface layer.

The diffusion barrier and the surface layer may be applied by electrodeposition.

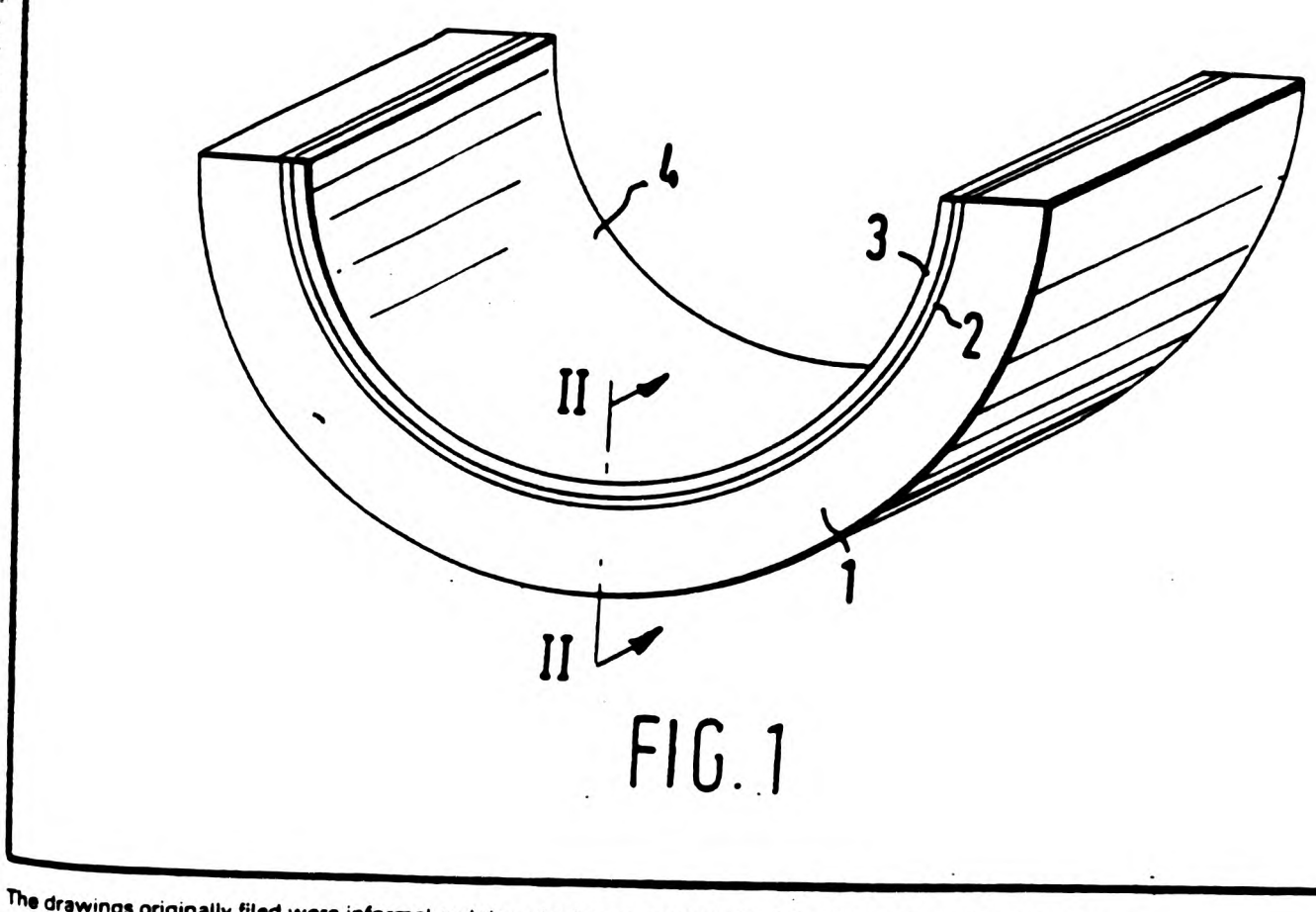

FIG. 1

GB 2 117 403 A

The drawings originally filed were informal and the print here reproduced is taken from a later filed formal copy.

2117403

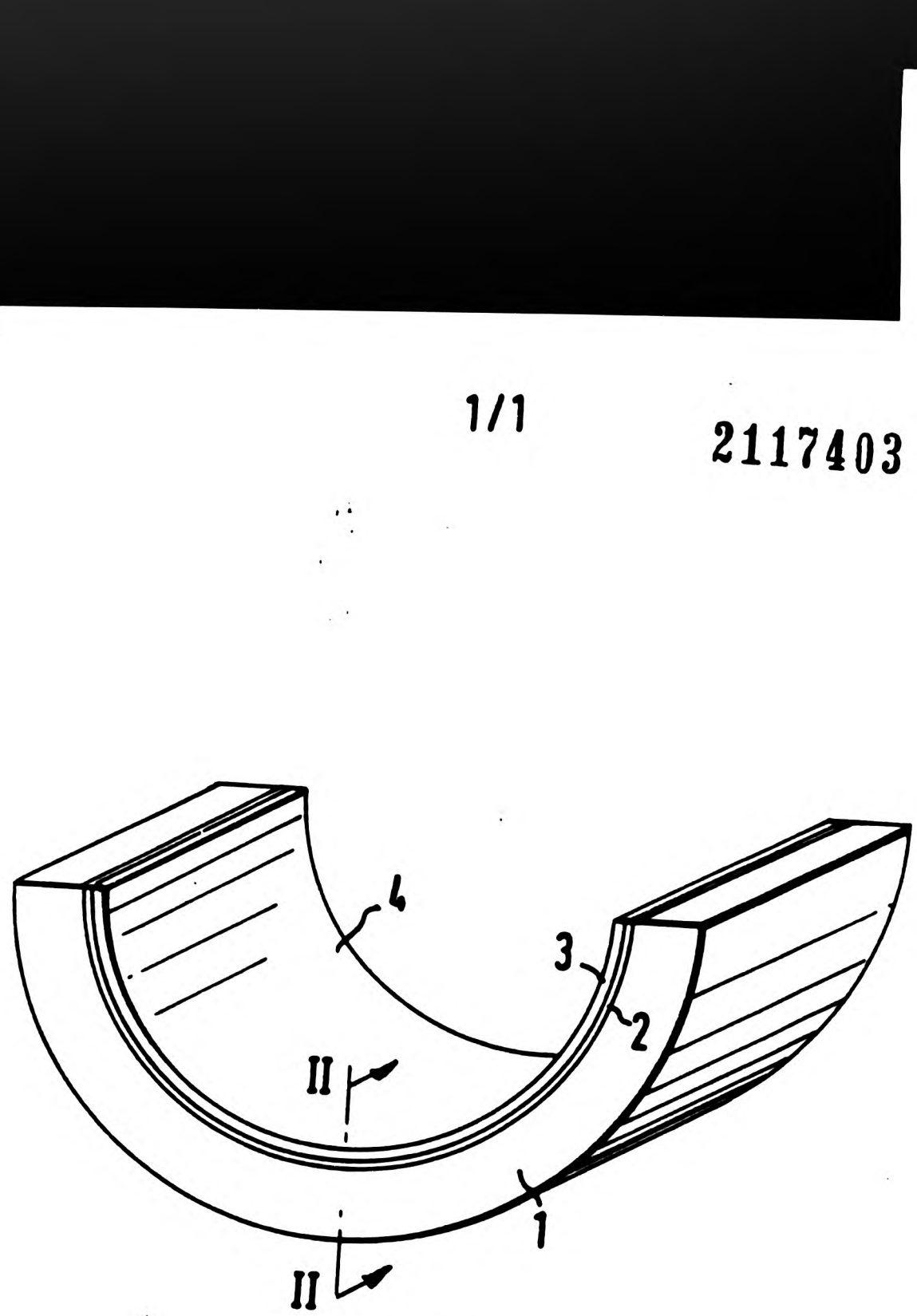

FIG. 1

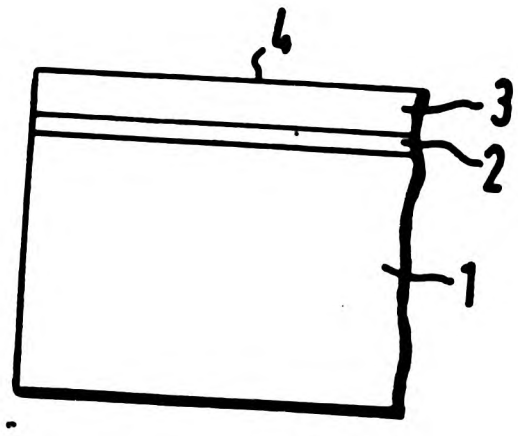

FIG. 2

SPECIFICATION

Composite antifriction bearing

The invention relates to a composite antifriction bearing comprising a base layer of a metal alloy containing at least copper and lead, a surface layer of lead alloyed with an anti-corrosion addition and a diffusion barrier arranged between the surface layer and the base layer, wherein the diffusion barrier slows down the reaction rate between the anti-corrosion addition of the surface layer and components of the base layer.

The base layer comprises generally a copper-lead alloy or a lead-bronze alloy.

The purpose of the surface layer is to increase the tolerance of the bearing to misalignment, dirt and wear debris, to enable it to operate against unhardened journals and to protect the bearing against corrosion.

The prime purpose of the anti-corrosion addition in the surface layer is to provide resistance to corrosion by hot-oxidised lubricating oils, or lubricating oils contaminated by partially decomposed fuels. The anti-corrosion addition generally is tin or indium.

From U.S. patent specification No. 3,307,926, a diffusion barrier is known consisting of a tin-nickel alloy for a composite antifriction bearing having a tin containing surface layer.

It is an object of the invention go provide a composite antifriction bearing having an improved diffusion barrier diminishing depletion of the anti-corrosion addition from the surface layer to a greater extent than the known diffusion barriers. For this purpbsk the composite antifriction bearing according to the invention comprises a base layer of a metal alloy containing at least copper and lead, a surface layer of lead alloyed with an anti-corrosion addition and a diffusion barrier arranged between the surface layer and the base layer, wherein the diffusion barrier comprises copper in combination with boron.

It is another object of the invention to provide a method of manufacturing such a composite anti-friction bearing. For this purpose said method comprises applying copper in combination with boron to the base layer by an electro-deposition process, in order to form the diffusion barrier and then applying the surface layer on top of the diffusion barrier.

The invention will now be further explained with reference to the accompanying drawings, wherein

Fig. 1 shows a perspective view of one half of an embodiment of a composite antifriction bearing according to the invention.

Fig. 2 shows a cross-section II—II of the embodiment of Fig. 1.

In the composite antifriction bearing as shown, the base layer is indicated by reference numeral 1, which base layer 1 is a metal alloy containing at least copper and lead, such as a copper-lead alloy or a lead-bronze alloy. The base layer 1 may be supported at the outside periphery by a support body (not shown), for example made of steel. The inner side of the base layer 1 is bonded to a diffusion barrier 2 comprising copper in combination with boron. The inner side of the diffusion barrier 2 is bonded to a surface layer 3. The surface layer 3 may have a thickness in the range of from about 6 μm to 25 μm. The surface layer 3 may be a lead-tin alloy, wherein the quantity of tin is in the range of from about 2% to about 20% by weight. Instead the surface layer 3 may be a lead-indium alloy, wherein the quantity of indium is in the range of from about 3% to about 10% by weight. The inner surface 4 of the surface layer 3 is adapted to cooperate with a journal (not shown), wherein the surface 4 and the journal may be separated by a film of a suitable lubricant.

The bearing according to the invention is manufactured by applying copper in combination with boron to the base layer 1 in order to form the diffusion barrier 2 by an electro-deposition process.

In this copper-boron electro-deposition process, an electroplating bath is used having the following composition:

Substance	*Concentration in g/l of aqueous solution*
Cupric sulphate, $CuSO_4.5H_2O$	30
Boric acid, H_3BO_3	40

The operating conditions are as follows:

Temperature	20—25°C
Cathode current density	0.5—1.0 A/dm²

The anode/cathode area ratio is for example 1:1 and the anodes are of copper.

The resulting product is Cu-B with a boron content of up to 0.02% wt.

Finally the surface layer 3 is applied on top of the diffusion barrier 2. This surface layer 3 can for example be applied by an electro-deposition process, which is a process known in the art as such.

Claims

1. A composite antifriction bearing comprising a base layer of a metal alloy containing at least copper and lead, a surface layer of lead alloyed with an anti-corrosion addition and a diffusion barrier arranged between the surface layer and the base layer, wherein the diffusion barrier comprises copper in combination with boron.

2. The antifriction bearing as claimed in claim 1, wherein the anti-corrosion addition is tin.

3. The antifriction bearing as claimed in claim 2, wherein the quantity of tin in the surface layer is in the range of from about 2% to about 20% by weight.

4. The antifriction bearing as claimed in claim

1, wherein the anti-corrosion addition is indium.

5. The composite antifriction bearing as claimed in claim 4, wherein the quantity of indium in the surface layer is in the range of from about 3% to about 10% by weight.

6. The composite antifriction bearing as claimed in any one of the claims 1—5, wherein the thickness of the surface layer is in the range of from about 6μm to about 25 μm.

7. A method of manufacturing a composite antifriction bearing as claimed in any one of the claims 1 to 6, comprising applying copper in combination with boron to the base layer by an electro-deposition process, in order to form the diffusion barrier, and then applying the surface layer on top of the diffusion barrier.

8. The method as claimed in claim 7, wherein the surface layer is applied by an electro-deposition process.

9. A composite antifriction bearing substantially as described with particular reference to the accompanying drawings.

10. A method of manufacturing a composite antifriction bearing substantially as described.

Printed for Her Majesty's Stationery Office by the Courier Press, Leamington Spa, 1983. Published by the Patent Office, 25 Southampton Buildings, London, WC2A 1AY, from which copies may be obtained

K-6201(US)
HWC:JN

AN ELECTRONIC CONDUIT AND A METHOD OF MANUFACTURING IT

Background of the Invention

The invention relates to an electronic conduit comprising a base conduit made of copper or containing mainly copper and provided with a coating of tin-lead or of tin.

Such electronic conduits are known and are used on a large scale in electronic equipment, for example on printed circuit boards, or as terminals of electronic components.

The coating of tin-lead or of tin protects the base conduit, so that corrosion of the base conduit is prevented and furthermore the coating facilitates the making of connections between various electronic components by soldering.

A problem with such electronic conduits is that material from the coating, in particular tin and copper of the base conduit tend to interdiffuse and react with each other, so that the intermetallic compounds Cu_3Sn and Cu_6Sn_5 are formed which are more difficult to solder. Said intermetallic compounds can be soldered only by the process of wetting which has the disadvantage that in soldering by modern automatised techniques the time may not be sufficiently long to promote wetting and hence good electrical contact.

In particular if the coating is very thin, for example about 5 µm, it is possible that the tin of the coating will react completely with the copper of the main conduit, so that only Cu_3Sn is formed and soldering is hardly possible. This will occur, for example, as a result of storage of the electronic conduit during a relatively short period of time, for example about six weeks.

In order to deal with this problem, it has been proposed to arrange a diffusion barrier, comprising for example iron, or nickel or cobalt, between the coating and the base conduit, said diffusion barrier

reducing the diffusion of tin from the coating into the base conduit and consequently the formation of intermetallic compounds. Such a diffusion barrier is described in U. S. Patent No. 3,872,356 which was published on March 18, 1975.

It is an object of the invention to provide an electronic conduit of the above kind having an improved diffusion barrier reducing the transfer of tin from the coating into the base conduit to a greater extent than the known diffusion barriers.

It is a further object of the invention to allow the application of a thinner coating of tin-lead or of tin, in the presence of the diffusion barrier, and thereby to effect a more economic use of the coating metal.

Summary of the Invention

The electronic conduit according to the invention comprises a base conduit containing mainly copper and provided with a coating of tin-lead or of tin, wherein a diffusion barrier is arranged between the coating and the base conduit and wherein the diffusion barrier comprises either copper in combination with phosphorus or copper in combination with boron.

A method of manufacturing such an electronic conduit comprises applying copper in combination with phosphorous or copper in combination with boron to the base conduit by an electro-deposition process, in order to form the diffusion barrier, and then applying the coating on the diffusion barrier.

After the application of the diffusion barrier on the base conduit, the coating may be applied by an electro-deposition process or by dipping the base conduit into molten tin or into molten tin-lead.

Brief Description of the Drawing

The drawing shows a cross-section of a printed circuit board constructed in accordance with the present invention.

Description of the Invention

As shown in the drawing a circuit board comprises a plate 1 made of suitable synthetic resin or glass. The plate carries a number of base conduits 2 made of copper or containing mainly copper. The base conduits 2 are applied on the plate 1 by an electro-deposition process or by any other suitable method known in the art.

Each of the base conduits 2 is provided with a diffusion barrier 3, which comprises either copper in combination with phosphorus or copper in combination with boron. The diffusion barrier 3 is applied on the base conduit 2 by means of suitable electro-deposition processes which will be described below.

On each diffusion barrier 3, a coating 4 of tin or of tin-lead is present. After the application of the diffusion barrier 3, the coating 4 may be applied by a suitable electro-deposition process or by dipping the base conduit 2 into molten tin or into molten tin-lead.

The diffusion barrier 3, comprising copper in combination with phosphorus, is applied by means of a copper-phosphorus electro-deposition process, wherein an electro-plating bath is used having the following composition:

Substance	Concentration in g/dm^3 of aqueous solution
Cupric chloride, $CuCl_2.2H_2O$ (s)	60-70
Phosphorous acid, H_3PO_3 (s)	10-15
Orthophosphoric acid, H_3PO_4 (l) (density 1.75 g/cm^3)	40-50

The operating conditions are as follows:

Temperature	40-45°C
Current density	0.3-1.5 A/dm^2
pH at 22°C	1-0.5

The resulting product is Cu-P with a phosphorus content of 0.05-0.15% weight.

The diffusion barrier 3, comprising copper in combination with phosphorus is also applied by means of a copper-phosphorus electro-deposition process, wherein an electroplating bath is used having the following composition:

Substance	Concentration in g/dm^3 of aqueous solution
Cupric sulphate, $CuSO_4.5H_2O$ (s)	25-35
Phosphoric acid, H_3PO_4 (l) (density 1.75 g/cm^3)	20-30
Phosphorous acid, H_3PO_3 (s)	10-15

The operating conditions are as follows:

Temperature	40-45°C
Current density	0.3-1.5 A/dm^2

The resulting product is Cu-P with a phosphorus content of 0.03-0.15% weight.

The diffusion barrier 3, comprising copper in combination with boron, is applied by means of a copper-boron electro-deposition process, wherein an electroplating bath is used having the following composition:

Substance	Concentration in g/dm^3 of aqueous solution
Cupric sulphate, $CuSO_4.5H_2O$ (s)	25-35
Boric acid, H_3BO_3 (s)	35-45

The operating conditions are as follows:

Temperature	20-25°C
Cathode current density	0.5-1.0 A/dm^2

The anode/cathode area ratio is for example 1:1 and the anodes are of copper.

The resulting product is Cu-B with a boron content of up to 0.02% weight.

Finally, the coating 4 is applied on the diffusion barrier 3. The thickness of the coating 4 is for example in the range of from about 0.25 µm to about 25 µm.

WHAT IS CLAIMED IS:

1. An electronic circuit board conduit comprising a base conduit made of copper or containing mainly copper and provided with a coating of tin-lead or of tin, wherein a diffusion barrier is arranged between the coating and the base conduit and wherein the diffusion barrier comprises either copper in combination with phosphorus or copper in combination with boron.

2. An electronic conduit as claimed in Claim 1, wherein the base conduit is a strip.

3. An electronic conduit as claimed in Claim 1, wherein the thickness of the coating of tin-lead or tin is in the range of from about 0.25 µm to about 25 µm.

4. A method of manufacturing an electronic conduit, comprising applying copper in combination with phosphorus to a base conduit made of copper or containing mainly copper by an electro-deposition process, in order to form the diffusion barrier, and then applying a coating of tin-lead or tin on the diffusion barrier.

5. A method of manufacturing an electronic conduit as claimed in Claim 4, comprising applying copper in combination with boron to the base conduit by an electro-deposition process, in order to form the diffusion barrier, and then applying the coating on the diffusion barrier.

6. The method as claimed in Claim 4, wherein the coating is applied by an electro-deposition process.

7. The method as claimed in Claim 4, wherein the coating is applied by dipping the base conduit into molten tin or into molten tin-lead.

K-6201(US)
HWC:JN

AN ELECTRONIC CONDUIT AND A METHOD OF MANUFACTURING IT

Abstract of the Disclosure

An electronic conduit comprising a base conduit (2) made of copper or containing mainly copper and provided with a coating (4) of tin-lead or of tin, wherein a diffusion barrier (3) is arranged between the coating (4) and the base conduit (2). According to the invention the diffusion barrier (3) comprises either copper in combination with phosphorus or copper in combination with boron. The invention relates as well to a method of manufacturing such as electronic conduit, wherein the diffusion barrier (3) is applied to the base conduit (2) by means of an electro-deposition process (see drawing).

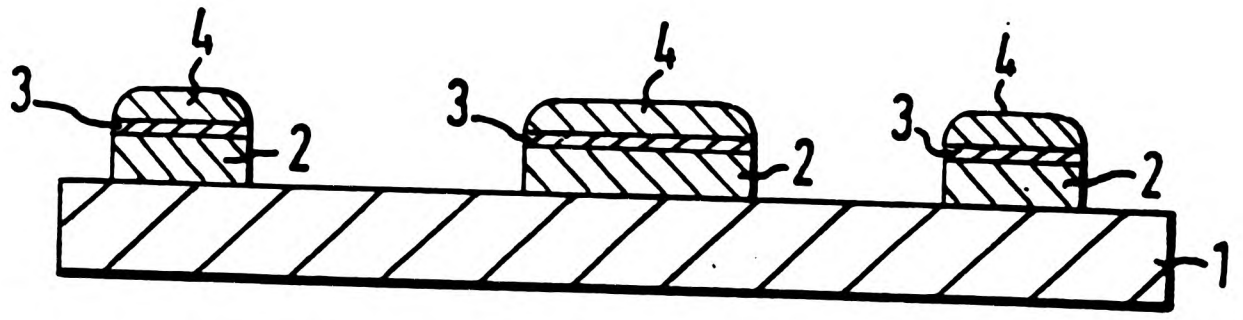
4
3
2
4
3
2
4
3
2
1

D688986

END